STUDIES OF THE FOULING OF HEAT EXCHANGER EQUIPMENT

by

G. FIELD, B.Sc.(Hons.), C.Eng., M.I.Mech.E.

Submitted in fulfilment of the requirements for
the degree of Master of Science

University of Aston in Birmingham
OCTOBER, 1969

Faculty of Engineering

Department of Mechanical Engineering

Head of Department and Supervisor:
Professor A. J. Ede

SYNOPSIS

The fouling of heat exchanger equipment has long been one of the most troublesome, and unpredictable aspects of heat exchanger operation.

In this thesis the nature of fouling is discussed, and the effect of a fouling film on a heat transfer surface is illustrated by numerical example. The various types of fouling are classified and comments on the factors affecting fouling are included. Problems related to the economics, design and maintenance of heat exchanger equipment subject to fouling are also discussed.

After these introductory comments, a comprehensive literature survey is presented which concludes with a general discussion on the papers.

A section describing the experimental work follows in which, first of all, the reasons are given for the choice of the experimental programme. This programme concerned the deposition of calcium sulphate on a heated surface, and was aimed at establishing a law relating the deposition rate both to the heat flux causing the deposition and to the mass flow rate of the circulating solution.

The experimentally derived law is subsequently applied to the analysis of a double-pipe heat exchanger in order to predict a thermal resistance - time relationship in both parallel flow and counterflow configurations.

The thesis concludes with a discussion summarising the main points established in the body of the report and making recommendations concerning future researches.

CONTENTS

CONTENTS continued

CONTENTS continued

DESCRIPTION OF PRESENTATION

The report is divided into seven main sections designated as Section A to Section G, the whole being preceded by a Synopsis.

Each section, where appropriate, is subdivided into chapters using a numerical system preceded by the section letter. For example, the third chapter in section C would be chapter C3 and so on. Where necessary paragraph location within a chapter is by decimal subdivision of the chapter as for example in A1.2.

Formulae are similarly designated so that formula C3.2 is the second formula in chapter C3.

Symbols appropriate to a section are listed at the beginning of that section except for Section F containing the Appendices. In this case, each Appendix includes its own list of symbols. Whilst uniformity has been aimed at, the re-defining of symbols for each section allows a degree of flexibility where appropriate.

Appendages in the form of tables, lists of data, diagrams and graphs appear at the end of the chapter in which they are first mentioned. The prefix Fig. is used in all cases so that Fig. A1.2 is the second appendage to chapter A1.

A complete bibliography appears as the final section of the report.

UNITS

S.I. units have been adopted in this thesis with the acceptable alternative time unit, the hour. It is felt that the hour unit is more suitable in the context of the work under discussion. The only departure from S.I. units occurs in the literature survey where any quantities quoted in the discussion are expressed in the units originally given in the reference.

SECTION A

A GENERAL DISCUSSION OF THE FOULING PROBLEM

CONTENTS

SYMBOLS USED IN SECTION A

h	surface coefficient of heat transfer
k	thermal conductivity of flowing liquid
k_s	thermal conductivity of scale material
k_w	thermal conductivity of tube material
Pr	Prandtl number of flowing liquid
R	inside radius of tube
R_s	thermal resistance at scale - liquid interface
R_{sc}	thermal resistance of scale layer
R_w	thermal resistance of tube wall
t_w	tube wall thickness
V	velocity of flowing liquid
x	scale layer thickness
ρ	density of flowing liquid
μ	dynamic viscosity of flowing liquid

CHAPTER A1

THE NATURE OF THE PROBLEM

A1.1 Definition of terms

The term fouling is used to describe any situation in which the designed geometry and thermal performance of a heat exchanger are changed as a result of the deposition of solids.

It may sometimes be that deposition occurs on the heat transfer surface so changing the thermal resistance by effectively lagging the surface. This type of fouling may be the result of the deposition of insoluble salts from the circulating liquid and is then referred to more specifically as scaling. It is this particular mode of fouling which is investigated in detail in this report.

In addition to this, fouling as dirt deposition can occur. Hudson(1)* subdivides this into three parts:

(a) Large solids in the circulating liquid may lodge in the flow passages. These solids would be of such dimensions that they would pass through strainers often becoming jammed near the inlet on either the shell or tube side.

(b) Dirt deposition can occur in near-stagnant areas of an exchanger. These areas would be in the headers on the tube side and around the baffles on the shell side.

(c) Dirt deposition on heat transfer surfaces. This would result from finely divided solids forming a thin film on the tube surface. Kern and Seaton(2) and later, Kern(3) discuss a possible mechanism for this manner of fouling. This will be reviewed later in the literature survey (chapters B2.2 and B2.5).

(*Numbers in brackets refer to reference list, Section G)

In addition to the above mentioned types of fouling, Kelly and Puckorius(4) mention corrosion products as a potential foulant.

Signs that equipment is becoming fouled might be in reduced heat transfer rates, or increased pumping costs. Other indications could be unexpected shutdowns or shortened equipment life. Corrosion of components or poor corrosion inhibitor performance could also result from fouling.

A1.2 Factors affecting fouling

If dirt is already present in the liquid upstream of the heat exchanger, the quantity present in the heat exchanger as a potential foulant depends on the efficiency of filtration.

However, by offering resistance to flow a better filtration system means increased running costs. Dirt which does enter a heat exchanger may not be troublesome if the liquid path is designed to minimise stagnant regions.

Scaling will generally increase with increase in temperature. This may be because a chemical reaction is involved which requires a high temperature for it to take place. Alternatively it may be due to the reduced solubility at higher temperatures of salts such as calcium sulphate. The solubility of salts can also be affected by a change in pH or alkalinity of the solution. It is also known that certain micro-organisms can influence the solubility of dissolved solids.

The composition of the cooling water with respect to dirt or scaling constituents is influenced by effluent, particularly for river water flowing through industrial areas. Even climatic conditions can change water composition.

Finally, velocity is a factor in that suspended particles are less likely to settle out at higher velocities. In the case of scaling, increasing the velocity results in reducing the tube surface temperature in a heat exchanger giving a reduced rate of precipitation of insoluble salts.

A1.3 The magnitude of the problem

It is common practice in textbooks, when dealing with heat exchanger theory, to mention fouling as a problem in the design of heat exchangers, quote specimen fouling factors (an additional fixed thermal resistance) and then omit the fouling resistance term from subsequent analyses for convenience.

Consequently one could be left with the impression that this additional thermal resistance is not of primary importance.

Although an analysis of a simple double-pipe heat exchanger with fouling is included later in the report, (Section D), it would be useful at this stage to look at a simple numerical example.

Consider water flowing at a constant rate through a tube of circular section, and suppose scale accumulates on the inside surface of the tube. Conditions on the outside surface are neglected although this is only omitting a constant surface coefficient of heat transfer if the heat transfer medium on the outside is assumed to be non-scaling. The importance of the scale layer will be indicated by its thermal resistance compared with the combined effect of the tube wall resistance, and the resistance associated with the surface coefficient of heat transfer at the scale - water interface.

The appropriate thermal resistances are calculated according to the following equations:

Tube wall

Treating the tube as a thin cylinder

$$R_w = \frac{t_w}{k_w} \qquad \text{(A1.1)}$$

Scale

This is treated as a thick cylinder, for which

$$R_{sc} = \frac{R}{k_s} \ln\left[\frac{1}{1 - x/R}\right] \qquad \text{(A1.2)}$$

Scale - Water interface

$$R_s = \frac{1}{(1 - x/R)h}$$

and using the Dittus - Boelter equation for the surface coefficient of heat transfer,

$$h = \frac{0.023\ k}{(2R - 2x)}\left[\frac{\rho V(2R - 2x)}{\mu}\right]^{0.8} (Pr)^{0.4}$$

so that

$$R_s = \frac{R}{0.0115\ k\ Pr^{0.4}}\left[\frac{\mu}{2\rho VR}\right]^{0.8}\left[1 - \frac{x}{R}\right]^{0.8} \qquad \text{(A1.3)}$$

Fig. A1.1 lists typical values for the variable and Fig. A1.2 summarises the resulting thermal resistances for x/R in the range 0 to 0.1.

The scale thermal conductivity is not necessarily that of the pure substance deposited due to the porosity of the scale.

Krupiczka (5) in his analysis of the thermal conductivity of granular materials indicates decreasing thermal conductivity with

increased porosity. A value of 1.25 W/m deg C for calcium carbonate scale is quoted by Hasson (6) and so the convenient value of 1 W/m deg C used in the calculation is considered to be representative.

The comparative resistances are plotted on Fig. A1.3 which shows that with a scale thickness - radius ratio of only 0.015 the scale is offering a resistance to heat flow equal to the combined resistance of the tube wall and of the liquid at the scale - liquid interface. Beyond this point its effect becomes progressively more serious.

The slight change in thermal resistance at the scale surface - water interface is due to the reducing internal diameter of the tube as the scale thickness increases.

DATA

TUBE RADIUS	R	0.025 m
TUBE WALL THICKNESS	t_w	0.0075 m
THERMAL CONDUCTIVITY(TUBE MATERIAL)	k_w	100 W/m deg C
THERMAL CONDUCTIVITY(SCALE)	k_s	1 W/m deg C
THERMAL CONDUCTIVITY (WATER AT 20° C)	k	0.6 W/m deg C
DYNAMIC VISCOSITY (WATER AT 20° C)	μ	10.1×10^{-4} kg/ms
DENSITY (WATER AT 20° C)	ρ	1000 kg/m^3
PRANDTL NUMBER (WATER AT 20° C)	Pr	7.0
WATER VELOCITY	V	1 m/s

FIG.A1.1

COMPARATIVE THERMAL RESISTANCES

$\frac{x}{R}$	R_w $\frac{m^2 \text{ deg C}}{W}$	R_{sc} $\frac{m^2 \text{ deg C}}{W}$	R_s $\frac{m^2 \text{ degC}}{W}$	$R_s + R_w$ $\frac{m^2 \text{ deg C}}{W}$
0		0	0.000291	0.000366
0.01		0.000248	0.000289	0.000364
0.02		0.000495	0.000287	0.000362
0.03		0.000765	0.000284	0.000359
0.04		0.00103	0.000282	0.000357
0.05	0.000075	0.00129	0.000279	0.000354
0.06		0.00155	0.000277	0.000352
0.07		0.00181	0.000275	0.000350
0.08		0.00209	0.000273	0.000348
0.09		0.00237	0.000270	0.000345
0.10		0.00263	0.000268	0.000343

FIG.A1.2

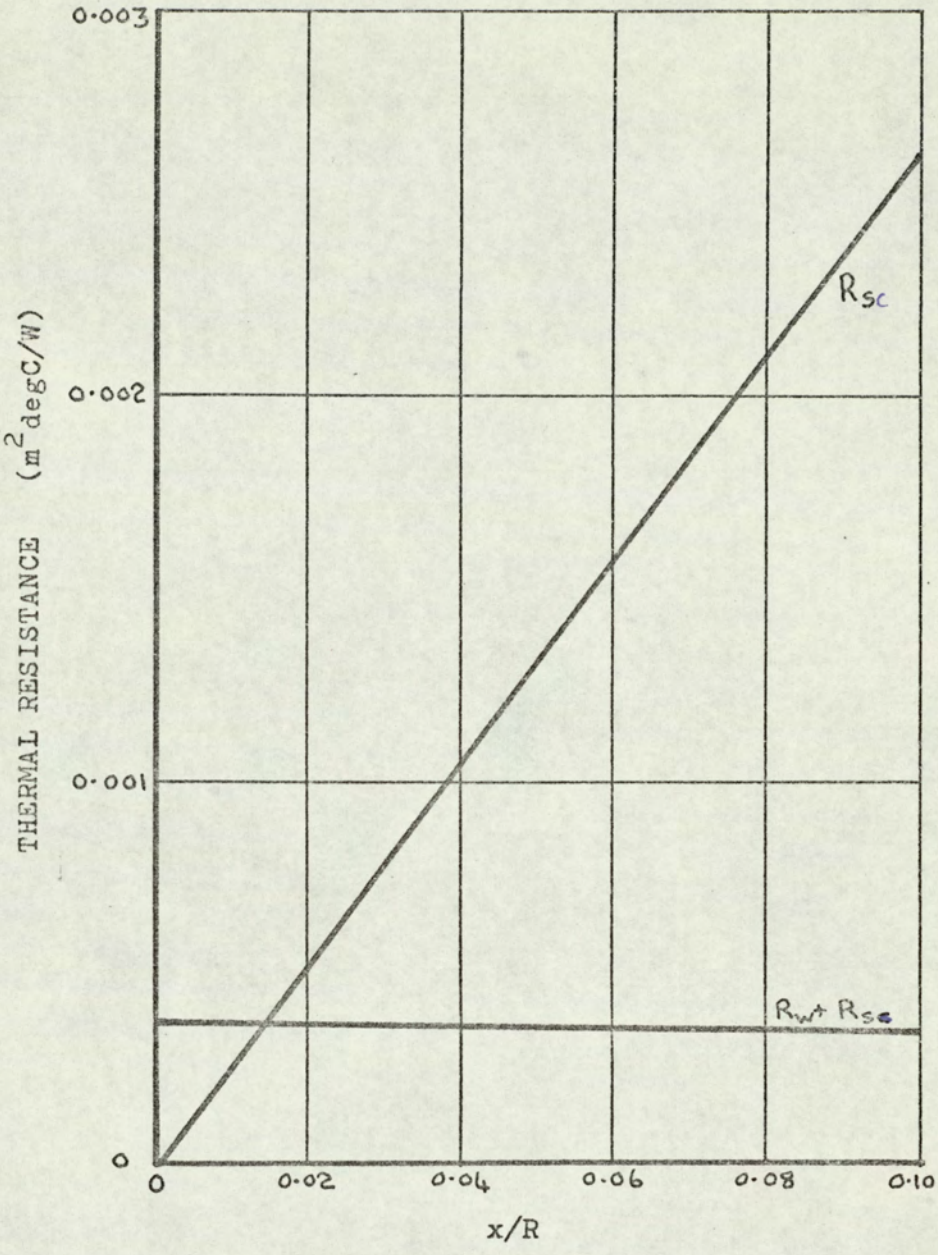

COMPARATIVE THERMAL RESISTANCES

FIG. A1.3

CHAPTER A2

THE INFLUENCE OF FOULING ON THE ECONOMICS, DESIGN, AND MAINTENANCE OF HEAT EXCHANGERS

The numerical example of the last section illustrates how a relatively small degree of fouling can radically change the thermal performance of a heat transfer surface.

Well established information on the design of heat transfer equipment becomes meaningless once a surface is fouled, the prediction of the future performance of the equipment cannot be established and the cost of maintenance together with 'out of service' time can be a serious economic factor.

It has been estimated (1) that in the U.K. alone, the cost of additional hardware to allow for fouling is in the region of £5,000,000 in one year. This figure assumes 30% oversurfacing because of fouling and does not include labour costs for maintenance.

Emerson (7) refers to the frustration caused to designers by this problem. This last comment arose from a symposium on Heat Exchangers (1,7) which the writer attended.

At this symposium it was generally acknowledged that fouling was a universal difficulty but potential investigations into the problem have so far failed on two counts. Firstly a lack of data precludes the possibility of a general quantative review. To obtain such information would necessitate a greater degree of plant instrumentation than is the case at present. Wider co-operation within industry would be essential in order to

accumulate the maximum quantity of information. It has been suggested that the government should coordinate the collecting of data.

Secondly, and possibly of greater importance than the collecting of data, is postulating what sort of questions are likely to lead to fruitful researches. It seems that this has been a real difficulty in at least two potential investigations mentioned at the symposium.

It is usual to allow for in-service fouling by introducing a fouling factor. This is a fixed thermal resistance invariably based on TEMA factors (8).

Alternatively an allowance based on operating experiences with similar equipment may be used. Even then the responsibility for assigning an allowance sometimes lies with the purchaser of heat exchangers, and occasionally with the manufacturer.

It has been suggested that as a result of fouling and other problems, deliberate over design is frequently practised and it is not uncommon to find figures as high as 75% quoted.

There are many shortcomings to the use of a fouling factor and these are documented by Kern and Seaton (2). Since deposition is a continuous process, a time factor is involved and one of the failings of the fouling factor is that it is not time dependent. If the performance of a heat exchanger is monitored it might be possible to extrapolate results on a time basis and predict at what time an allowable maximum thermal resistance is reached. Further comment related to this point is made in the discussion on the published work (Chapter B4).

The application of a fouling factor will overdesign equipment

so that it will tolerate some degree of fouling before its performance falls below a stipulated minimum value. However the absence of a time factor precludes the designer from saying at what point in time this situation will occur.

Again, fouling cannot be considered in isolation when designing heat exchanger equipment. It may be necessary or desirable to take a heat exchanger out of service for other reasons at a particular time. Failure may result from corrosion, or maintenance schedules might be dictated by considering an entire plant rather than isolated units within the plant.

Under these circumstances, too high a fouling allowance at the design stage would mean that a heat exchanger would still be oversized at the time of shut-down and cleaning.

This is clearly wasteful and one would like to be able to make an allowance such that the performance had deteriorated to its minimum value at a time when routine maintenance was due.

The present state of knowledge on the subject is indicated briefly in Fig. A2.1 which gives a historical review of published work. Authors are listed in chronological order of their publications and brief reference is made to the nature of their work. It must be emphasised that Fig. A2.1 highlights either work aimed at providing practical data on fouling phenomena or those papers specifically concerned with relevant theories. The list omits those references which make general comment on the problem.

SUMMARY OF THEORETICAL AND PRACTICAL WORK PUBLISHED

AUTHOR	DATE	THEORY SUGGESTED OR DISCUSSED	PRACTICAL WORK	
			FULL SCALE PLANT	LABORATORY
McCabe & Robinson(9)	1924	YES	Limited number of results	-
Weiland, McCay, and Barnes (10)	1949	NO	Fouling resistance - time graphs	-
Kern and Seaton (2)	1959	YES	-	-
Banchero and Gordon (11)	1960	NO	-	Observed initiation of scale as a function of % supersaturation
Kerst (12)	1960	NO	-	Scale deposition on hair-pin specimen. Mainly corrosion testing.
McAllister, Eastham, Dougharty, and Hollier (13)	1961	NO	Change in overall co-efficient with time for condensers using river water	
Kerst (14)	1962	NO	-	Scale deposited on various materials and using various water treatments. Rate of build-up not measured.
Hasson (15)	1962	YES	-	Change in overall thermal resistance with time for simple steam condenser

continued over ...

FIG.A2.1

SUMMARY OF THEORETICAL AND PRACTICAL WORK PUBLISHED (continued)

AUTHOR	DATE	THEORY SUGGESTED OR DISCUSSED	PRACTICAL WORK	
			FULL SCALE PLANT	LABORATORY
Fisher (16)	1963	NO	-	Some scale measurement. Mainly corrosion testing.
Chandler (17)	1964	YES	-	Concerned with rate of nucleation
Reitzer (18)	1964	YES	-	-
Gutziet (19)	1965	BRIEF REFERENCE	-	Corrosion and fouling comparison for steel, aluminium, and Admiralty brass tubes
Kern (3)	1966	YES	Theory applied to full-scale plant with some improvement claimed	-
Hasson et al (6)	1968	YES	-	Scaling obtained in constant flux heat exchanger

FIG.A 2.1

CHAPTER A3

INTRODUCING A TIME FACTOR

Relating thermal resistance or scale growth to time is at the root of the fouling problem.

Since the thermal resistance is a function of the amount of deposit then it follows that the scale growth rate is important. The experimental work reported later (Section C) and the heat exchanger theory (Section D) are both based on considerations of the rate of scale growth due to the precipitation of insoluble salts. At this stage it is of interest to evaluate the change in thermal resistance with time for a simple configuration.

Suppose we consider a circular tube held at a constant temperature. The scaling liquid flows through the tube depositing scale on its inner surface.

If a growth rate law is stipulated then it is possible to set up equations which will lead to a relationship between the overall thermal resistance and time. Appendix F.1 details the analysis which has been applied to cases allowing for different overall temperature differences, different scale thermal conductivities, and different fluid flow rates, using water as the scaling fluid. A list of symbols is given at the beginning of the analysis.

Results and graphs are presented at the end of this section. The following features emerge from the analysis.

For the particular growth rate law assumed the general form of the thermal resistance characteristic shows a sharp increase

initially, the rate of increase diminishing as time progresses. Fig. A3.1 shows a family of curves for varying differences between the tube wall temperature and the bulk water temperature. For various mass flow rates of water another family of curves is obtained and shown in Fig. A3.2. Again similar curves showing the effect of different scale thermal conductivities appear in Fig. A3.3.

In looking at the effect of changing either the overall temperature difference or the mass flow rate it is best to compare the times taken to achieve a specified thermal resistance; that is, the time taken to reach a predetermined level of fouling. For the purposes of illustration a value of 2.5×10^{-3} m^2 deg C/W or about ten times the initial resistance has been chosen.

Fig. A3.4 demonstrates the effect of changing the overall temperature difference. It is clear that a progressively improved time interval results from reducing this temperature difference as one might expect from the nature of the scale rate law.

However, in most applications, the extreme temperatures would be specified, and invariant. Even if the overall temperature difference could be reduced, it would lead to a larger, and more costly heat exchanger for a given duty.

The effect of altering the mass flow rate is to change the surface coefficient of heat transfer which, in turn, changes the temperature at the scale - liquid interface for a given overall temperature difference. Fig. A3.5 shows that the time taken to reach a particular degree of scaling varies as the 0.8 power of the mass flow rate. The 0.8 clearly originates from the Reynolds' number term in the Dittus-Boelter equation.

This would suggest that an increase in mass flow rate could be beneficial in suppressing this type of scale growth, but it must be remembered that this can only be achieved at the expense of greater power input. This is due not only to the increased flow rate but also to the associated increase in pressure required to drive the liquid through the heat exchanger system. The line shown in Fig. A3.5 cannot be extrapolated towards the origin since it arises from considerations of the turbulent flow regime only. In fact the mass flow rates chosen correspond to a Reynolds' number range of 10 000 to 50 000.

It will be apparent from the literature surveys which appear later (Section B) that fouling is usually characterised by the thermal resistance of the heat exchanger. For this particular example of heat exchange between two isothermal fluids the real measure of performance is the quantity of heat transmitted. A typical heat flow characteristic is shown in Fig. A3.6 in which the quantity of heat transmitted is seen to fall rapidly in the initial scaling period. (The time scale on this graph is ten times that used for the thermal resistance characteristics). This would suggest that whilst anything which reduces fouling is bound to be beneficial to the performance of equipment, the real savings can only be realised by the complete elimination of the problem. That such a goal is very remote is not in dispute but it must be the ultimate object of work on the fouling problem.

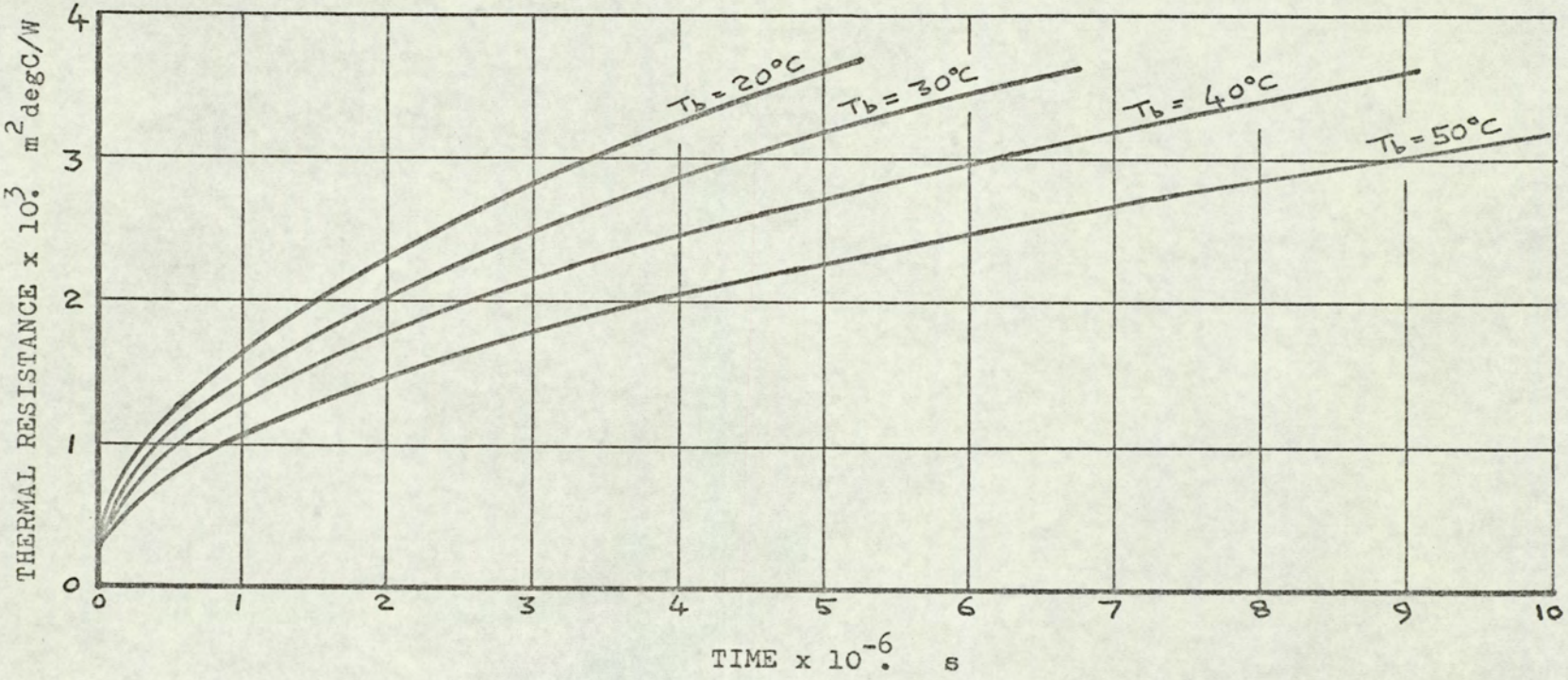

FIG. A 3.1

THERMAL RESISTANCE CHARACTERISTIC - VARYING T_b

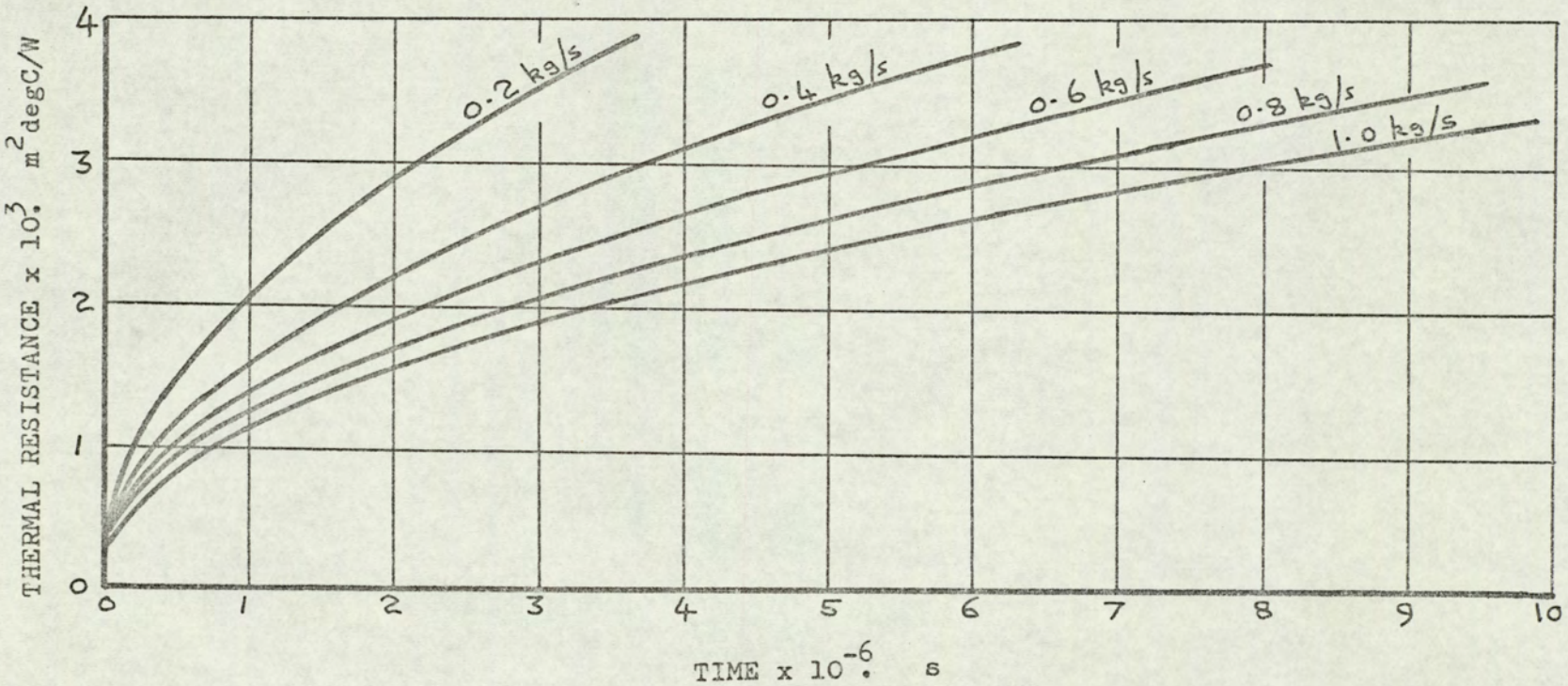

FIG. A 3.2

THERMAL RESISTANCE CHARACTERISTIC - VARYING $\dot{m}$

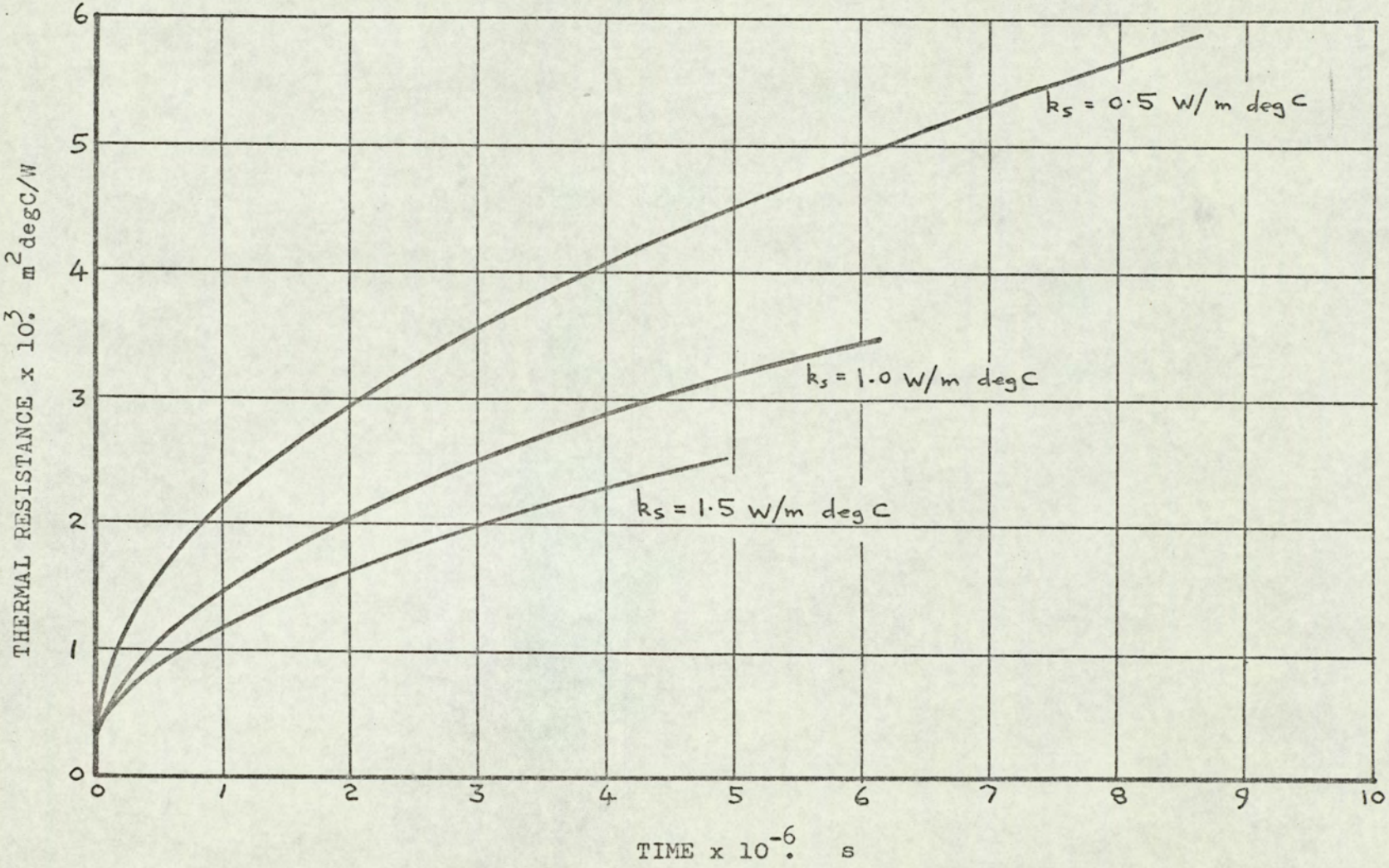

FIG. A 3.3

THERMAL RESISTANCE CHARACTERISTIC - VARYING k_s

TIME TO REACH A SPECIFIED THERMAL RESISTANCE

(a)FOR VARYING TEMPERATURE DIFFERENCE ($T_w - T_b$)

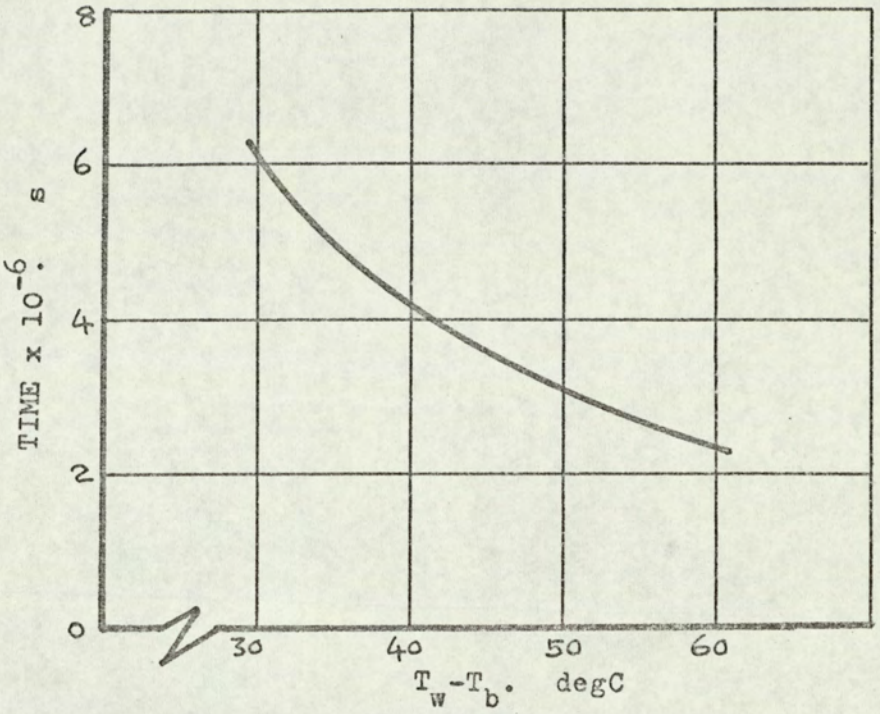

FIG. A 3.4

(b)FOR VARYING MASS FLOW RATE $\dot{m}$

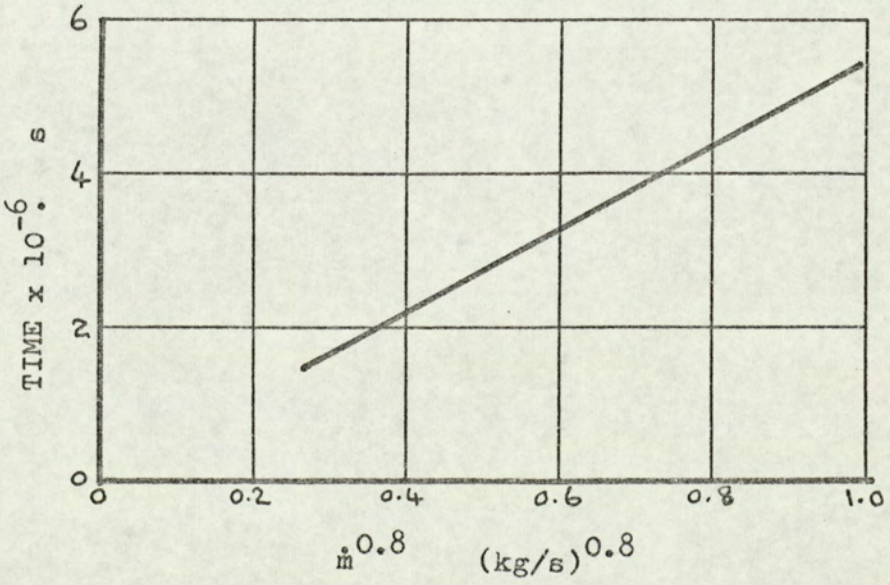

FIG. A 3.5

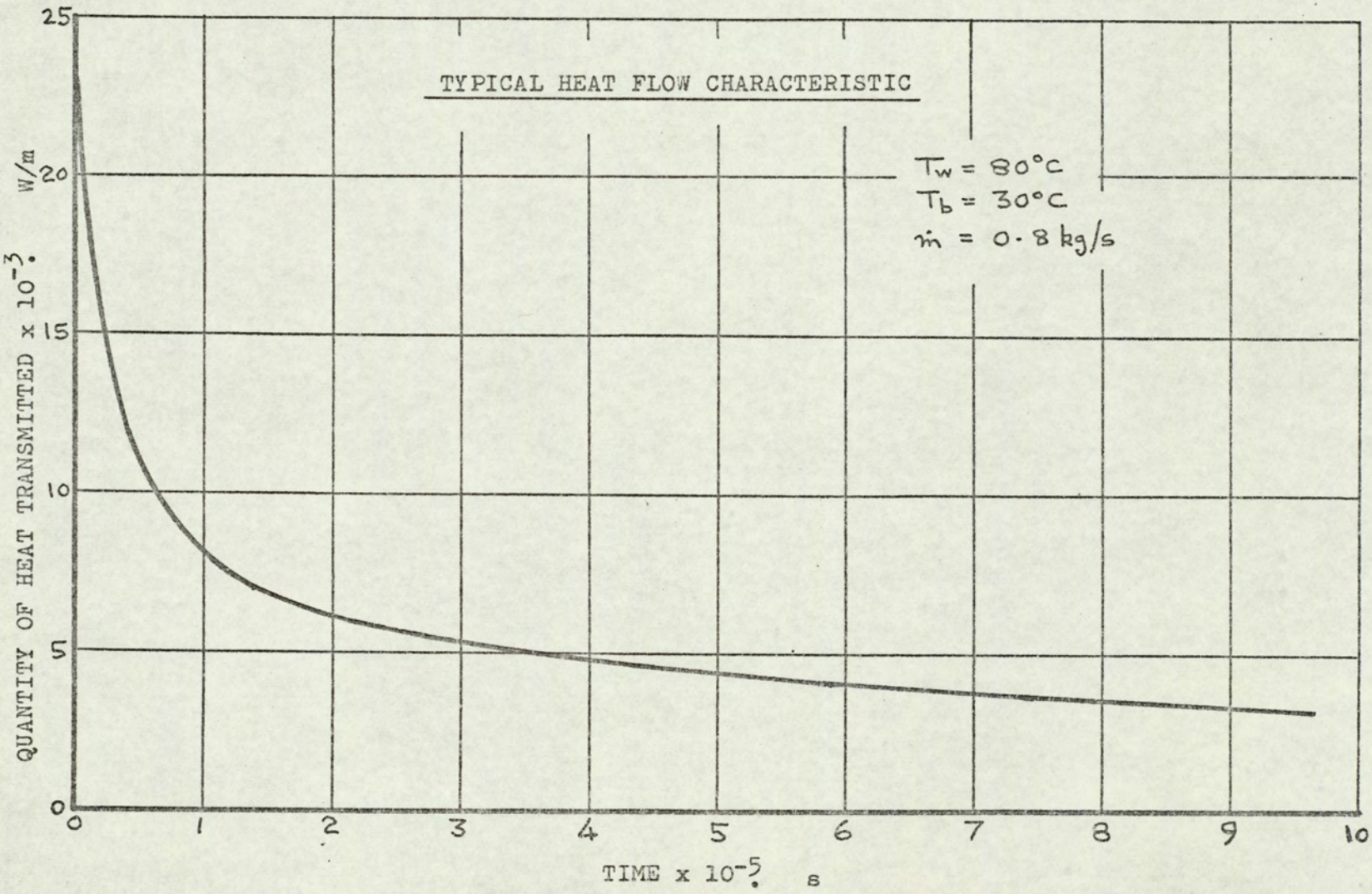
TYPICAL HEAT FLOW CHARACTERISTIC
T_w = 80°C
T_b = 30°C
$\dot{m}$ = 0·8 kg/s
QUANTITY OF HEAT TRANSMITTED x 10^{-3}. W/m
TIME x 10^{-5}. s
0
5
10
15
20
25
0
1
2
3
4
5
6
7
8
9
10

FIG.A 3.6

SECTION B

CONTENTS

LITERATURE SURVEY

SYMBOLS USED IN SECTION B

a	a constant in equation B2.8
A	area
b	slope of solubility curve
B	a constant in equation B2.4
B_1	a constant in equation B3.1
B_2	a constant in equation B2.2
B_n	a constant in equation B2.7
C	a constant in equation B2.3
c_b	concentration of scale material at T_b
c_s	concentration of scale material at T_s
E	energy of activation
f	Fanning friction factor
g	gravitational acceleration
h	surface coefficient of heat transfer
k'	pseudo crystallisation velocity factor
k_s	thermal conductivity of scale
K	reaction rate coefficient
K_o	characteristic reaction constant
K_D	diffusion mass transfer coefficient
K_R	overall mass transfer coefficient
L	tube length
$\dot{m}$	mass flow rate
m_s	mass of scale
n	exponent in equation B2.7
p	exponent in equation B2.14

(symbols continued over...)

SYMBOLS USED IN SECTION B (continued)

P	pressure
q	heat flow rate
Q	quantity of heat
R'	molar gas constant
Re	Reynolds' number
R_o	thermal resistance at time zero
R_T	overall thermal resistance at time t
R_s	thermal resistance of fouling material
t	time
T	absolute temperature
T_b	bulk liquid temperature
T_s	temperature at scale - liquid interface
U	overall heat transfer coefficient
V	liquid velocity
x	scale thickness
w	weight of scale
ρ	liquid density
ρ_s	density of scale material

Subscripts

*	refers to asymptotic condition
1	operating condition 1
2	operating condition 2

CHAPTER B1

INTRODUCTION

In this section a number of papers are reviewed, many of which have already been cited in Fig. A2.1.

Several papers are concerned with a theoretical approach to fouling, and these are conveniently grouped as chapter B2. The remaining papers, of varied content, have been grouped as chapter B3.

In both chapters, papers are presented in date order. They are reported factually so that opinions expressed in the review are solely those of the appropriate author. A general discussion on the papers follows the reviews in chapter B4.

CHAPTER B2

THEORETICAL PAPERS

B2.1 McCabe and Robinson 1924 (9)

This paper claims to offer a new theory on fouling in that the authors say that they had failed to locate any other work dealing qualitatively with the problem of scale build-up. McCabe and Robinson point out that engineers are aware that an increasing deposit of scale occurs with time and that this leads to a progressive reduction in heat transfer.

The paper is specifically concerned with evaporator operation and in developing a theory the following assumptions are made:

(a) Constant fluid velocity

(b) Constant temperature difference which necessitates that

(c) the feed water enters the evaporator at almost boiling temperature

(d) The amount of scale deposited on the heating surface is directly proportional to the total amount of water evaporated from the time of going into service.

The last assumption, which is the speculative one on which the theory depends, is interpreted in a modified form for the purpose of stating it as an equation. For example, since the amount of water evaporated depends on the quantity of heat transmitted, Q, the latter is more conveniently used as a variable. Also, providing the scale is thin, the amount of scale deposited is proportional to the thickness, x. Assumption (d) then

becomes $x = \text{constant} \times Q$

If the original thermal resistance R_o increases to a value R_T in time t, the analysis leads to an equation which has since become well known; that is

$$R^2_T = R^2_o + B_2 t \qquad (B2.2)$$

where B_2 is a constant.

McCabe and Robinson quote a limited amount of data collected from evaporators in service to support their theory.

B2.2 Kern and Seaton 1959 (2)

In this paper the authors refer to a dearth of information on the nature and mechanism of fouling to the extent that the only mathematical work available is that by McCabe and Robinson (9).

Kern and Seaton attempt to distinguish between dirt and scale in the following way. Dirt, they suggest, means non-polar particles with no particular attraction either for each other or for the tube wall. Scale, however, implies true crystal growth involving binding forces between one crystal and another. For the purpose of their analysis, Kern and Seaton treat the distinction as a matter of degree.

They claim that increasing fluid velocity can decrease the rate of deposition and therefore that fluid shear may result in a removal mechanism. Against this there is a continuous deposition on the surface. The authors conclude from this that the net accumulation of dirt on a heat transfer surface results from the combined effect of the deposition and removal processes. The paper offers two approaches to a theoretical treatment.

In the first approach, Kern and Seaton express the net

accumulation as a quotient; that is the ratio of the deposition term to the removal term. For the shear removal term, they use well-known formulae which relate the shear stress to a friction factor. In postulating a removal term they argue as follows. In their experience, practical results demonstrate that the overall thermal resistance of a heat exchanger increases with time such that the thermal resistance asymptotically approaches some constant value. Therefore they propose a driving force equation describing the removal mechanism which has the form:

$$\text{driving force} = C\, e^{-Bt} \qquad \text{(B2.3)}$$

where t is time, and B and C arbitrary constants.

By equating the ratio of the driving force and the shear stress removal term to the rate of increase of thermal resistance, they arrive at a relationship between the thermal resistance of the deposit, R_s, and the time, t. That is:

$$R_s = \frac{4Cg}{2fV^2 B\rho}\,(1 - e^{-Bt}) \qquad \text{(B2.4)}$$

In this equation, f is the friction factor, V the fluid velocity, and ρ the fluid density.

The alternative approach considered by Kern and Seaton is to consider the difference between the deposition and removal terms, in order to arrive at a net rate of accumulation. Their analysis is developed for flow through a circular pipe, and, in assessing the shear stress, due allowance is made for the reduction in diameter due to the increasing scale thickness. The following assumptions are made:

(a) constant flow rate,

(b) constant rate of deposition,

(c) removal is due to shearing action at the surface,

(d) dirt is sheared off at random planes of weakness,

(e) these planes of weakness may occur at any depth,

(f) based on (c), (d) and (e), the rate of removal is proportional to the product of the shear stress and the thickness of the dirt.

The resulting differential equation yields a relationship between dirt thickness x and time t which shows, for arbitrary constants in the equation, an asymptotic build-up as in Fig. B2.1.

However, the main purpose of the paper is to relate scale thickness to pressure drop; particularly at the asymptotic condition. Since this limiting case depends on the allowable pressure drop the object is to determine to what extent a changed pressure drop can reduce the asymptotic thickness to an acceptable level. The thermal resistance is assumed to be proportional to this thickness. The equation developed is:

$$\frac{(x^*)_2}{(x^*)_1} = \left(\frac{L_2}{L_1}\right)^{0.8} \left(\frac{\Delta P_1^*}{\Delta P_2^*}\right)^{0.8} \left(\frac{\dot{m}_2}{\dot{m}_1}\right)^{0.6} \qquad \text{(B2.5)}$$

This relates the asymptotic dirt thickness x^* to the associated pressure drop ΔP^*, the tube length L and mass flow $\dot{m}$ for two operating conditions for a fluid whose fouling properties remain unchanged.

Kern and Seaton point out that a favourable inverse relationship exists between the asymptotic dirt thickness and the pressure drop required to suppress it.

Although this work concerns itself with tube side fouling, the authors suggest that shell side fouling may be treated in a similar way. This is because shell side coefficients are usually obtained from equations originating from dimensional

analysis on the tube side.

Kern and Seaton warn that increasing fluid velocities for the purpose of dirt suppression carries with it the possibility of increasing erosion of parts of the equipment. If this is so care must be taken not to increase fluid velocities (with a resultant increase in cost) to such an extent that the equipment corrodes out of service before an acceptable build-up time is reached.

The authors conclude by suggesting that the practice of designing on a fixed pressure drop might be abandoned to allow for increasing tube pressure drop so that a tolerable dirt thickness could be maintained.

B2.3 Hasson 1962 (15)

The purpose of this paper is to review the work of McCabe and Robinson, and Kern and Seaton, and particularly to propose a more fundamental approach based on recognised principles of mass transfer.

The work is concerned with experimental results obtained from a simple double-pipe heat exchanger in which scale was deposited from mains water on the tube side. Steam on the shell side was used as the heating medium.

Four tests were conducted in which the average scale thicknesses were determined from the weights of scale deposited at the end of a run and the density of a scale sample.

For each test, the change in overall thermal resistance with time was obtained and the results are shown on Fig. B2.2. The thermal resistance was obtained from the inlet and outlet water temperatures, water flow rate and steam temperature.

Hasson analyses these results in the light of various empirical methods for relating the change in overall thermal resistance with time.

The analysis of McCabe and Robinson (9) is quoted but being concerned with heat exchange between a condensing fluid and an isothermal scaling liquid, it is not directly applicable to these tests. However, Hasson modifies the analysis for heat exchange between a condensing fluid and a non-isothermal scaling liquid. That is to say, a liquid flowing at a constant rate suffers a decrease in bulk temperature, and also the scale surface temperature diminishes as the scale builds up. This reduction in temperature would reduce the rate of deposition and the consequent rate of increase of thermal resistance.

The original analysis of McCabe and Robinson gave:

$$\frac{dR_T}{dt} = \text{constant} \times \frac{1}{R_T} \qquad \text{(B2.6)}$$

for an overall thermal resistance R_T at time t.

For the non-isothermal liquid case, Hasson suggests:

$$\frac{dR_T}{dt} = \text{constant} \times \frac{1}{R^p_T}$$

where p is a constant. The resulting equation is given as:

$$R_T^n = R_o^n + B_n t \qquad \text{(B2.7)}$$

where B_n and n are constants.

The author's test results suggest that for the three tests at the lowest velocities, a reasonable correlation is obtained with n = 3·5. However, the results of test four deviate from this law and Hasson concludes that the practical value of the analysis for high liquid velocities is doubtful.

Dealing next with the analysis of Kern and Seaton (2), Hasson restates their relationship between the scale thermal resistance, R_s and time, t, in the form

$$\frac{dR_s}{dt} = a - B R_s \qquad (B2.8)$$

where a is constant.

The author assumes that the scale thickness is small compared with the inside diameter of the tube, so that the increase in velocity, at a constant mass flow rate, due to the reduction in diameter is small. This means that B can be assumed constant and integration of equation B2.8 yields

$$R_s = R^*_s \ (1 - e^{-Bt}) \qquad (B2.9)$$

where R^*_s is the asymptotic thermal resistance of the scale.

An alternative form of equation (B2.9) is obtained by differentiation, giving

$$\ln \frac{dR_s}{dt} = \ln R^*_s B - Bt \qquad (B2.10)$$

The test results plotted in the form $\ln \frac{dR_s}{dt}$ against t show the predicted linear relationship after an initial deviation. Hasson suggests that this deviation seems to correspond to a very marked reduction in scale surface temperature in the initial stages. In fact this temperature never achieves a constant value which is implied in the work of Kern and Seaton when specifying a constant rate of deposition.

Hasson's own analysis concerns the principles of mass transfer, and is as follows:

He suggests that the scale growth rate is determined by the combined effects of diffusion and crystal formation providing the velocity is sufficiently low so that crystals are not sheared from the surface. This means that the growth rate $\frac{dm_s}{dt}$ is given by

$$\frac{dm_S}{dt} = K_R (C_b - C_s) \qquad (B2.11)$$

where C_b is the concentration of the scaling material in the bulk of the fluid, C_S is the equilibrium concentration corresponding to the scale surface temperature and K_R is the overall mass transfer coefficient for the deposition of the scaling material.

The diffusion effect is distinguished from the so called 'surface reaction' by introducing the relationship

$$\frac{1}{K_R} = \frac{1}{K_D} + \frac{1}{K} \qquad (B2.12)$$

in which K_D is the mass transfer coefficient for the diffusion of the scaling material through the boundary layer and its value can be established from the well-known empirical rule applying to turbulent flow through pipes.

K is the reaction rate coefficient which is a function of the absolute temperature of the scale surface, T, according to the Arrhenius equation

$$\ln K = \ln K_o - \frac{E}{R'T} \qquad (B2.13)$$

Hasson describes the following procedure for checking the validity of his approach.

Equation (B2.11) is used to calculate the overall mass transfer coefficient, K_R, since the concentrations C_b and C_s can be found, and the growth rate $\frac{dm_S}{dt}$ as a function of time is obtainable from the overall thermal resistance characteristics. In order to relate the growth rate to thermal resistance an average thermal conductivity is found from the final scale thickness and the corresponding thermal resistance.

Again, from known water and steam temperatures and calculated thermal resistances it is possible to estimate an average scale surface temperature T as a function of time.

Combining the results of these calculations gives the variation of K_R with T.

The diffusion mass transfer coefficient K_D can be determined as a function of the scale surface temperature T by using the accepted empirical equation applying to turbulent flow through pipes.

Finally, equation B2.12 is used to give the 'rate' coefficient K as a function of T and these results are compared with the Arrhenius equation B2.13.

For the low velocity tests Hasson shows reasonable agreement. However, the higher velocity test did not conform and Hasson suggests that this is due to crystals being sheared from the surface at the higher velocities.

B2.4 Reitzer 1964 (18)

This paper is concerned with relating equations governing the rate of crystallization from a solution having an inverse solubility curve with equations governing heat transfer. In this way a relationship is developed between the overall coefficient of heat transfer with time.

If a linear relationship between solubility and temperature is assumed and the rate of increase of mass varies as the p^{th} power of the supersaturation, then Reitzer shows that

$$\frac{dx}{dt} = \frac{k' b^p}{\rho_s} (T_s - T_b)^p \qquad \text{(B2.14)}$$

where x is the scale thickness at time t, k' is the pseudo-crystallisation velocity factor (assumed constant), b is the slope of the solubility curve, ρ_s is the scale density, T_s is the scale surface temperature, T_b is the liquid temperature. Reitzer

states that, for surface reaction controlling, p is the order of that reaction, and for mass transfer controlling p = 1. Between these limits the value of p is empirical.

The author combines equation (B2.14) with the conventional heat transfer equations pertaining to radial heat flow through a 'composite' tube arriving at

$$\frac{dx}{dt} = \frac{k' b^p}{\rho_s} \left[\frac{k_s \Delta T/h}{R_o k_s + x} \right]^p \qquad \text{(B2.15)}$$

where k_s is the thermal conductivity of the scale, h is the surface coefficient of heat transfer, R_o is the initial overall thermal resistance before scaling and ΔT is the overall temperature drop from the heating to the cooling medium.

An alternative presentation in terms of the rate of heat flow q through area A is given as

$$\frac{dx}{dt} = \frac{k' b^p}{\rho_s} \left[\frac{q}{Ah} \right]^p \qquad \text{(B2.16)}$$

Integration of equations (B2.15) or (B2.16) is obtained by restricting either ΔT or $\frac{q}{A}$ constant.

1. Constant overall temperature drop

This gives the case of scaling between two isothermal fluids and, if the restriction p = 1 is imposed, equation (B2.15) reduces to

$$R_T^2 = R_o^2 + B_2 t$$

which is the form proposed by McCabe and Robinson

2. Constant heat flux

For this case, equation (B2.16) becomes

$$R_T = R_o + \frac{k'}{\rho_s k_s} \left(\frac{b}{h}\right)^p \left(\frac{q}{A}\right)^p t \qquad \text{(B2.17)}$$

or, in terms of the overall temperature drop,

$$\Delta T = \Delta T_o + \frac{k'}{\rho_s k_s} \left(\frac{b}{h}\right)^p \left(\frac{q}{A}\right)^{p+1} t \qquad \text{(B2.18)}$$

Reitzer concludes that in either case, a linear relationship is predicted between thermal resistance, or temperature and time. The influence of changing heat flux is to alter the rates of change.

In the second part of the paper Reitzer refers to scaling from an unsaturated solution. This may occur since it is still possible for supersaturation to occur at the hot surface of the tube. Analysing this case under conditions of constant heat flux the author finds that the equations are of the same form as (B2.17) and (B2.18) but with modified rates of change.

B2.5 Kern 1966 (3)

Following a preamble on the inadequacy of the fouling factor concept in the design of heat exchanger equipment a mathematical treatment is developed.

Reference is made to an earlier paper by Kern and Seaton (2) in which the net accumulation of deposit is assumed to depend on two factors. The first of these is the 'deposition' factor which is the primary cause of fouling, but opposing this is a 'removal' factor dependent on fluid shear. In the earlier paper, the interaction of these terms was considered both in the form of a quotient and as a difference (summarised in paragraph B2.2).

In this paper, Kern suggests that the better approach is that in which the net accumulation is expressed as the difference between the deposition and the removal terms. The earlier analysis (for constant weight flow) is presented again in a briefer form and it is modified slightly by assuming that

$$R_T = \frac{x}{k_s}$$

where R_T is the thermal resistance of the deposit, and x the

thickness of the deposit at time t, and κ_s is the thermal conductivity of the deposit.

The result is, that equation (B2.5) now becomes

$$\frac{R^*_{T2}}{R^*_{T1}} = \left(\frac{L_2}{L_1}\right)^{0.8} \left(\frac{\Delta P_1}{\Delta P_2}\right)^{0.8} \left(\frac{\dot{m}_2}{\dot{m}_1}\right)^{0.6} \qquad \text{(B2.19)}$$

which relates the thermal resistance R_T to the length of the heat transfer path L, the pressure drop ΔP, and mass flow $\dot{m}$.

Kern explains that the purpose of developing this equation was not for use in design, but to show the dependence of the fouling resistance on pressure drop. That is to say, an increase in the allowable pressure drop should result in an almost proportional decrease in the asymptotic fouling resistance. Although the pumping costs would increase as a result of the greater pressure drop Kern suggests that this may be more than offset by the saving in capital equipment.

A further development in the paper is to relate the thermal resistance of the deposit R_s at time t to the asymptotic thermal resistance R_s^*. If the dirt thickness is considered to be small compared with the tube diameter the analysis simplifies to give

$$R_s = R_s^* \left(1 - e^{-Bt}\right) \qquad \text{(B2.20)}$$

where B is a constant. (This equation is arrived at in Hasson's paper, equation (B2.9).)

A trial and error solution of this equation is possible once two resistances (at times other than zero) are known. With the aid of standard curves Kern gives an example in which information obtained from a heat exchanger in service can be used to predict a suitable fouling resistance to apply to the design of a similar heat exchanger where an operating time is stipulated. This means

that two thermal resistances and their corresponding times are obtained from the exchanger in service and, with the aid of equation (B2.20) values of R_T^* and B can be established. It is then possible to find a suitable design thermal resistance corresponding to a selected operation time.

The author also shows how the effect of changing, for example velocity, can be predicted by using equation (B2.19).

Kern claims that these procedures have been effectively applied to improve the continuous operating period of several plants subject to severe fouling; in fact the fouling was more severe than that implied in developing the theory.

Kern emphasises that the removal mechanism does not imply any cleaning action due to fluid shear but is concerned only with the tendency for particles to be carried into the stream rather than being deposited on the heat transfer surface.

The relationship between the thickness of the deposit and time for the case of a variable weight flow at constant pressure drop is developed in the Appendix to the paper.

B2.6 Hasson et al. 1968 (6)

This paper describes an extension of the previous paper (summarised in B2.3) and is concerned with the deposition of calcium carbonate scale from hard water in turbulent non-boiling flow adjacent to a heat transfer surface.

The authors describe a constant flux heat exchanger in which a tube was heated by an electrical element running along its axis. The scaling liquid passed through an annulus around the heated tube.

They argue that under conditions of constant heat flux and constant weight flow rate the scale surface temperature will

remain constant and consequently the rate at which mass is deposited will remain constant with time.

Providing the scale thickness is small compared with the tube radius the authors show that the scale growth rate is proportional to the rate of increase of the radial temperature difference. In other words a linear increase in radial temperature difference with time is expected and indicated by results.

Tests carried out at a variety of average liquid velocities in the range 0.82 to 2.69 ft/s with both the scale surface temperature and the bulk liquid temperature held constant are reported and show a relationship between the weight of scale deposited per unit time and area, w, to the Reynolds' number Re. This relationship is given as

$$w = 0.054\ (Re)^{0.68} \qquad (B2.21)$$

An analysis applied to diffusion controlled scale growth and using the j - factor analogy between heat and mass transfer predicts

$$w = 0.03\ (Re)^{0.716} \qquad (B2.22)$$

showing close similarity with the observed result.

Tests are described in which a constant velocity of 1.62 ft/s was maintained whilst surface temperatures were varied in the range 67.5°C to 82.5°C. These results show a linear increase in rate of scale growth with increase in temperature amounting to some 20%.

In the final set of tests reported, the authors were concerned with the effect of different water compositions and the tests were conducted at constant flow velocity, scale surface temperature and bulk water temperature. For these conditions the paper shows that the rate of scale growth can be predicted

to be proportional to the calcium concentration driving force. The experimental results are shown graphically in comparison with the predicted line. The authors attribute deviations for the case of low concentration to the omission of a nucleation term in the analysis. For the high concentrations they suggest that discrepancies between the practical results and theory occur as a result of the escape of gaseous CO_2 from the reaction surface.

VARIATION OF DIRT THICKNESS WITH TIME (Reference(2))

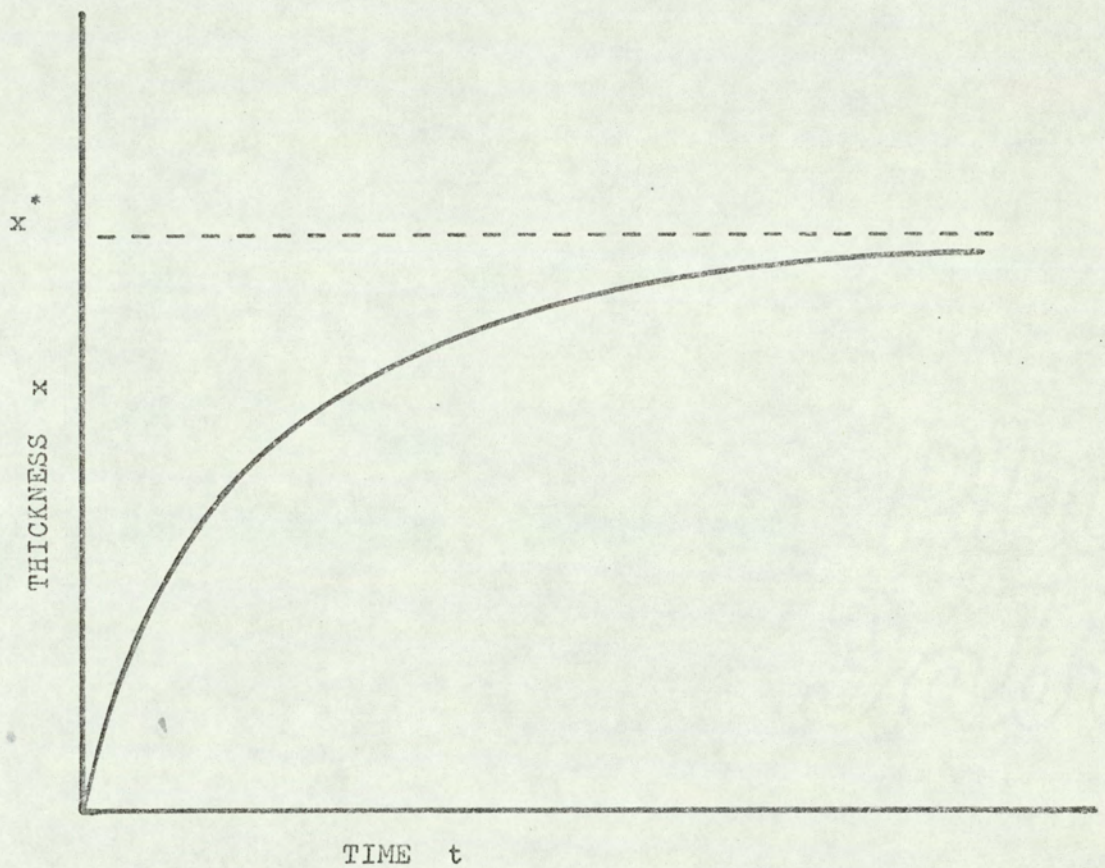

FIG.B2.1

OVERALL THERMAL RESISTANCE AS A FUNCTION OF TIME

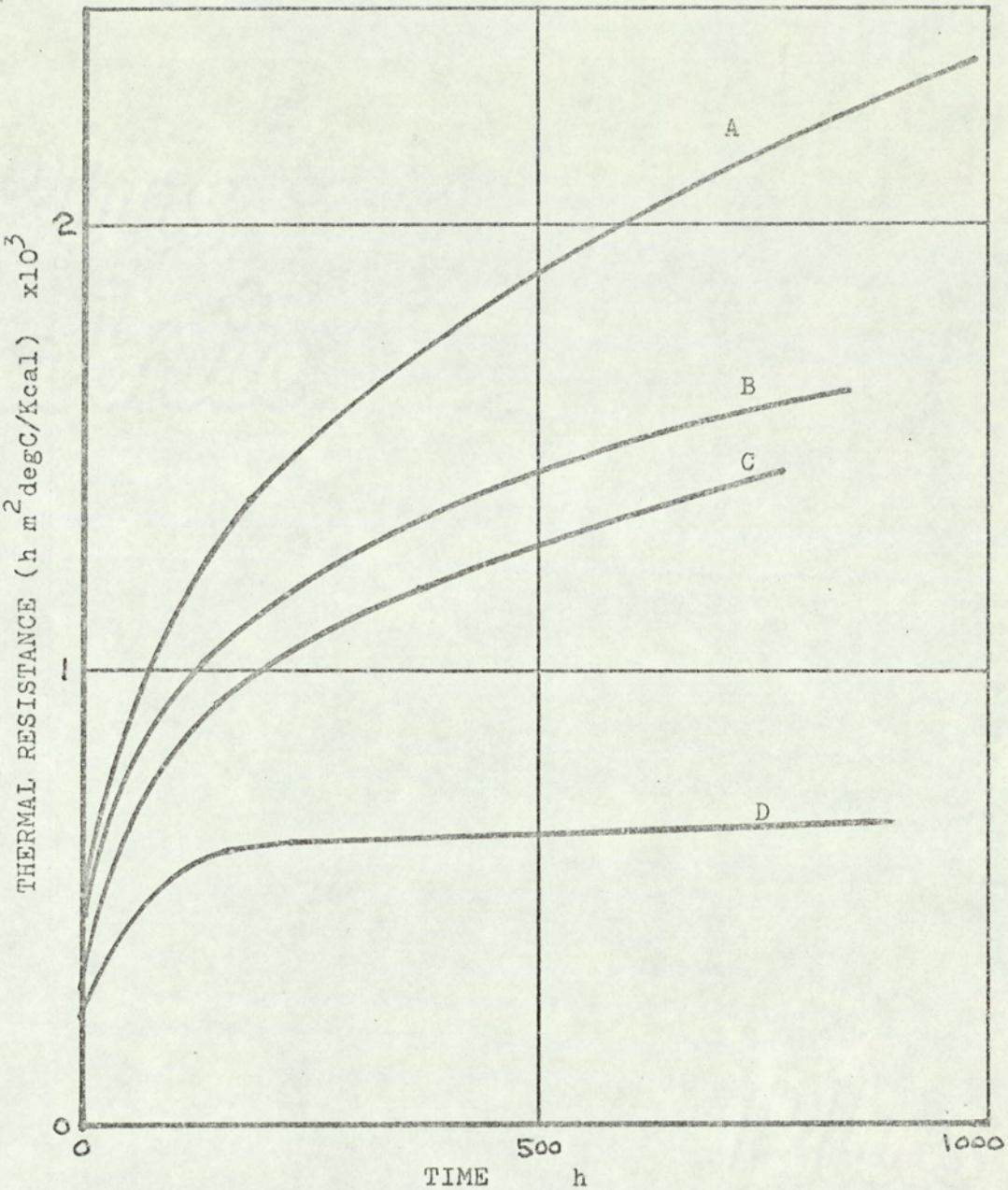

TEST	WATER VELOCITY cm/s
A	21-39
B	36-50
C	33-42
D	94-125

FIG.B2.2

CHAPTER B3

GENERAL PAPERS

B3.1 Weiland, McCay and Barnes 1949 (10)

The paper describes cleaning methods used in various types of heat exchanger and tabulates performance data.

The heat exchangers referred to are Cycle fuel-oil-heated naptha reboilers, depropanizer reflux condensers, absorption oil coolers, and gas oil-catalyst slurry exchangers.

The type of fouling varied in each application. For example, loose coke deposition was experienced on the tube side of the reboilers. In the case of the condensers and oil coolers, water flowing in the tubes left a sediment deposit whilst a loose flaky scale developed on the shell side. The gas slurry exchangers accumulated a viscous gummy sludge on the shell side of the tubes.

Various graphs of fouling resistance against time are presented in the paper and these show quite severe rates of increase of fouling resistance. An increase in fouling resistance from 0.01 to 0.03 ft^2 h deg F/Btu took place in four months for the gas slurry exchangers, and in only one month for the oil coolers.

No comment on the fouling resistance characteristics appear in the paper since the data quoted is given primarily as supporting evidence for the cleaning techniques used.

B3.2 Banchero and Gordon 1960 (11)

A laboratory test is described in which the initiation time

for scale formation was observed. The results are presented as a function of the solution concentration and percentage supersaturation. Either increasing the solution concentration or the degree of supersaturation reduced the time required to start scale formation.

The apparatus was designed to simulate conditions found in evaporators used to produce potable water.

A copper cylinder with a helical groove cut into the outer surface was fitted with a spiral gasket and assembled in a precision bore glass cylinder. The liquid under test flowed along this helical path.

A second cylinder having a similar groove on its surface fitted inside the copper cylinder, and pressurised hot water was fed along this groove in counterflow to the test solution. Thermocouples were located under the solution groove.

Results were obtained for aqueous solutions of lithium carbonate, calcium sulphate, calcium hydroxide, and sodium sulphate, all of which have inverse solubility characteristics.

The effect of liquid velocity was investigated and it was concluded that, in the range 2 to 10 ft/s, the initiation time was independent of velocity.

B3.3 Kerst 1960 (12)

Tests were conducted in the laboratory to investigate the effect of chemical treatments on corrosion and scale formation in the presence of high process side temperatures. In one series of tests 'hairpin' specimens were used. These consisted of ¼ inch bore seamless steel tube bent to the shape of a hairpin and mounted in a standard 1½ inch pipe plug. This allowed the

specimen to be inserted into a cooling stream and hot liquid could be circulated through the steel tube.

For other tests a simple double-pipe heat exchanger was used. This had a ½ inch outside diameter seamless steel tube mounted in a 1 inch standard pipe to form the shell.

High skin temperatures were obtained by circulating hot Ucon through the hairpin specimen or through the heat exchanger. Temperatures in the range 350°F to 390°F were obtained.

Generally, corrosion rates were found and in most tests the weight of scale was measured. The scale was mostly tri-calcium phosphate arising from the polyphosphate water treatment being used.

There is no attempt in the paper to investigate rates of deposition.

B3.4 McAllister, Eastham, Dougharty and Hollier 1961 (13)

Condenser tube failure at a power station on the Neches river, Texas, led to a project concerned with the corrosion and fouling of condenser tubes. So that the water would be identical to that used on full scale condensers, the test apparatus was set up at the power station.

The equipment was designed to allow velocities both greater and less, and also the same as those used in the actual plant. Tubes of various materials were tested and the effect of tube coating was investigated.

Thirteen condensers were arranged in parallel so that river water could be fed through the tube side of each one. The shell side hot water was circulated through the condensers in series

from one to the other so that some flow was concurrent and some flow countercurrent relative to the flow of river water. A copper tube carrying steam was coiled in the annulus of the condenser to maintain a constant temperature in the shell side water throughout the tube length.

In addition to measurements of flow velocity, pressure drop, and the water temperatures, a record was made of the river water pH, hardness and chloride-ion concentration.

Reference is made to the work of McCabe and Robinson (9) and Kern and Seaton (2), (these are reviewed in paragraphs B2.1 and B2.2 respectively), and the paper concludes that a linear growth of resistance with time is representative of the results. That is,

$$R_T = R_o + B_1 t \qquad (B3.1)$$

which relates the overall thermal resistance R_T at time t to the initial thermal resistance R_o.

A comparison of tube materials showed no marked difference between copper-nickel, aluminium-brass, alloy 77, and admiralty brass tubes. An Alclad aluminium tube showed rapid deterioration whilst the stainless steel tubes seemed to result in the lowest rate of increase of thermal resistance.

Coated and uncoated admiralty brass tubes showed similar rates of increase of thermal resistance which suggested that the fouling was a function of the river water condition.

The effect of velocity was examined by running tests at 3.86 ft/s, 7.72 ft/s, and 11.6 ft/s. Considerable scatter of results was experienced and 'best' lines were constructed using the method of least squares. During the initial scaling period the resistance to heat transfer increased at the same rate for

each velocity. Only in the later stages of the test did the tube having the higher velocity of flow suggest a decrease in the scaling rate. It is suggested that this decreased rate is the only indication of the behaviour predicted by Kern's model.

The river water hardness and chloride-ion concentration were recorded and it is suggested that there is some correlation between these values and the rate of deposition.

What appears to be a general scatter of results of thermal resistance against time is shown to be a series of gradients whose values rise and fall. These gradient changes follow the general pattern of rising and falling hardness and chloride concentration values. For this reason Kern's theory is rejected because of its implication of a constant rate of deposition.

Fouling is also characterised by the pressure drop in the heat exchanger and one graph shows the Fanning friction factor increasing linearly with time.

B3.5 Kerst 1962 (14)

This paper was written as an extension of the earlier work (paragraph B3.3) and again deals with corrosion and scale.

In a discussion on calcium carbonate scale it is suggested that by suitable water treatment this type of scale can be controlled. Kerst goes on to say: "Difficulties resulting from carbonate scales in industrial heat exchange equipment now are rare and usually occur under abnormal conditions when control by known methods is prevented."

In a reference to calcium sulphate scaling Kerst comments that whilst control is usual at normal hot side temperatures

(300 to 350°F) at higher temperatures (500°F upwards) serious deposition can occur. This deposition is often uncontrollable and can lead to the plugging of heat exchanger tubes.

Further remarks concern the fact that polyphosphates used for corrosion and scale control can result in a scale or sludge forming when normal amounts of calcium are present in the water.

The important point is made that scale and corrosion are not inseparable and that corrosion products are usually to be found in the composition of heat exchanger scale. In reporting an increased amount of deposit on steel tubes compared with admiralty brass tubes it is suggested that this is mainly due to the additional corrosion products arising on the steel surface.

B3.6 Fisher 1963 (16)

A laboratory test rig is described for investigating corrosion rates using various inhibitors. Treated water was circulated in a closed loop system containing two simple double-pipe heat exchangers. The first heat exchanger used a cartridge heater to heat the tube whilst the second heat exchanger was used as a cooler. Cooling was effected by circulating glycol through the tube. , In both cases the water was fed through the shell side of the heat exchanger.

Following a discussion on corrosion the report deals with scale evaluation. Fisher defines scale, for his purpose, as being all deposits affecting heat transfer in the system.

In a series of tests in which the deposit was weighed it was found that more deposition had occurred on the cool surface than on the hot surface. Scale analyses revealed similar

composition and it is suggested that the scale, having a normal solubility characteristic is more soluble in water at the higher temperatures.

Scale thickness measurement by caliper was attempted but proved difficult because of surface roughness.

Another approach to detecting scaling is by temperature measurement. Fisher argues as follows. The heat transfer rate for the heat exchanger is

$$q = U A \Delta T_m$$

For a given system with a constant heat flow

$$\Delta T_m \propto \frac{1}{U}$$

Now $\frac{1}{U} = \sum$ thermal resistances

These thermal resistances are the inside and outside surface convective resistances, the tube wall resistance, and the scale resistance. For a system in operation only the scale resistance, R_s, changes, and, approximately

$$\frac{1}{U} \propto R_s$$ (Fig. A1.3 confirms this).

Therefore it can be concluded that

$$\Delta T_m \propto R_s$$

and if the thermal resistance of the scale is directly related to the scale thickness x, then

$$\Delta T_m \propto x$$

Temperature tests revealed no significant correlation with time. It is concluded that the rig was inadequately designed for the collection of this data.

Finally it was decided to monitor the pressure drop across the heat exchanger. During a run of six weeks duration the flow control valve was not adjusted and the flow rate dropped to

three-quarters of its original value. Correspondingly, the pressure drop reduced rather than increased as anticipated. Before stopping the test the flow rate was reset to the original value and the pressure drop was also found to return to its original value.

Again it was concluded that the rig was unsuitable for this type of test.

B3.7 Gutziet 1965 (19)

A test programme was devised for investigating the possibility of replacing costly admiralty brass tubing in coolers and condensers by steel or aluminium tubes.

Heat exchangers consisted of tubes of the appropriate material under test. Condensing steam on the shell side was the heating medium and treated water was passed through the tubes.

Graphs of overall thermal resistance against time indicate linear relationships where the rates of increase of thermal resistance depend on the water treatment.

For the results described, the water velocity was continuously adjusted to its initial value. When the velocity was allowed to fall as a result of an increase in tube pressure drop an increased rate of fouling was observed.

Bearing in mind the results on corrosion as well as fouling it is concluded that steel tubes could be justified as replacements for admiralty tubes providing suitable corrosion protection was maintained and water velocities were not allowed to fall below 4 to 5 ft/s.

Aluminium tubes would not be suitable because of their greater tendency towards corrosion and fouling.

B3.8 Gilmour 1965 (20)

Gilmour writes a forceful paper in which he says that fouling is largely a result of bad design. He admits that fouling exists but engineers are criticised for thinking too much in terms of a fouling factor, and not enough in terms of design, particularly in the realm of fluid mechanics.

On the tube side it is pointed out that uneven distribution of the tube side liquid often means that only part of the tube bundle is effective in transmitting heat. The remaining tubes may contain near stagnant liquid and are subject to rapid fouling. The overall performance may not be worse than predicted on a balanced distribution of liquid because those tubes accepting higher flow rates would develop higher surface coefficients than allowed for in the design.

It follows that oversurfacing as the result of incorporating a fouling factor in the design does not necessarily improve the performance of a heat exchanger. If additional tubing causes a poor distribution of the liquid then it is possible that the performance could be worse than if no fouling factor had been allowed for at all.

Shell side design is severely criticised and Gilmour suggests that the use of a fouling factor merely offsets the poor heat transfer coefficients resulting from bad design. Baffle cuts, and the use of the rods and dummy tubes are discussed to show how the correct siting of these components can lead to improved flow paths of the shell-side liquid.

In a reference to tube materials Gilmour compares the life of carbon steel to that of stainless steel in one application. The rapid deterioration of the carbon steel soon offset the

original saving in capital cost.

In one instance where a carbon steel tubed exchanger was available for a plant it was decided to chromium plate the tubes in order to avoid fouling. The cost involved was considerably less than would have been the case for retubing in stainless steel.

At the end of the paper, Gilmour gives an example of a reboiler which was packed with tubes, on the philosophy that this gave a large surface area. When half of the tubes were removed, and the remaining ones finned to regain some surface, there was a substantial reduction in both fouling rate and cleaning time. It seemed that the turbulence induced by the fins and the sharp fin edges prevented the foulant from completely surrounding the tubes.

It is also argued, contrary to some opinion, that it is simpler to clean the shell side of a heat exchanger than clean the numerous long tubes having a comparatively small diameter. Therefore the stream most likely to foul should be placed on the shell side.

CHAPTER B4

DISCUSSION

B4.1 Introduction

In section A of the thesis attention has been drawn to the scope of the problem, in that the word fouling is a term used loosely to describe any phenomenon in which deposition of unwanted material occurs on a heat transfer surface.

Therefore, in a practical application of a heat exchanger, it is necessary to recognise the type of fouling that could occur so that necessary counter measures can be taken at the design stage. The situation is particularly complicated in cases where different types of fouling occur simultaneously.

In the literature survey we see that the emphasis is on scaling, and this is understandable to the extent that scaling due to chemical action is likely to be the most predictable form of fouling.

Both Reitzer (18) and Hasson (6, 15) have concerned themselves with scaling from saturated solutions of salts having inverse solubility characteristics. Whilst Hasson justified the deposition of calcium carbonate as a mass transfer process in his tests, Reitzer developed a theory resulting in a time dependent expression for the overall thermal resistance.

It is clear from the reviews of other workers in the field that much of their interest has been concerned with the relationship between thermal resistance and time.

For example, McCabe and Robinson suggest that, for evaporators,

$$R_T^2 = R_o^2 + B_2 t$$

Reitzer, working from crystallisation theory, develops more generalised results of the form

$$R_T^n = R_o^n + B_n t$$

in which the power n is determined by the deposition process. It was said in B2.4 that Reitzer's equation agrees with McCabe and Robinson for a particular growth rate index $p = 1$ but it should be emphasised that this is coincidental. There is no question of McCabe and Robinson's theory being a particular case of that proposed by Reitzer.

For the case of constant heat flux, Reitzer shows the thermal resistance to increase linearly with time. Therefore, it follows from the fundamental relationship between heat flux thermal resistance, and temperature difference that, providing the bulk liquid temperature is constant, the scale surface temperature will also increase linearly with time. This fact was used as a means of detecting scale build-up by Hasson (6).

Kern (3) has approached the problem from a different point of view and is unique in attempting a theory for dirt deposition. He arrives at a thermal resistance - time relationship which tends to some asymptotic value of thermal resistance. That is:

$$R_T = R_o + R_s^* (1 - e^{-Bt})$$

The theory assumes that deposition occurs at a constant rate but it is arguable to what extent this is true. Certainly for the precipitation of insoluble salts one would only anticipate a constant rate of deposition under conditions of constant heat flux.

Two main questions arise at this point. Firstly, how can a thermal resistance - time relationship help in the design and maintenance of heat exchangers? Secondly, what practical evidence is there to support these relationships?

B4.2 Design and Maintenance

The ideal situation from the design point of view would be to know the exact form of the thermal resistance - time equation and to be able to predict the constants involved. Whilst Reitzer develops his equations from crystallisation theory there is no comment concerning the practical determination of the various constants and coefficients.

The work of Hasson seems to be the only case where a fundamental approach through principles of mass transfer has been developed with experimental support.

At this time it seems that progress would be made if a suitable type of law could be established. For example, suppose there is reason to believe that in a particular application the thermal resistance will increase according to

$$R_T^2 = R_o^2 + B_2 t$$

Then, knowing the initial thermal resistance R_o it only requires one further check on the heat exchanger performance at some time t to establish the constant B and so predict the future performance.

This is a compromise solution but it would give a positive indication of the future deterioration in performance, and would allow a revision of maintenance schedules. It may be that for a small tolerable increase in thermal resistance beyond the limit specified at the design stage, the heat exchanger could have a usefully extended in-service time. This introduces a degree of flexibility which would assist the efficient planning of a maintenance programme.

It follows that if this approach is adopted then, as far as possible, one would look for a generalised law and one

which is straightforward to use.

Undoubtedly a linear law of the form

$$R_T = R_o + B_1 t$$

would be the most desirable. Otherwise, the general power law

$$R_T^n = R_o^n + B_n t$$

offers more scope in fitting the data.

The asymptotic law proposed by Kern is the least attractive from this point of view.

In his paper, Kern (3) cites an example of performance prediction which involves a trial and error solution based on two operating points to determine the constants. This labour would be justified only if a performance prediction could be proved to be much more reliable on this basis than by using the simpler power law.

It is conceded that to determine the index n in the power law from operating data has to be done by trial and error but generally one would expect experience from similar plant to indicate a suitable value.

If the foulant is a precipitation of an insoluble salt then a knowledge of the deposition rate for the salt will suggest a value for n. This will be demonstrated in a later section of the thesis (Section D) in which this type of deposition is considered in relation to a simple double-pipe heat exchanger analysis for both parallel flow and counter flow arrangements.

B4.3 Practical evidence supporting thermal resistance - time relationships

McCabe and Robinson give limited support for their theory

by quoting three sets of data. However, in one of these cases only three operating points are available whilst in a second case, two distinct laws are apparent.

Reitzer mentions one reference to practical work to support his theory.

Kern implies support for his theory from practical data in that he states that observation of the asymptotic nature of the thermal resistance characteristic formed the basis of his shear removal theory.

Hasson, in his earlier paper (15) tests the theories of both McCabe and Robinson, and Kern. In fact the operating conditions of his apparatus contravened the assumption made in both theories and therefore the results are inconclusive. What does emerge is the fact that the results of three tests indicate a law of the form

$$R_T^n = R_o^n + B_n t$$

in which n = 3.5 for his results.

From the reviews of papers covered in chapter B3 there is a limited amount of data on thermal resistance characteristics.

Gutziet (19), and McAllister et al (13) suggest the simple linear relationship

$$R_T = R_o + B_1 t$$

is a reasonable fit to their respective sets of data. Results generally lie within ± 20% of the proposed line. This is important since, within these limits it is possible to fit alternative laws equally well. For example, in one set of results represented graphically by McAllister, the scatter is such that the data is fitted equally well by

$$R_T = R_o + \text{constant} \times t \quad \text{or} \quad R_T^2 = R_o^2 + \text{constant} \times t$$

In this case one would certainly choose the linear law to describe the performance unless there was theoretical justification for using the power 2. The example shows that even if a law is predictable from a theory, the practical performance of the equipment may be sufficiently erratic to allow a simplified version of the thermal resistance law to be applied.

The practical scatter of data presents a further problem. It has been explained that the application of the thermal resistance characteristic is to predict future performance. The difficulty is that the form of the characteristic needs to be established early in the in-service time of the equipment to be of real value. To compute the thermal resistance at two specific times is unsatisfactory because of the variations in performance. Therefore frequent and regular checks are necessary with results presented graphically to indicate the trend.

If a linear law is anticipated then a 'best' line drawn through the results is the most expedient solution. Otherwise, the average thermal resistances at two particular times can be interpolated from the results to enable the equation constants to be found.

This discussion has so far been concerned with thermal resistance - time data which, with a scatter band, show a smooth progression. It is as well to introduce a caution at this point and say that such a smooth progression is not always true.

McAllister documents one test where the overall trend of test results showing a rising thermal resistance with increasing time presents a different picture if looked at over shorter time intervals.

For example, the total time of the test is 120 hours. If

the results are isolated into groups ~~occurring~~ covering the periods 0 to 40 hours, 40 to 80 hours, and 80 to 120 hours, then within each group a unique trend is apparent. (The fluctuation of results may be due in part to the variation in river water composition during the test - see paragraph B3.4). It should be said that in 40 hours, approximately 70 results are recorded, so that the trend is well established in that time.

By looking at the results in this way it is clear that, for a given law, a thermal resistance prediction based on the first 40 hours of service would be different from that based on the first 80 hours, and different again from that based on the first 120 hours.

This being so, not only is it necessary to anticipate the nature of the thermal resistance - time relationship, but there is the added difficulty of deciding how much in-service time should be allowed so that the trend of results in that period can be considered to be reliable.

Some of the papers comment on the effect of using different tube materials but they are mostly concerned with corrosion resistance.

It is clear from the discussion that most of the work has been concerned with the time-dependent thermal resistance characteristic. Perhaps the final comment should be to emphasise the theme of Gilmour's paper (20) which draws attention to the importance of good design in helping to minimise fouling.

SECTION C

EXPERIMENTAL WORK

CONTENTS

(continued over ...)

SECTION C CONTENTS continued

SYMBOLS USED IN SECTION C

A	area
E	energy of activation
h	surface coefficient of heat transfer
K	reaction rate coefficient
K_o	characteristic reaction constant
K_1	rate constant
K_2	constant
K_R	overall rate coefficient
K'	constant in equation C3.8
L	tube length
$\dot{m}$	liquid mass flow rate
m_s	mass of scale
N	exponent in equation C3.5
p	exponent in equation C2.1
P	wetted perimeter
q''	heat flux
r	radius
R	tube outside radius
R'	molar gas constant
s	supersaturation
t	time
T	absolute temperature

(continued over ...)

SYMBOLS USED IN SECTION C continued

T_b	bulk liquid temperature
T_s	scale-liquid surface temperature
x	scale thickness
ρ_s	density of scale material
μ	dynamic viscosity of liquid
Pr	Prandtl number
Re	Reynolds' number
Sc	Schmidt number
Sh	Sherwood number

CHAPTER C1

Introduction and summary

From previous sections it might be said that the problem of fouling is universal and costly, and yet relatively little work has been done since the paper of McCabe and Robinson (9) in 1924. Again, earlier comments (Chapter A1) were made concerning the classification of fouling and this immediately opens up four avenues of investigation based on these subdivisions.

From the literature survey, the most significant parts of which have been summarised in Fig. A2.1, it was clear that rarely has there been a combination of theory supported by experimental work; Hasson et al (6) making their work on calcium carbonate deposition the exception.

Therefore it was necessary to decide broadly what facet of the fouling phenomenon would be investigated. Because of the nature of the general problem requiring a deposition over a considerable period of time it was realised that, in the time available, research would have to be confined to one aspect of the problem and even then the work might be restricted.

It was felt that a useful theory concerning the deposition of salts had been developed by Reitzer (18) and so it was decided to test the validity of this theory using a simple heat exchanger.

Consequently the decision was made to study that aspect of scaling concerned with chemical deposition. Chapter C2 discusses the chemistry involved and deals essentially with salts having inverse temperature solubility characteristics.

According to Brennan (21), the most predominant scaling salts are calcium and magnesium sulphates and carbonates. Generally calcium carbonate is associated with sea water scaling and calcium sulphate with fresh water scaling, although it is not unknown for calcium sulphate to be present in sea water scale.

This is confirmed by Levene (22) who reports its presence in evaporators at the C.E.G.B. station at Dungeness. Brennan (21) also refers to calcium sulphate as the most common and the most troublesome scale constituent. The seriousness of calcium sulphate deposition is emphasised by Kerst (14) who refers to uncontrollable scaling at high temperature which can lead to the plugging of heat exchanger tubes.

Bearing in mind these comments and the fact that certain aspects of calcium carbonate deposition have been documented by Hasson et al (6) it was decided to base the research on calcium sulphate scaling.

The experimental work which was accordingly carried out has resulted in the establishment of a relationship between deposition rate, heat flux, and liquid mass flow rate at low Reynolds' numbers for scaling on the shell side of a simple shell and tube heat exchanger. The results substantiate the fundamental rate law suggested by Reitzer (18) and used in the earlier theory (Chapter A3 and Appendix F1).

A performance analysis of both a parallel flow and a counterflow heat exchanger subject to this type of scaling is discussed in Section D.

For the range of variables tested the results are summarised on a carpet curve Fig. C1.1 which shows the experimental results

in relation to the surface whose equation is

$$\frac{dx}{dt} = \frac{9.64}{10^8}\left[\frac{q''}{\dot{m}^{0.81}}\right]^2$$

This relates the rate of increase of scale thickness $\frac{dx}{dt}$ (mm/h) to the heat flux q" (kW/m^2) at a mass flow rate $\dot{m}$ (kg/s).

The mass flow index of 0.81 generally suggests that the experiments were in the turbulent flow regime.

The heat flux index of 2 characterises the calcium sulphate deposition law, and enables a prediction of the thermal resistance - time relationship one might expect in a heat exchanger subject to this type of scaling.

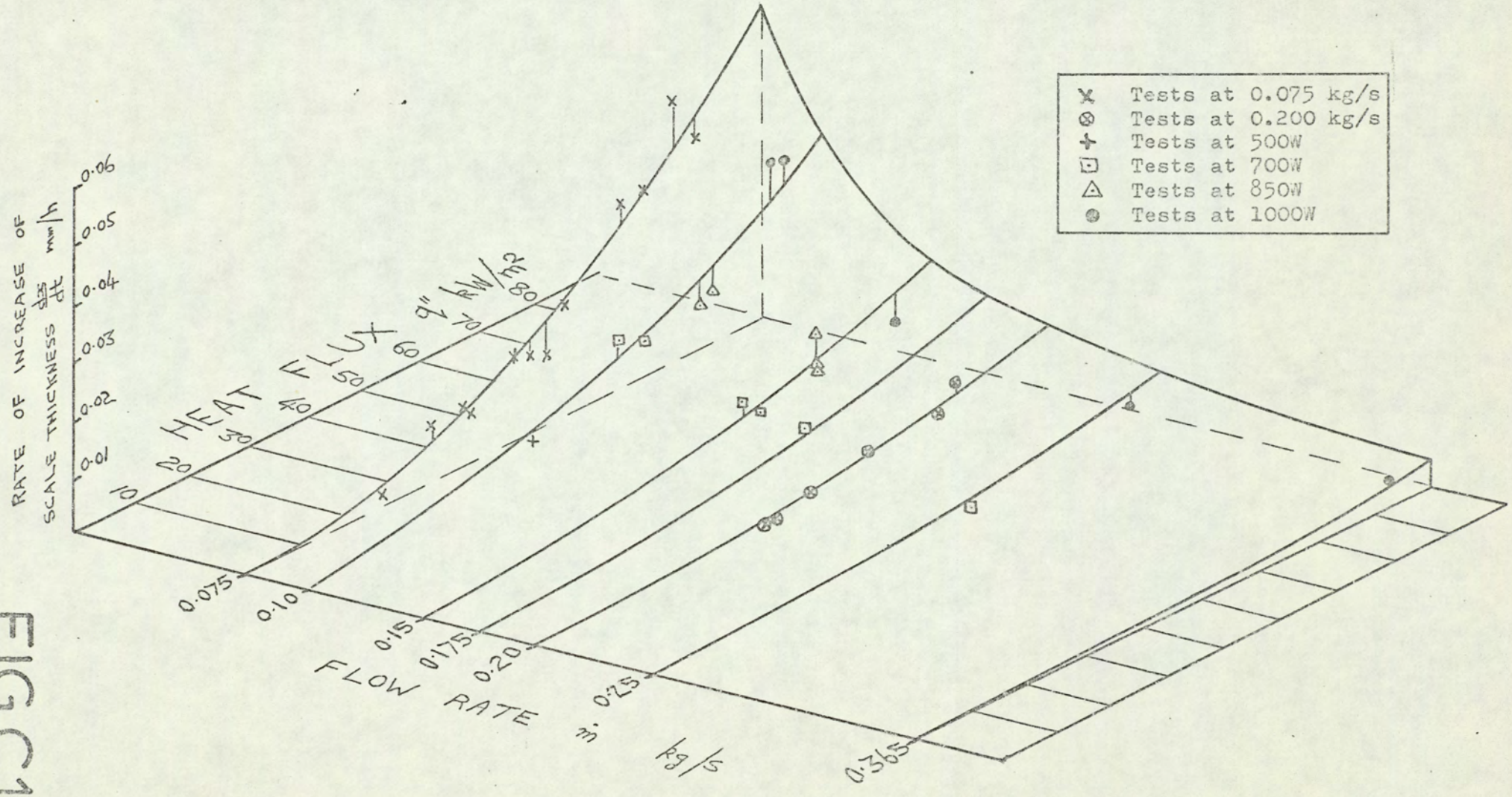

FIG. C1.1

CARPET GRAPH RELATING THE RATE OF INCREASE OF SCALE THICKNESS TO MASS FLOW RATE AND HEAT FLUX

CHAPTER C2

NOTES ON THE CHEMISTRY OF SCALING

C2.1 Preamble

At this stage it is worth discussing in more detail some aspects of the scaling process. This is essentially a discussion on chemical scaling as opposed to dirt deposition although the two are not entirely inseperable.

A deposition rate equation was postulated in the analysis of scaling inside a circular tube (Appendix F1) and further remarks on this equation appear later.

The build-up process can be thought of in two stages. First, nucleation must occur on the surface and then growth of these nucleii will follow. In both cases the driving potential is the supersaturation of the liquid. Thus the principle applied in laboratory scaling is to provide a saturated solution of a substance having an inverse temperature - solubility characteristic, and then to bring the solution into contact with a heated surface. An inverse temperature - solubility characteristic is one in which the saturation concentration of the solute decreases with increasing temperature. Therefore when such a solution encounters a heated surface supersaturation occurs and the necessary driving potential is set up.

The form of the solubility characteristic for calcium sulphate is shown in Fig. C2.1. The decrease in solubility with increasing temperature is apparent beyond a maximum solubility which occurs at about 40°C. Sherwood Taylor (23)

quotes a typical solubility value for calcium sulphate in water at 15°C as 2.6 g/l.

We consider now the nucleation and growth processes in more detail.

C2.2 Nucleation

The nucleation rate is influenced by several factors which could be present in heat exchanger equipment. The primary influence is supersaturation. Chandler (17) investigated the effect of surface supersaturation on the nucleation rate for disodium phosphate and sodium sulphate. He found the deposition rate 'to be very sensitive to the supersaturation at the heat transfer surface.' Fig. C2.2 illustrates this point and shows a critical supersaturation as that below which nucleation is unlikely to occur.

A further factor affecting the rate of nucleation is mechanical impact. For example the action of pump could result in the solution impacting on its internal components and a heat exchanger would contain many potential impact areas due to the tortuous flow path of the liquid. This would be particularly true for example on the shell side of a baffled shell and tube exchanger.

Not unconnected with the impact concept is nucleation resulting from agitation of a solution. In this context it might be thought that surface roughness could influence nucleation in so far as a rough surface could cause local agitation. However, this point has not emerged in Chandler's work.

In comparing polished with corroded surfaces he concludes

that the nucleation rate is fairly insensitive to surface roughness, and suggests that an increased growth rate on a rough surface is more likely to be due to the better adhesion of nucleii as compared with a smooth surface although the rate of forming the nucleii might be the same.

Grove et al (24) mention, in addition to the previous factors the catalytic effects of foreign nucleii or existing crystals, particularly those having the same lattice structure as the crystal being formed.

Soluble impurities may affect nucleation in an unpredictable way and dirt deposition could influence nucleation by causing localised high temperatures on the heat transfer surface.

Finally Levene (22) mentions that aeration can increase nucleation and the subsequent rate of scale growth and this is substantiated by the experimental work of Golightly and McCartney (25).

A model of deposition due to bubble formation is suggested by Freeborn and Lewis (26) and by Golightly and McCartney (25). Fig. C2.3 illustrates the salient features in which evaporation from the liquid near to the triple interface occurs. Dynamic equilibrium is maintained by the subsequent condensation at the cooler inner surface of the bubble remote from the heating surface. There will also be a tendency to an inflow of solution towards the bubble which will maintain a high degree of supersaturation in the region of the triple interface.

C2.3 Growth rate

In their introductory textbook on Chemical Engineering Badger and Banchero (27) comment significantly that the laws for the rate of crystal growth are not completely understood.

Both reaction at the crystal surface and diffusion towards the surface affect the growth rate and generally the growth rate is sensitive to temperature if the surface reaction predominates and sensitive to the degree of agitation if mass transfer is controlling.

The most generalised law (18) can be expressed in the form

$$\frac{dm_S}{dt} = K_R A\, s^p \qquad (C2.1)$$

which relates the rate of increase in mass to the surface area A and the degree of supersaturation s.

It is suggested that this equation is empirical between the limits of either surface reaction or mass transfer controlling.

In the first case p would represent the order of reaction whilst for the second case p would be unity. The rate coefficient K_R would be a function of Reynolds' number as proposed by Bransom (28) for mass transfer controlling. If the surface reaction predominates then K_R would be the temperature dependent rate coefficient referred to by Grove et al (24)

For the mass transfer case, the rate coefficient would be obtained from a correlation of the general form

$$Sh = f(Re, Sc) \qquad (C2.2)$$

At the other extreme the rate coefficient would become the reaction rate coefficient which varies exponentially with the inverse of the absolute temperature so that

$$K_R = K = K_o\, e^{-\frac{E}{R'T}} \qquad (C2.3)$$

This emphasises that the reaction process is very sensitive to temperature.

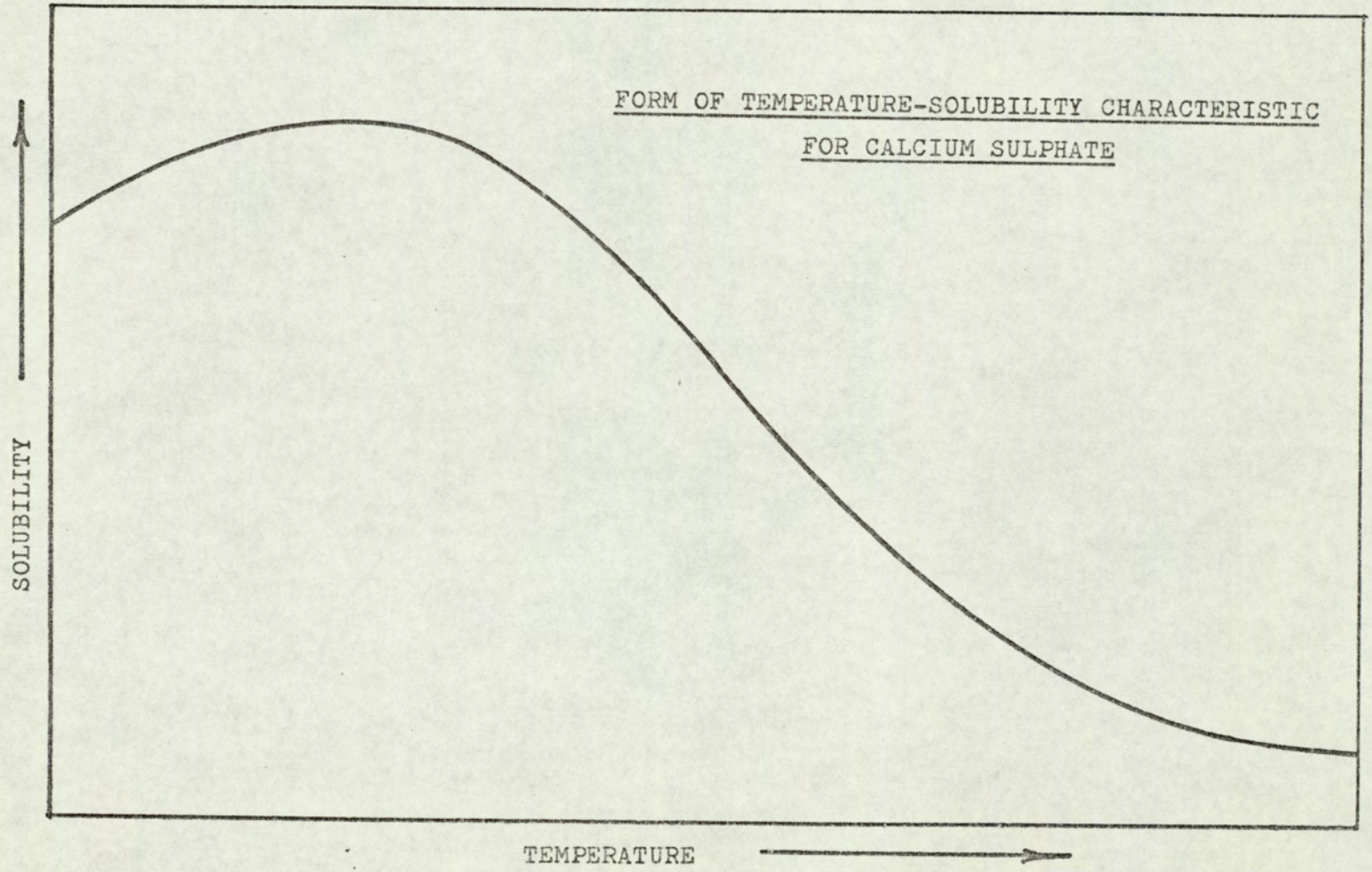
FORM OF TEMPERATURE-SOLUBILITY CHARACTERISTIC
FOR CALCIUM SULPHATE
SOLUBILITY
TEMPERATURE

FIG.C2.1

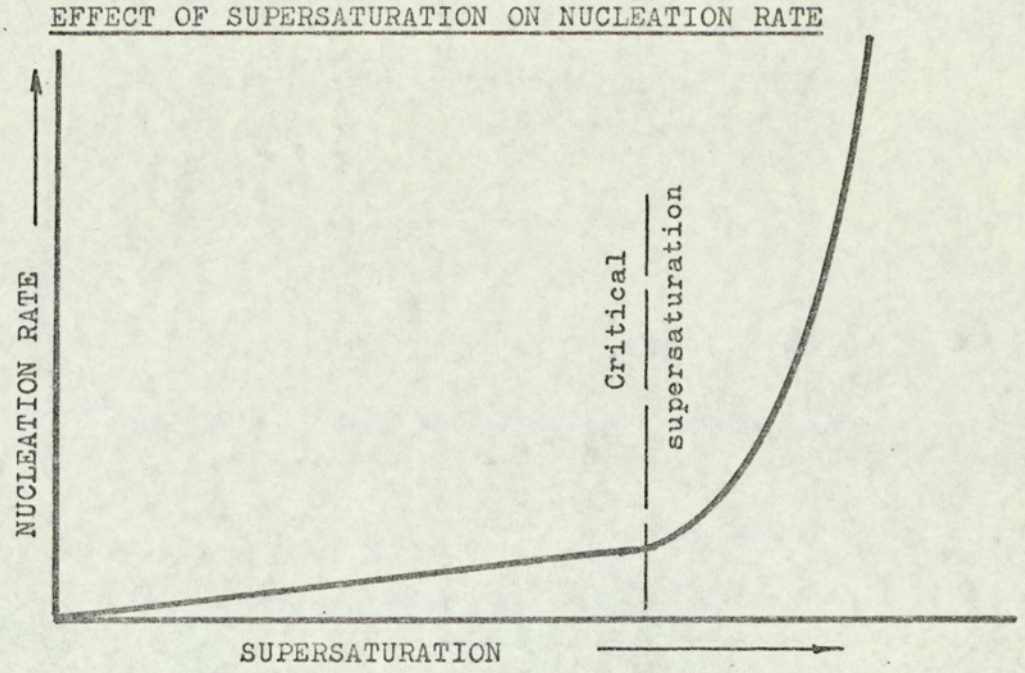

FIG.C2.2

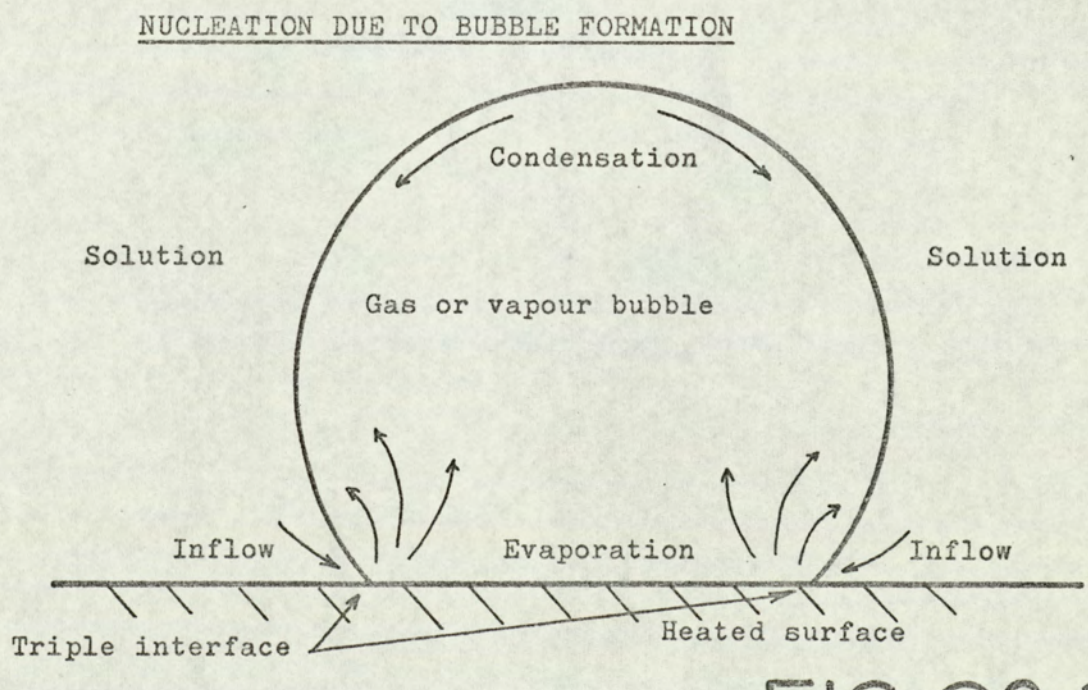

FIG.C2.3

CHAPTER C3

BACKGROUND THEORY

The generalised growth rate law as stated in chapter C2 formula C2.1 is

$$\frac{dm_s}{dt} = K_R A s^p$$

If an inverse temperature - solubility characteristic is assumed to be linear in the temperature range being considered, then the supersaturation s at the heated surface is proportional to the difference in temperature between the heated surface and the bulk liquid and so we have

$$\frac{dm_s}{dt} = K_1 A (T_s - T_b)^p \qquad (C3.1)$$

For a restricted range of flow rate and scale surface temperature, K_1 may be considered constant.

To suit the operating parameters on the rig this can be modified into a more useful form as described below.

Consider first the heat transfer parameters.

In terms of an overall coefficient h at the scale surface - liquid interface the heat flux q" can be expressed as

$$q'' = h(T_s - T_b)$$

$$\text{or} \quad T_s - T_b = \frac{q''}{h} \qquad (C3.2)$$

In turn, h can be generally written in the form $h = f(Re, Pr)$ and if the bulk liquid temperature is constant then the Prandtl number will be constant.

The Reynolds' number can be written conveniently in terms of a mass flow rate $\dot{m}$ and the wetted perimeter P of the flow

section so that

$$Re = \frac{4\dot{m}}{\mu P} \qquad (C3.4)$$

The dynamic viscosity will be constant at constant temperature and for a particular flow geometry the wetted perimeter will be fixed so that the Reynolds' number is proportional to the mass flow rate.

Therefore the heat transfer coefficient can be expressed in the form $h = f(\dot{m})$ and bearing in mind the nature of the empirical formulae for forced convection heat transfer in conduits it is reasonable to suggest

$$h \propto \dot{m}^N \qquad (C3.5)$$

where N is the index associated with the Reynolds' number.

Combining C3.1, C3.2 and C3.5 leads to

$$\frac{dm_s}{dt} = K_2 A \left[\frac{q''}{\dot{m}^N}\right]^p \qquad (C3.6)$$

Now consider the rate of deposition term $\frac{dm_s}{dt}$.

For deposition of scale having a density ρ_s on the outside of a tube of length L and radius R as shown in the diagram

$$\frac{dm_s}{dt} = \rho_s 2\pi r L \frac{dr}{dt}$$

$$= \rho_s A \frac{dr}{dt}$$

and since $r = R + x$

$$\frac{dm_s}{dt} = \rho_s A \frac{dx}{dt} \qquad (C3.7)$$

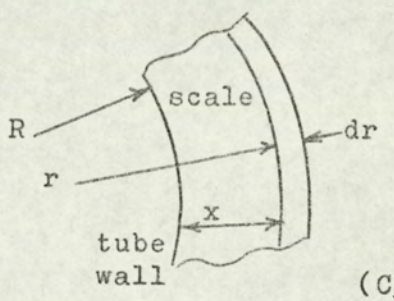

Substituting C3.7 in C3.6 gives $\frac{dx}{dt} = \frac{K_2}{\rho_s}\left[\frac{q''}{\dot{m}^N}\right]^p$

and since ρ_s is constant

$$\frac{dx}{dt} = K^1\left[\frac{q''}{\dot{m}^n}\right]^p \qquad (C3.8)$$

The test programme was designed to verify the form of equation C3.8 and to establish the index p for the deposition of calcium sulphate on a heat transfer surface.

CHAPTER C4

THE TEST RIG

C4.1 General

In the first place a pilot rig was built to check the scaling ability of the system.

The final rig was developed from the pilot rig and due to the pressing time factor it had to retain some features which might otherwise have been changed. This point is made to emphasise that the results obtained whilst indicating the pattern of behaviour are specifically for the arrangement under test.

Fig. C4.1 shows the schemmatic arrangement of the rig and Fig. C4.2 shows a photograph of the actual rig.

Water from a 0.3 m^3 reservoir was circulated through two experimental heat exchangers mounted in series via a flow measurement section. Flow control was obtained by a valve downstream of the heat exchanger together with a by-pass valve situated between the pump discharge and the flow meters. These valves were adjusted so as to give the required flow rate whilst maintaining a small pressure in the system to prevent air leakage into the circulating water.

Calcium sulphate was introduced into the water by placing pieces of Plaster of Paris in the reservoir. These pieces were concentrated near the inlet and discharge points in the reservoir so that they were constantly being washed during testing. A small quantity of calcium hydroxide in the form of commercial lime was added to the water to increase the

availability of calcium ions. The reservoir was open to atmosphere and the lime had the secondary effect of preventing dust entering the water due to the scum formed on the water surface.

The presence of solid calcium sulphate resulted in a saturated solution at the temperature of the reservoir (the solution analysis is given in paragraph C6.7.2). This concentration would not be measurably changed as the result of deposition on the heated surface since the quantity of solid removed was very small compared with that dissolved in the reservoir.

Cooling was effected by circulating town mains water through a small shell and tube heat exchanger.

The experimental heat exchanger section is shown in Fig. C4.3 and the detail drawing appears as Fig. C4.4.

Scaling was induced on a thin wall copper tube 20.6 mm outside diameter heated by a removable electric element. A stainless steel tube was also available for comparative testing.

The square section shell was chosen originally to facilitate observation and measurement. By fitting a flat perspex window on the side of the exchanger it was hoped to measure the tube diameter in situ but this proved impossible in the event due to the nature of the deposition process.

Because of the measurement problem it was apparent that the tube would have to be removable and so the copper tube was brazed to a square brass flange which could be screwed to a mating flange on the shell. Fig. C4.5 shows the tube construction together with the removable heater element. The copper tube was blanked off at the inner end and the flow geometry was

maintained by having a dummy brass rod screwed into the other end flange as can be seen in Fig. C4.4.

Thermostats were attached to the shell of each heat exchanger and they were arranged to cut off the power to the heaters in the event of an abnormal temperature rise of the shell. This was to guard against either pump failure or loss of water through the exchanger due to pipe failure. An additional precaution related to pipe failure was the inclusion of a level switch in the reservoir controlling the pump motor. These controls were essential since tests involved continuous running of the rig.

C4.2 Equipment data

The heaters were rated at 1 kW and they had an effective length of 180 mm. This resulted in a maximum heat flux of about 85 kW/m^2 with a clean tube. The heaters were designed to give a concentrated heat flow over that part of the tube area well within the heat exchanger. Heat flow along the thin walled copper tube would be small and any heat transmitted in this way or directly from the heater leads within the tube would be absorbed by the cold water entering near to the tube end. The dummy rod at the opposite end of the exchanger ensured no heat leakage in that direction. That heat transmission was occurring essentially over the central area of the tube was confirmed by the distribution of scale on the tube.

Heating loads were varied by Torovolt voltage regulators, and power was measured on a Weston Sangamo precision wattmeter.

Rotameters were used for water flow measurement and temperatures were recorded variously by thermometer and chromel-alumel thermocouples.

For continuous recording a Philips 12 point recorder was used in conjunction with a Zeref automatic ice junction.

A Bourdon pressure gauge was situated downstream of the pump to check the system pressure.

The pH value of the water was checked periodically using a Cambridge portable pH meter.

Measurements of the scaled tube diameter were made using a Pye cathetometer; the procedure is described in detail in chapter C5, paragraph C5.4.

SCHEMMATIC ARRANGEMENT OF RIG

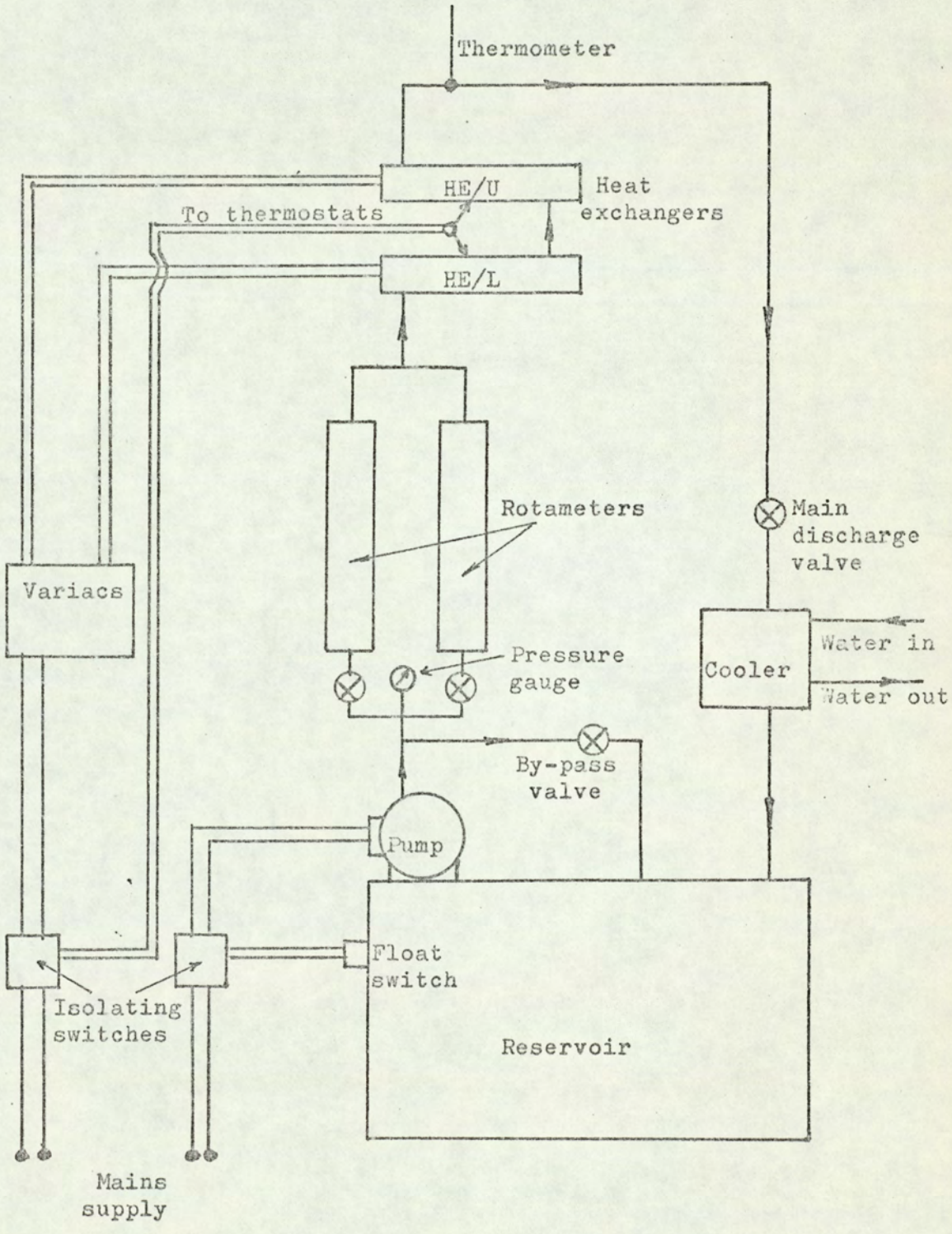

FIG.C4.1

TEST RIG

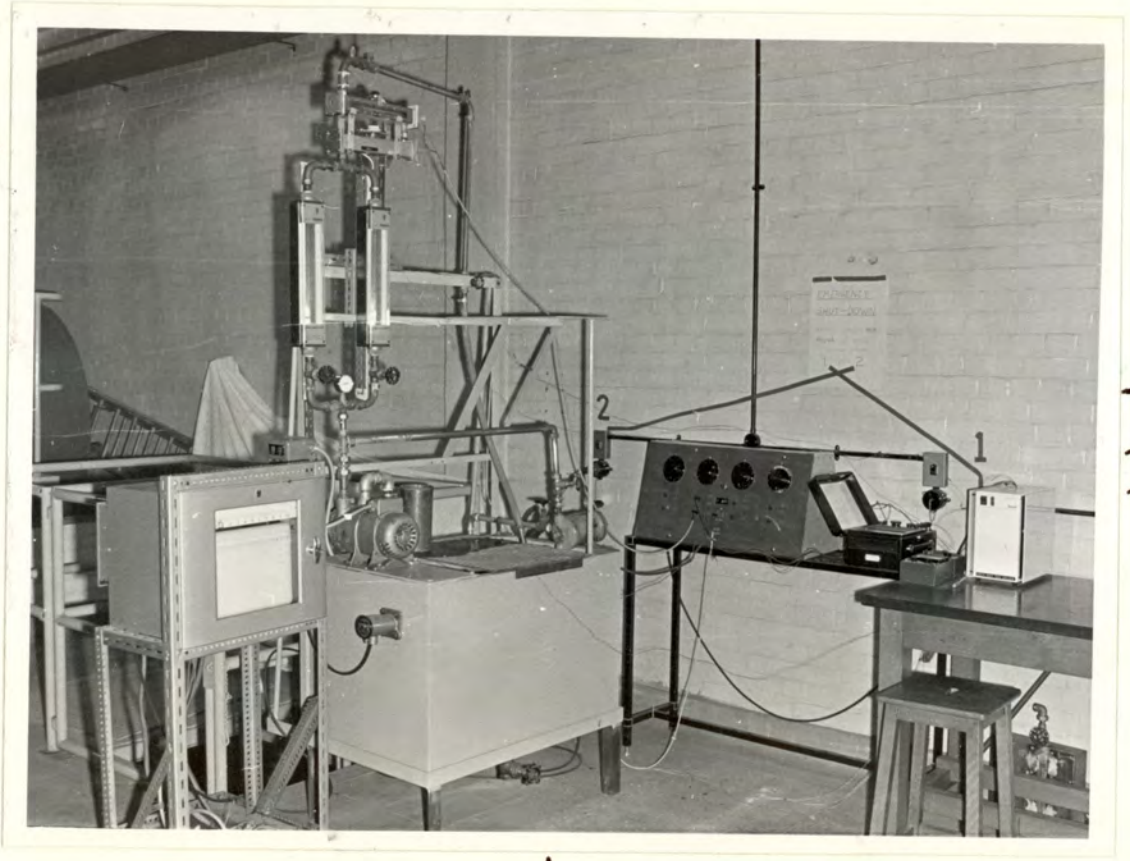

FIG.C4.2

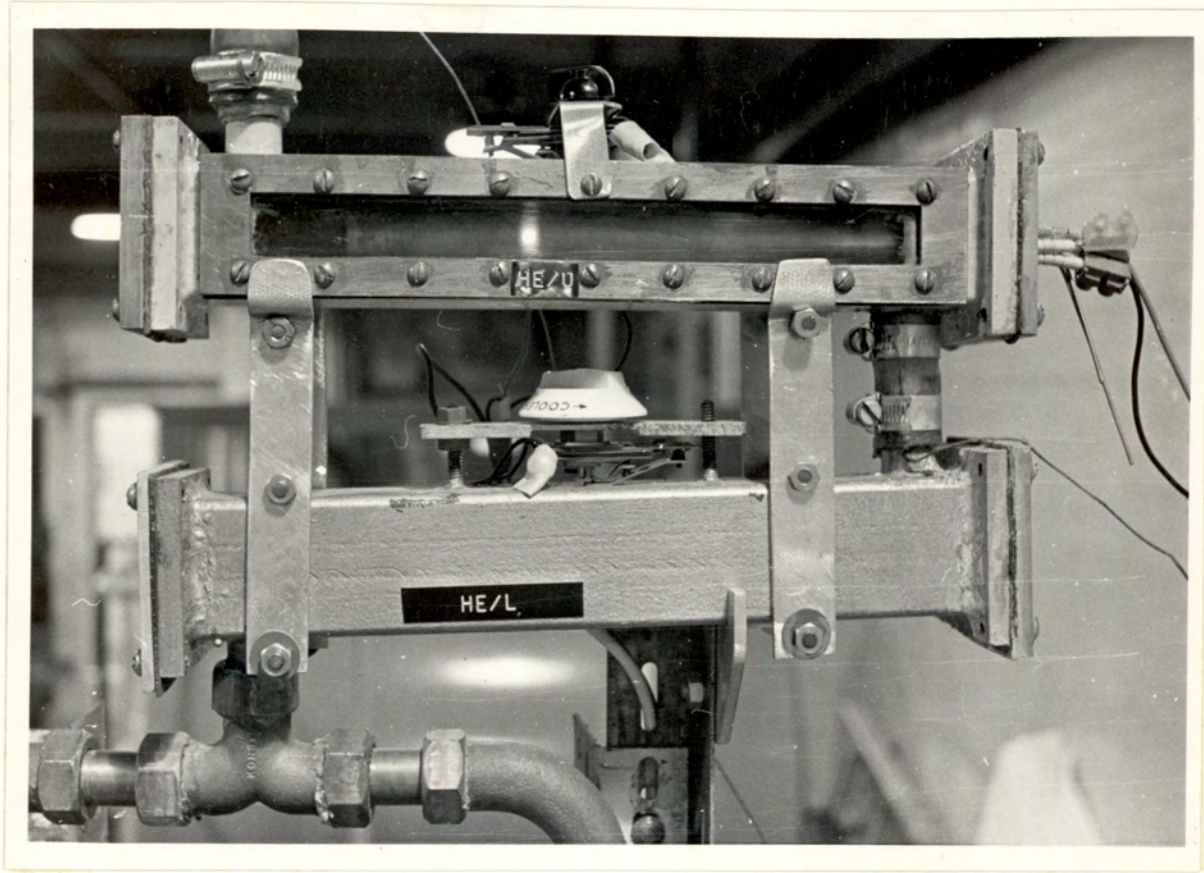

EXPERIMENTAL HEAT EXCHANGERS

FIG.C 4.3

EXPERIMENTAL HEAT EXCHANGER SHOWING PRINCIPAL FEATURES AND DIMENSIONS

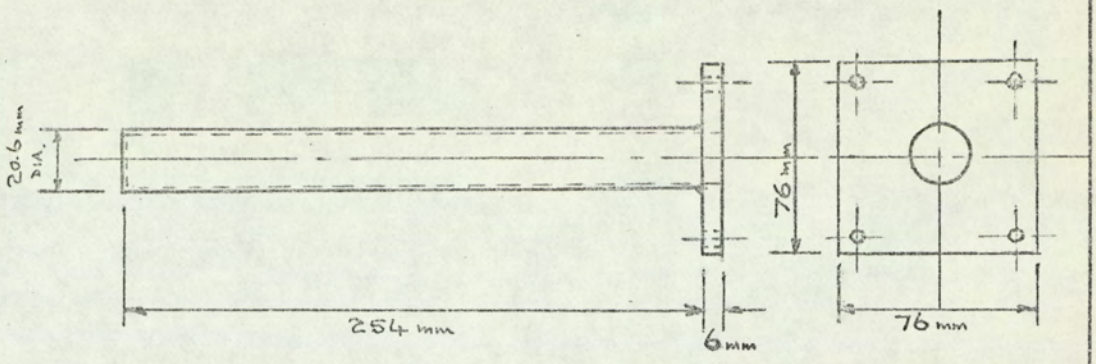

TUBE

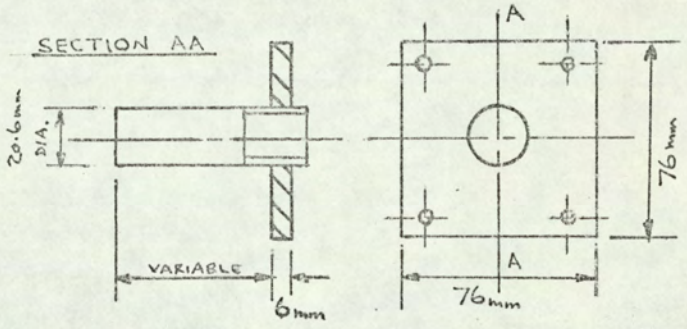

DUMMY END

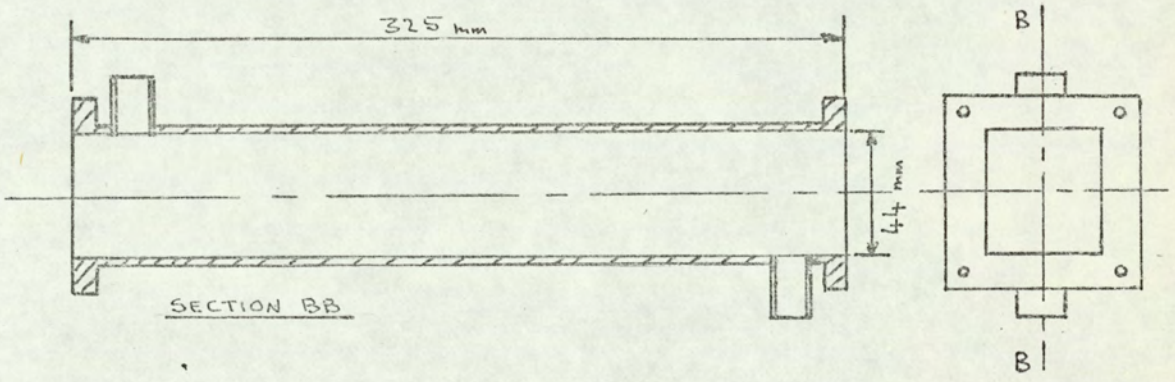

SHELL

MATERIALS

Tube: copper or stainless steel
Tube flange and dummy end: brass
Shell: mild steel

NOT TO SCALE

FIG.C4.4

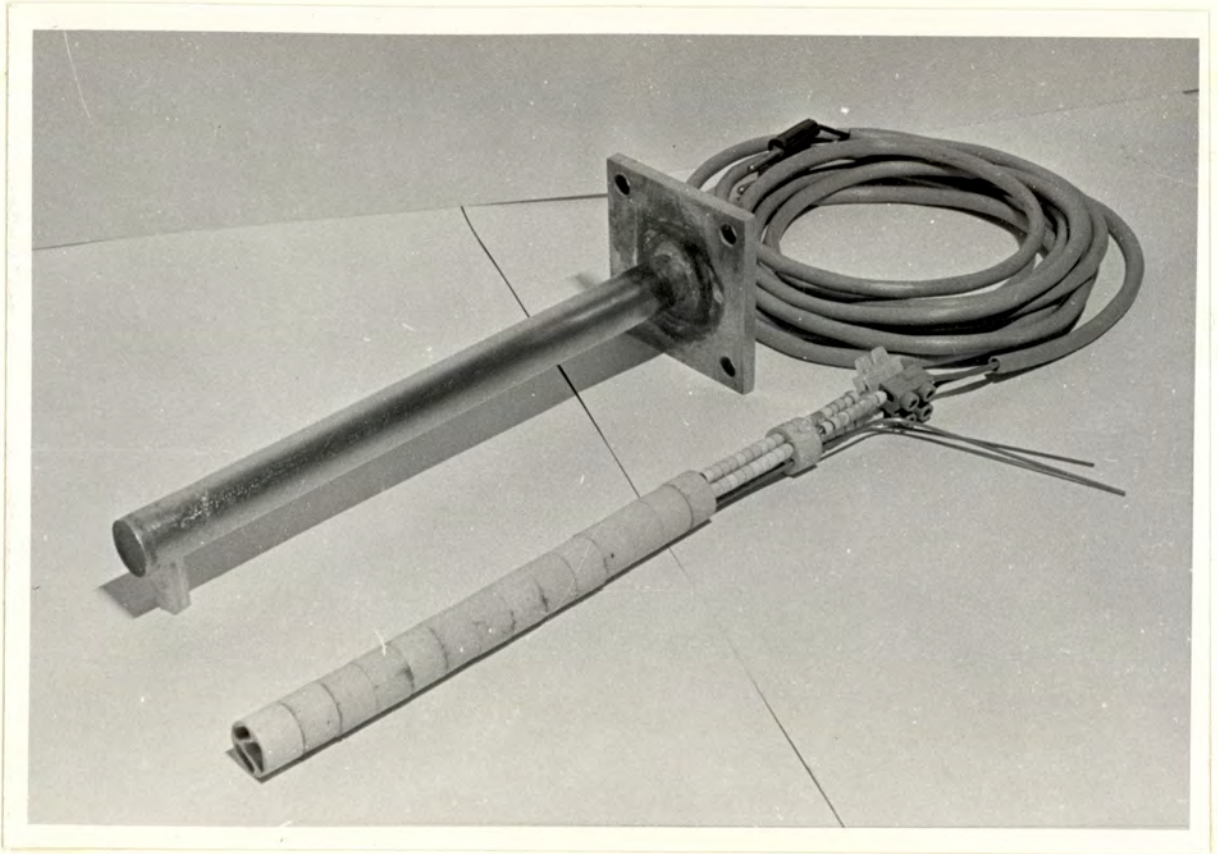

TUBE AND HEATER ASSEMBLY

FIG.C4.5

CHAPTER C5

EXPERIMENTAL PROCEDURE

C5.1 Introduction

The object of the test programme was to investigate the validity of equation C3.8 and therefore, within certain limitations, scaling rates at various heat fluxes and flow rates were determined by measuring the rate of increase of scale thickness. The experimental determination of these three variables is discussed below. The accuracy of results is discussed later in paragraph C6.3.

C5.2 Mass flow rate

The mass flow rate was indicated by a Rotameter graduated at intervals of 0.01×10^{-3} m^3/s (0.01 kg/s). A required flow rate was set by mutual adjustment of the main flow control valve and the by-pass valve so that a small system pressure was maintained.

There was no detectable variation in flow rate during a run.

C5.3 Heat flux

By arranging for deposition to take place on the outside of the tube there was a consequent increase in surface area through which the heat was dissipated. Therefore a constant heat input gave a progressively reducing heat flux during a test. For this reason maintaining a constant heat flux was not practical, and tests were run at a constant heating load. The heat flux was calculated using the area based on the average scale thickness

during the test. The heating load was measured using a precision wattmeter, the power being taken from the 230 V 50 Hz mains supply.

Fluctuations in power remained generally within ± 1% although variations of the order of ± 5% sometimes occurred at the beginning or the end of a day when there were large load changes within the building. However, the necessary adjustments were made as soon as possible after these load changes and the duration of these peak loads was small in comparison with the total running time.

C5.4 Rate of increase of scale thickness

This proved to be the most troublesome measurement for several reasons.

For example, deposition was not uniform along the tube as can be seen on Fig. C5.1. This is due partly to the flow pattern in the heat exchanger giving a varying surface temperature along the tube, partly to the fact that the heater lay slightly eccentrically in the tube, and partly to lack of uniformity in the heating element coils.

A typical longitudinal distribution of scale is shown in Fig. C5.2 (a) in which the water would be flowing from right to left. The deposit was greatest in the centre section decreasing rapidly to zero in the last 20 mm at either end and always lay within the first 180 mm of the length of the tube.

The effect of eccentricity is illustrated in Fig. C5.2 (b) and (c). At the early stages of scaling, or at the ends of the scaling region the deposit did not completely surround

the tube (Fig. C5.2 (b)). Where heavier deposition occurred the tube was completely covered but with an eccentric distribution (Fig. C5.2 (c)).

This distribution of scale will be referred to more specifically in the following chapter (chapter C6) in which the test results will be analysed. However, this preliminary description has been necessary in order to explain the measurement procedure.

It was decided to work on average values of scale thickness and so the following method was adopted.

At each measuring station indicated on Fig. C5.2 (a) two mutually perpendicular diameters were measured using a cathetometer graduated to read to 0.05 mm. These axes were designated V (vertical) and H (horizontal) in relation to the location of the tube in the heat exchanger. From these readings it was possible to plot a graph of the average tube diameter against length in order to find the overall mean diameter from the area under the curve. This was taken as the equivalent uniform diameter for the same quantity of scale deposited. This area mean is not a precise solution due to the curvature of the tube surface but since the scale thickness is small compared with the tube radius it was felt that the not inconsiderable extra computation required to determine the exact mean was not justified.

The area under the diameter - length graph was measured using a planimeter and the average scale thickness was based on a common length of 180 mm for all tests. Again, details of actual test results will be discussed in chapter C6. Fig. C5.3 shows the measuring arrangement with the tube held in

front of a board on which the locations A to J are marked. The cathetometer lens system was selected to focus at about 0.6 m.

C5.5 Temperatures

The temperature of the water in the reservoir was noted during tests using a thermometer graduated at intervals of 0.2 deg C. A thermometer situated downstream of the heat exchanger section was used to make occasional checks on the heat received by the circulating water.

In one series of tests the average tube wall temperature over the scaling region was recorded. Whilst scale thickness measurement by cathetometer was direct it had the disadvantage of interrupting a run by about three-quarters of an hour for each set of readings. It has already been argued by Hasson et al (6) that, under conditions of constant heat flux, a linear increase in scale thickness should be accompanied by a linear increase in tube wall temperature. Therefore it was felt that, whilst sacrificing the direct measurement of scale thickness, continuity of testing might be gained by temperature recording.

Three equi-spaced chromel - alumel thermocouples were attached to the copper tube at locations B, D and F and at the end of a horizontal diameter relative to the tube position in the heat exchanger. Records of individual temperatures and later of the average temperature were made on the pen recorder.

C5.6 Solution composition

Once the initial solution had been prepared it was only necessary to add water when required to compensate for

evaporation since a minimum level had to be maintained to hold the float switch in the on position.

Checks of the pH value were made from time to time using a portable pH meter and a sample of the water has been analysed by a chemist.

C5.7 Scale composition

Samples of scale have been analysed and the results of the analysis are presented later in paragraph C6.7.1.

C5.8 General procedure

The copper tubes were prepared for a test by first breaking off any scale from a previous test and removing the more tenacious scale by light filing and rubbing with emery paper. A fine grade of emery paper was used to give a smooth surface and Brasso was used to give a final polish. This left the tube with a slight shine, and before assembly in the heat exchanger the tube was degreased and its diameter checked.

Once the rig was assembled, the desired flow rate and heating load were set and the run was allowed to continue until a noticable deposition had occurred. Because initial nucleation on the surface was likely to behave differently from subsequent scaling this effect was ignored by discounting the initial build-up rate from results. In fact high heating loads and low flow rates were often used initially to induce rapid nucleation on the clean tube after which the test conditions could be set up.

In the first series of tests, having selected a heating load and flow rate, a series of tube measurements was made at intervals until the end of the test; this being determined by the scale

cracking and lifting off the surface. In the reported test on the pilot rig, for example, ten measurements of average scale thickness were made. It became clear in these earlier tests that so many measurements would be unnecessary in order to establish the rate of increase of scale thickness. A few tests were then conducted basing results on three or four measurements. The need or otherwise for a fourth result was usually decided by the scatter of the first three measurements.

Even by reducing the number of interruptions in a test it was still felt that each test run was too time consuming. Also, as results were being accumulated it became apparent that a considerable scatter was emerging although it was not clear why this was so. Since each test was independent of another and therefore there might be variations in the reservoir temperature or tube surface condition between tests, an alternative approach was adopted.

The idea was to maintain continuity between tests by progressively scaling the tube under a sequence of different test conditions. Thus, once a scaling rate had been obtained for one condition, the scaled tube was replaced in the heat exchanger, and a new heat load and mass flow rate applied. By this means it was possible to obtain several results in sequence before scale cracking terminated a test. In addition to providing continuity in each sequence of tests it also meant that more results became available in a given time. Again, bearing in mind the scatter of results it was important to complete as many tests as possible so that results could be analysed statistically.

C5.9 Range of tests

Tests were conducted generally within a range limited by the equipment. For example, the highest heating load that could be used was 1000 W. Even then the heaters had a very limited life and heater failures occurred several times in attempting to obtain results at this maximum heating load.

In turn, the maximum flow rate achieved on test was 0.365 kg/s at a heating load of 1000 W. Beyond this, the surface temperature would be insufficient to induce deposition.

This point has also been made by Freedman et al (29) in discussing the effect of velocity on scaling. Whilst increased velocity may have some scouring action its primary effect is to reduce surface temperature and so lessen the precipitation of scale material.

For the same reason a heating load of less than 300 W at the lowest flow rate was the minimum necessary to promote scaling.

The lowest flow rate used was 0.075 kg/s equivalent to a Reynolds' number of 1230. In work on heat transfer and pressure drop in annulii Davis (30) suggests that transition from laminar to turbulent flow can begin at a Reynolds' number of 1 000 compared with 2 000 for circular pipes. A similar comment has been made by Gunn and Darling (31) in connection with flow through non-circular conduits.

PARTIALLY SCALED TUBE

FIG.C5.1

DIAGRAM SHOWING DEPOSITION PATTERN AND MEASURING STATIONS

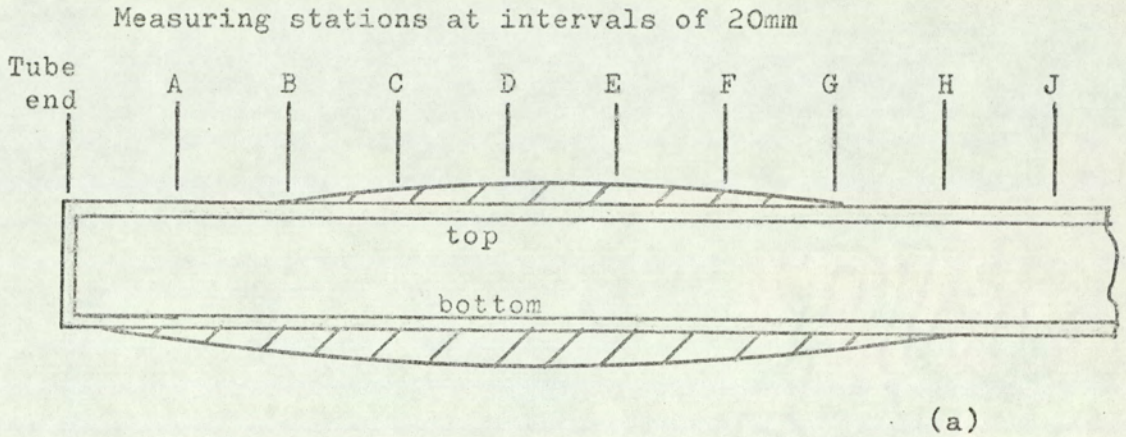

(a)

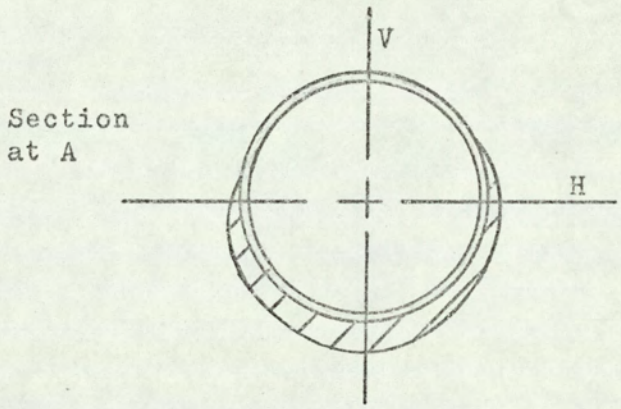

(b)

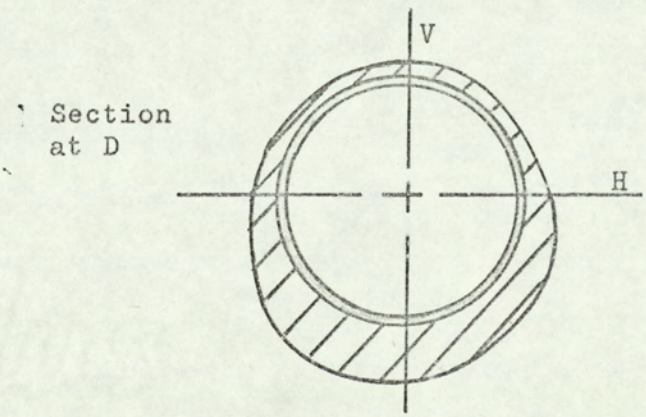

(c)

FIG.C5.2

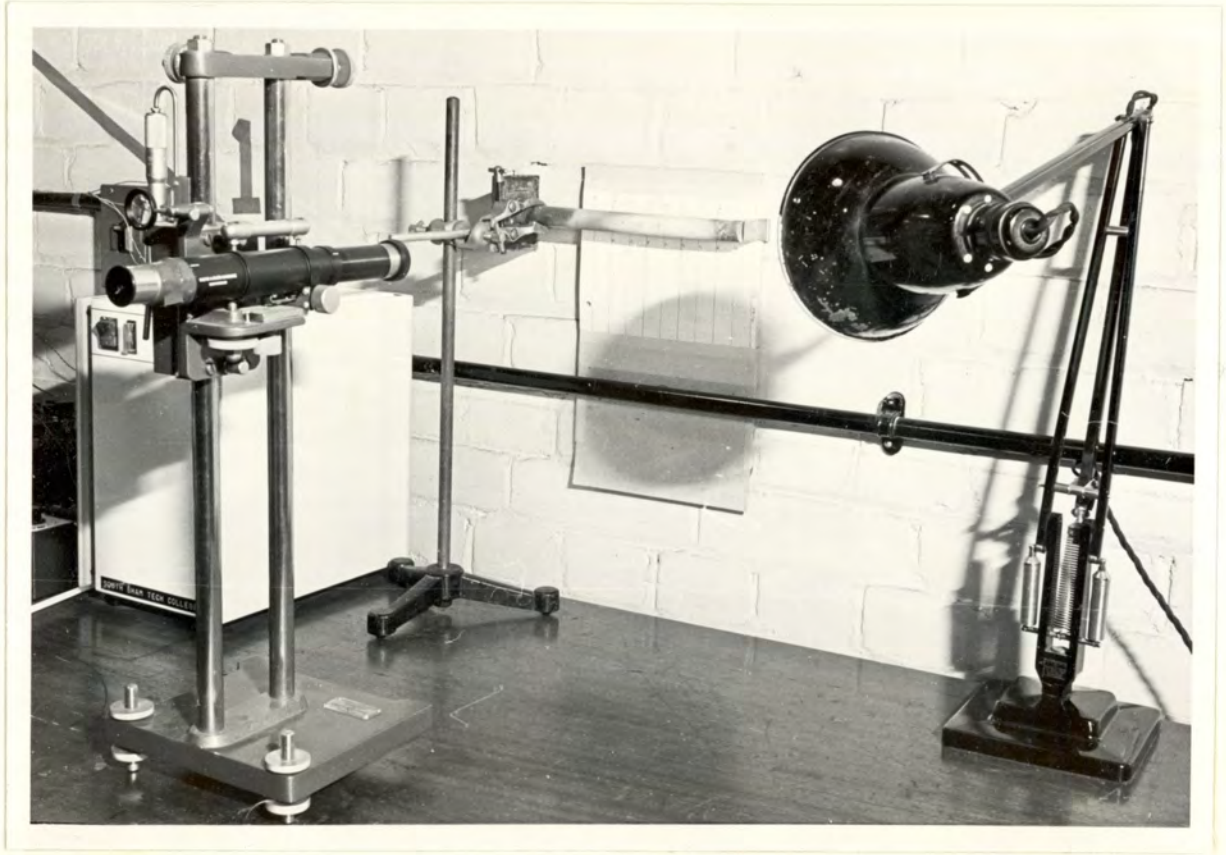

TUBE MEASURING ARRANGEMENT

FIG.C5.3

CHAPTER C6

RESULTS ANALYSIS AND DISCUSSION

C6.1 Preliminary tests on a pilot rig

Although several preliminary tests were run on a pilot rig details are not reported here. This is partly because the water treatment was slightly different in that there was no calcium hydroxide present. Also, the tube and heating arrangement was slightly different. Therefore the final analysis has been based only on results taken on the rig described in chapter C4, but the preliminary tests confirmed one important fact. That is that the rate of increase of the average scale thickness was constant for any particular heating load and flow rate.

One such test is reported here to illustrate the point.

In these early tests diameters were measured at three equi-spaced stations, 50 mm apart, along the length of the tube. The growth of the average scale thickness for a test at a flow rate of 0.075 kg/s and a heat input of 600 W is shown on Fig. C6.1. The uncertainty of the initial nucleation period is illustrated by the failure of the line to pass through the origin. Once initial deposition has occurred, however, the scale thickness is seen to increase linearly with time with little scatter of experimental results.

This behaviour was confirmed by other tests on the pilot rig and so the basis of the main test programme evolved. That is to establish rates of increase of scale thickness at various conditions of heating load and mass flow rate.

C6.2 Main test programme

It has been mentioned in the previous chapter how, for various reasons it was thought desirable and safe to reduce the number of readings and the time spent in any chosen test condition. It can be seen from Fig. C6.1, where ten average scale thicknesses were found over a period of 60 hours, that the same line would have been found from any group of results spanning between 15 and 20 hours.

Therefore the results for the main test series are based generally on three or four measurements of average scale thickness.

Fig. C6.2 to Fig. C6.14 inclusive show the experimental points used to establish the rates of increase of scale thickness. Fig. C6.15 tabulates these rates of increase as $\frac{dx}{dt}$ for all the tests.

One or two comments should be made about the scale thickness - time graphs.

Where little deviation from linearity occurred as in Fig. C6.2 (600 W) three points were considered sufficient to establish the line.

Where there was doubt about the severity of the scatter of results, as for example in Fig. C6.6 (750 W), then a fourth point was taken.

Whether three or four points were obtained, the slope of the best line was calculated using the method of least squares(32).

In a few tests only two points were taken. In Fig. C6.4 (500 W), for example, this was simply because scale cracking occurred after the second point and the test had to be stopped.

It was at this stage that the idea of successive tests

developed and Fig. C6.5 shows the result of the first such test. In this case, with the exception of the 800 W test, the heating load was changed point to point in order to achieve as many changes as possible before the scale began to crack and lift. Nevertheless it was considered that, whenever possible, for subsequent testing three points should be obtained to establish the rate of increase of scale thickness.

At this point, before taking these results to the next stage, it is worth showing in more detail the calculations involved in finding each value for the average scale thickness. Fig. C6.16 shows a typical extract from the log of results which tabulates the cathetometer readings. The variation in mean diameter along the tube was plotted and the area under the curve measured. The average scale thickness was calculated from this area. A representative series of diameter variations along the tube is shown on Fig. C6.17.

The analysis of the gradients obtained from the series of graphs Fig. C6.2 to Fig. C6.14 is as follows.

The first tests were conducted under conditions of constant flow rate in order to relate the rate of increase to the heat flux. (Perhaps it would be advisable here to emphasise that the term heat flux is used throughout to mean a rate of heat flow per unit area.)

The difficulty of measuring the heat flux was mentioned in paragraph C5.3 in which it was explained that, whilst the heating load was kept constant, the progressively increasing scale surface area resulted in a reducing heat flux. A subsidiary advantage of shortening the duration of a run was that the variation in heat flux through a test was reduced. It was

decided to base the heat flux on the average area during a particular test condition, this area being calculated from the average scale thickness indicated by the scale thickness - time graphs.

Fig. C6.15 tabulates average radii and the calculated heat flux values.

Having completed a series of tests at a flow rate of 0.075 kg/s covering twelve values of heat flux, a trend was apparent as can be seen on Fig. C6.18.

It was felt that, whilst more results would have been helpful, bearing in mind the scatter, the time involved might be better spent in broadening the test range. (The twelve results mentioned involved a running time of over 500 hours.) Therefore at that stage it was decided to analyse the curve since, as will be explained, the result is essential to complete the overall analysis.

Adopting the method of least squares, the rate of increase of scale thickness $\frac{dx}{dt}$ (mm/h) varies with the heat flux q"(W/m^2) according to:

$$\frac{dx}{dt} = \frac{5.05}{10^6} \; q''^{2.07} \qquad \text{(C6.1)}$$

This appeared close to a 'square' law and a sufficiently precise equation was considered to be:

$$\frac{dx}{dt} = \frac{6.65}{10^6} \; q''^{2} \qquad \text{(C6.2)}$$

These equations are shown comparatively on Fig. C6.18 and the test results, with two exceptions, lie within ± 20% of equation C6.2.

Having arrived at a dependence of deposition rate on heat flux further tests were carried out at various heating loads

and mass flow rates. These and the previous results are summarised in Fig. C6.15.

One approach to these tests would have been to run a series of varying heat flux tests at another flow rate and then to investigate the effect of varying flow rate under constant heating load (nearly constant heat flux) conditions. However, the number of tests required to establish the behaviour using this technique would have been formidable.

The following alternative approach was used. Accepting the square law relationship obtained from the first series of tests it was possible to adjust deposition rates at any heat flux to equivalent rates at an effective heat flux of 100 kW/m^2. These scaled results would then be a function of mass flow rate only.

Again Fig. C6.15 tabulates the effective rate of increase of scale thickness at 100 kW/m^2 for all results. By this process not only were new tests contributing to the analysis but also the original twelve tests could be included. The graph of these results is shown on Fig. C6.19 in which the trend is clear. The scatter band is fairly consistent over the range tested which suggests that the flow regime does not change materially although the Reynolds' number falls to 1230. Two results, not documented, taken at a flow rate of 0.05 kg/s departed radically from the reported results, and these were rejected as not being in a consistent flow regime.

The slope of the line shown on Fig. C6.19 is -1.62.

Referring this and the previous result (equation C6.2) to the general rate equation C3.8 shows that the heat flux index $p = 2$ and the mass flow rate index n is 0.81. The latter index

suggests that the tests were in the turbulent flow region.

Combining these results produces the equation describing the deposition behaviour in the range of tests undertaken as:

$$\frac{dx}{dt} = \frac{9.64}{10^8}\left[\frac{q''}{\dot{m}^{0.81}}\right]^2 \qquad (C6.2)$$

Alternatively, in terms of Reynolds number, Re,

$$\frac{dx}{dt} = 0.65\left[\frac{q''}{Re^{0.81}}\right]^2 \qquad (C6.3)$$

Having established the general law results have been separated into constant mass flow rate groups of 0.1, 0.15, 0.175, 0.2, 0.25, and 0.365 kg/s supplementing the first results at 0.075 kg/s. Equation C6.2 has been plotted for each group and the results are shown as Fig. C6.20 and Fig. C6.21 using the notation indicated on Fig. C6.19.

The complete summary of results in the form of a carpet graph, Fig. C1.1, has already been mentioned in chapter C1. This graph shows equation C6.2 plotted over the test range together with the individual experimental points.

The amount of scatter involved in the results clearly creates a difficulty in their interpretation. In looking for the cause there are three areas of the experimental work that could have bearing on the problem. These are the accuracy of individual results, the effect of the bulk liquid temperature, and the mechanism of deposition.

C6.3 Accuracy of individual results

It is not considered that any inaccuracy of observation or calculation is significant in the magnitude of the deviations of the test results from the 'best' curve.

For example, individual diameter readings, measured on

separate occasions agreed to within less than 0.5%

The areas under the diameter variation curves were rechecked periodically and agreed to within less than 0.3%. Possible inaccuracy inherent in drawing the curves was checked by drawing two curves through the same points independently, and measuring each area twice. It was found that the maximum and minimum areas were within ±0.6% of the mean.

The conversion of the area reading into a value for the average scale thickness was computed with a slide rule, and a random set of values was rechecked using a desk calculator. These calculations agreed to within 0.15%.

The average time interval between measurements was 16 hours. Since the heater was switched off and removed immediately before measurements were taken, the tube cooled rapidly to the temperature of the circulating water, and therefore deposition would cease at this time. Restarting was less definite in that a warming up time was involved. From the tests in which pipe temperatures were being investigated it seems that a reasonable estimate of the warming up period would be about 15 minutes. This represents approximately 1.5% of a typical running time.

All the measurements discussed above contribute to finding corresponding average scale thickness and time values from which the scaling rates are determined. That is, they form the basis for Fig. C6.2 to Fig. C6.14 inclusive. The accuracy involved in the drawing of these graphs is not of consequence since gradients have been calculated from the test points in all cases, using the method of least squares where appropriate.

C6.4 The effect of bulk liquid temperature

Reference to Fig. C6.22 will show that variations occurred in the bulk liquid temperature during the range of tests. Where temperatures were recorded continuously on a chart (Fig. C6.27 and Fig. C6.28) it was evident that the temperature after the heater exchanger remained constant during a test, and since the heat input and flow rate were constant it follows that the bulk water temperature in the reservoir remained constant. Therefore any variations in temperature through the test programme were due mainly to changes in ambient temperature in the laboratory.

By adjusting all test results to a common heat flux of 100 kW/m^2 and a common mass flow rate of 0.1 kg/s according to the exponents derived in equation C6.2 it has been possible to plot the results on a basis of reservoir temperature.

Fig. C6.22 tabulates these proportioned rates of increase of scale thickness together with the associated reservoir temperatures and the results are shown graphically on Fig. C6.23. There does not appear to be any temperature correlation from this analysis.

C6.5 Mechanism of deposition

From what has already been said, it would seem that the scatter of results arises most likely from the behaviour of the deposition process. Whilst this must be supposition at this stage it is worth looking at the pattern of deposition in the early stages of scaling.

Photographs have been taken showing the experimental tube at various stages of deposition during the first six hours of

scaling. The photographs appear as Fig. C6.24 to Fig. C6.26 inclusive, and they were taken when the heating load was 1 000 W and the mass flow rate was 0.1 kg/s.

The initial nucleation areas are clearly seen as small bubbles of gas mainly on the underside of the tube. As time progresses these bubbles become more numerous and their coverage extends around the tube. As the pocket of gas in the bubble gets hotter, it expands until eventually the bubble is carried off the tube surface into the flowing liquid. It is suggested that it is this random forming and detachment of bubbles that is responsible for the erratic deposition pattern.

The overall form of the build-up on the tube was discussed in paragraph C5.4 and these photographs supplement that description.

C6.6 Tube wall temperature

In paragraph C5.5 the argument is given for attempting to monitor the scaling rate indirectly by recording changes in tube wall temperature.

A typical extract from a test recording temperatures at the end of a horizontal diameter at stations B, D and F is shown on Fig. C6.27. The fluctuation of points is clear, and a slope was established by constructing a line through the minimum points of the fluctuations. The resulting lines have the same slope and it was thought that the variations in recorded temperature might be reduced if an average temperature were recorded. This proved not to be the case as can be seen on Fig. C6.28.

Notwithstanding this difficulty, a series of successive

combinations of heating load and flow rate were set up and conditions were held constant until the recorded temperatures showed a definite trend.

Temperature - time gradients were measured using the minimum temperatures as described above but there was no correlation on either a heat flux or a mass flow basis.

It became obvious that if this approach to the problem was to be pursued, bearing in mind the difficulties that had to be overcome, the original test programme might be jeopardised. Therefore it was decided to abandon temperature measurement as an indication of deposition rate and concentrate on the direct method of measurement.

C6.7 Chemical analyses

C6.7.1 Scale

Samples of scale were submitted to the Chemistry department of the University of Aston for analysis and the relevant section of their report is as follows:

'The following anions and cations were found to be present.

(a) calcium as the predominant element

(b) trace amounts of iron was detected

(c) sulphate was found to be the predominant anion

(d) trace amounts of phosphate were detected

(e) a slight effervesence was noted on acidification which indicates the possible presence of carbonate. This could not be determined however.'

C6.7.2 Solution

A sample of water from the reservoir was also analysed,

and its calcium ion content was 816 ppm at 20°C. This is equivalent to a calcium sulphate solubility figure of 2.75 g/l which is 6% higher than that given in paragraph C2.1.

However, as quoted figures can differ by as much as 10% the analysis confirms that the solution was saturated with calcium sulphate.

The pH value of the water was checked regularly and was found to be 12.3 ± 0.1 throughout the test programme.

C6.7.3 Appearance of scale

The scale was brittle and porous. Fig. C6.29 shows a photograph of a scaled tube with part of the scale broken off, and also photographs of a fragment of scale.

In some areas the scale would be firmly attached to the tube surface suggesting some chemical attack on the surface, whilst in other areas the scale would break cleanly from the tube. In the latter case growth had taken place circumferentially by deposition on the periphery of existing scale rather than by nucleation on the clean tube surface. A white powdery deposit was sometimes present but its thickness was insignificant compared with the hard porous scale.

C6.8 Effect of different tube materials

The test programme as reported was concerned with deposition on copper. It had been hoped to accumulate data using stainless steel but this proved to be too ambitious in the available time.

A stainless steel tube was used in one recorded test (marked S.S. on Fig. C6.15). Visually the deposition mechanism was similar to that observed on the copper tubes and the result

referred to lies within the band of test results.

Once a tube has an initial layer of scale then the process is independent of the original surface material. Therefore one might expect different materials to be effective, if at all, only in the initial nucleation stages. If there is any reaction between the scaling salt and the tube material then different materials could result in different strengths of adhesion between the scale layer and the tube wall. This could be important from the point of view of cleaning the heat transfer surface.

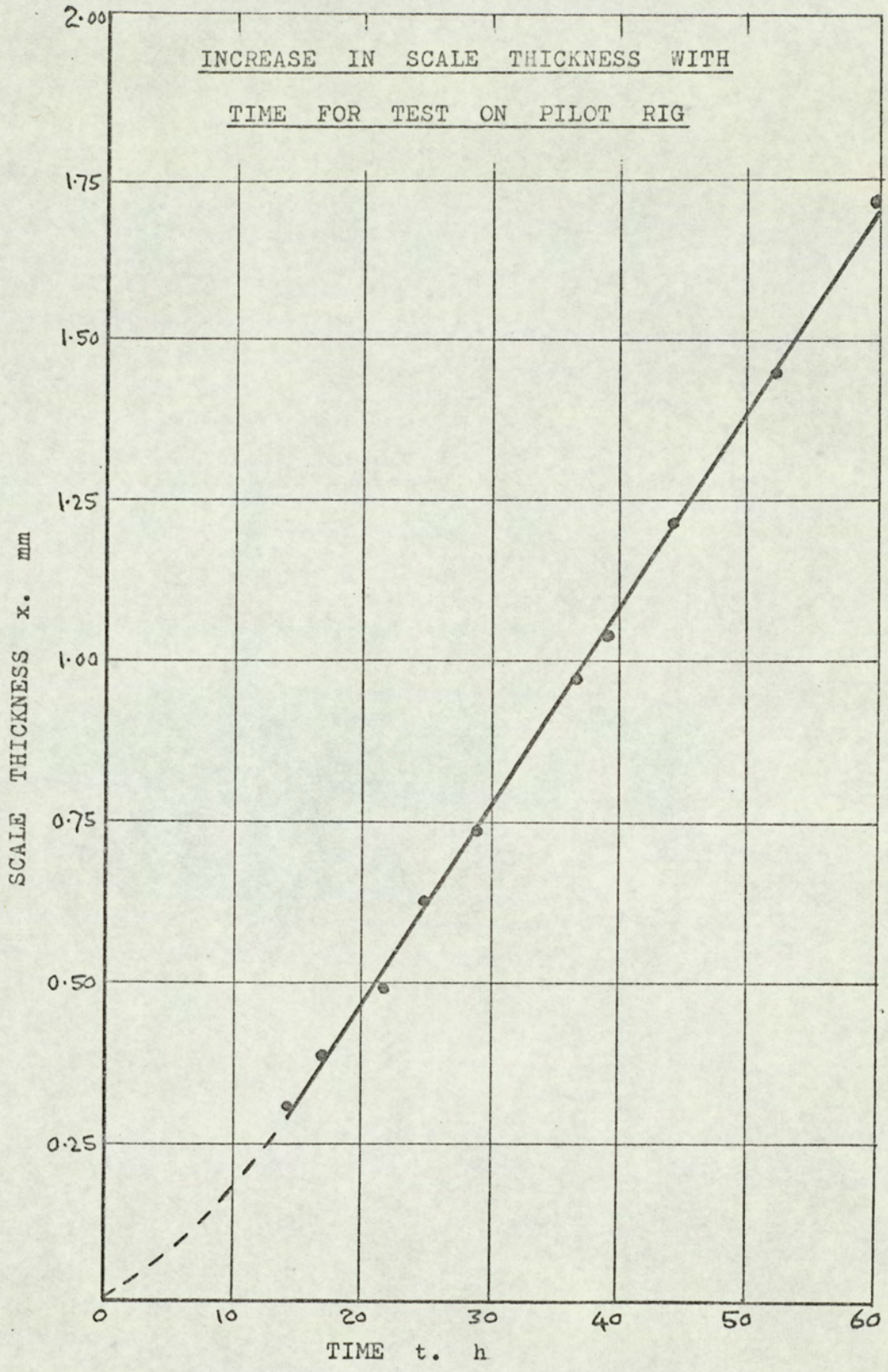
INCREASE IN SCALE THICKNESS WITH
TIME FOR TEST ON PILOT RIG
SCALE THICKNESS x. mm
2·00
1·75
1·50
1·25
1·00
0·75
0·50
0·25
0
10
20
30
40
50
60
TIME t. h

FIG. C6.1

INCREASE IN SCALE THICKNESS WITH TIME

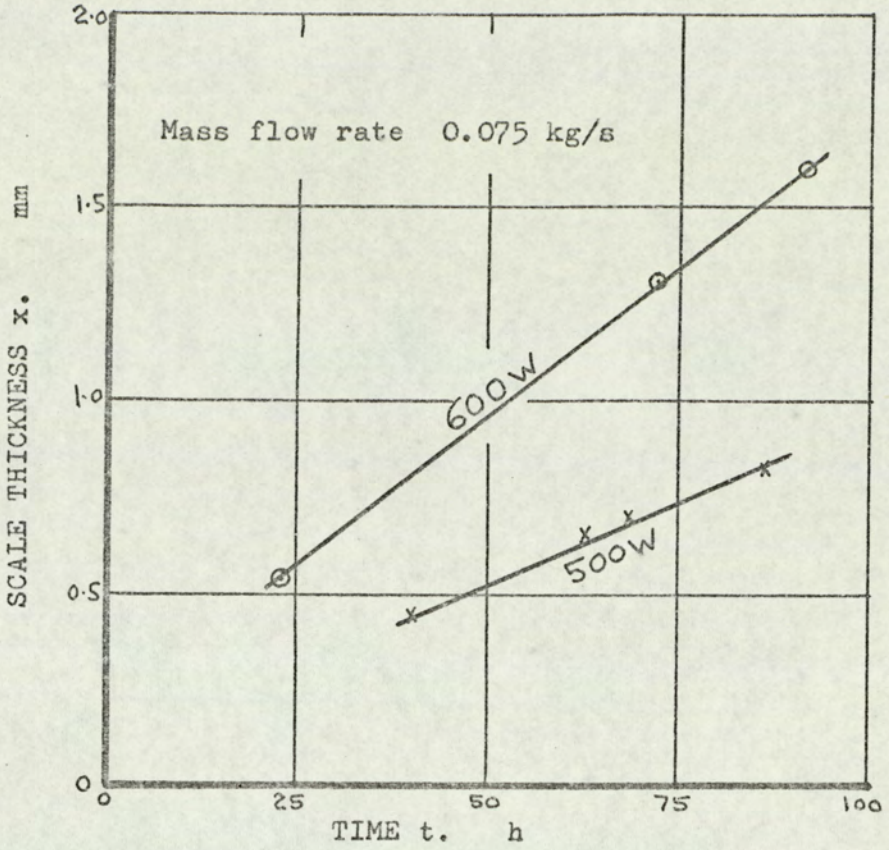

FIG.C6.2

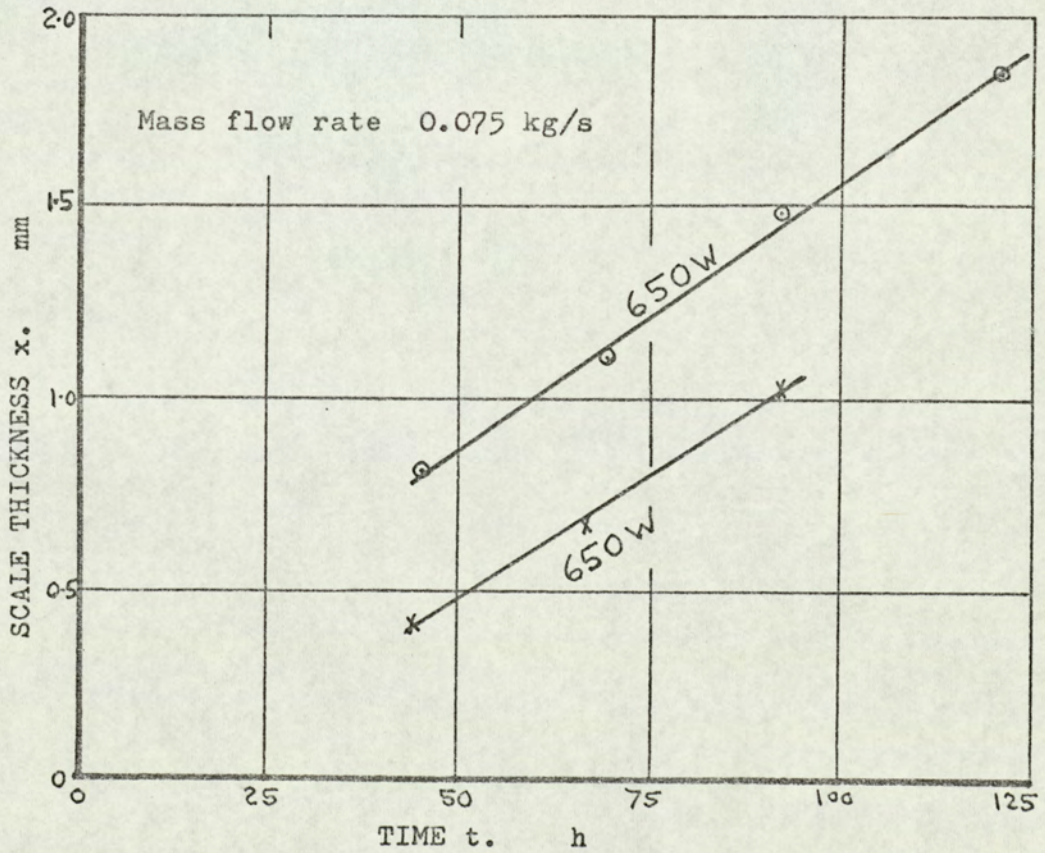

FIG.C6.3

INCREASE IN SCALE THICKNESS WITH TIME

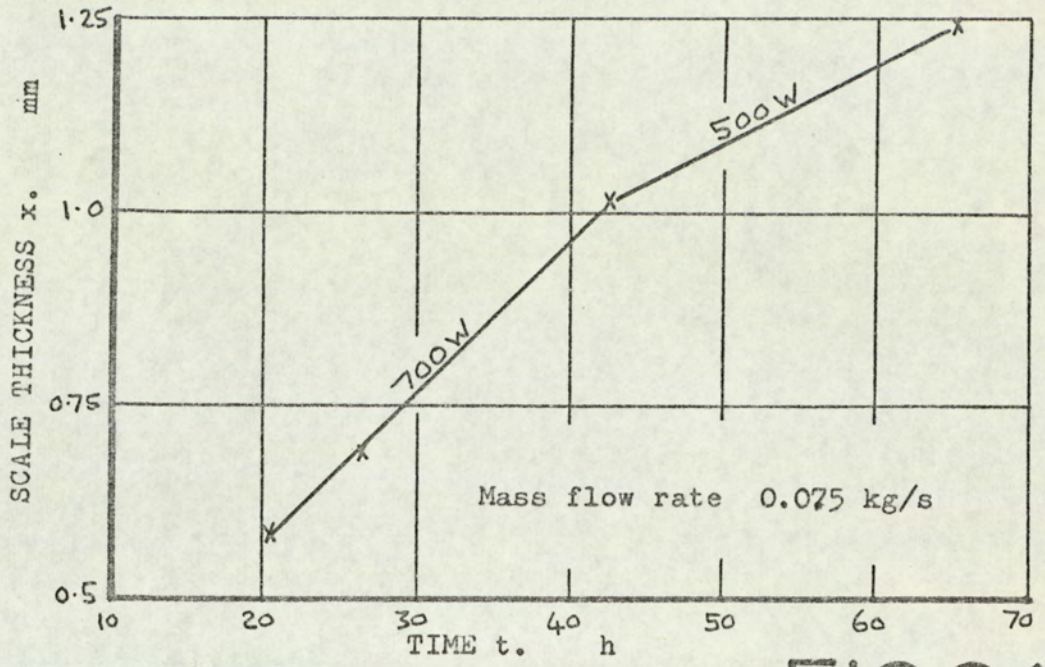

FIG.C6.4

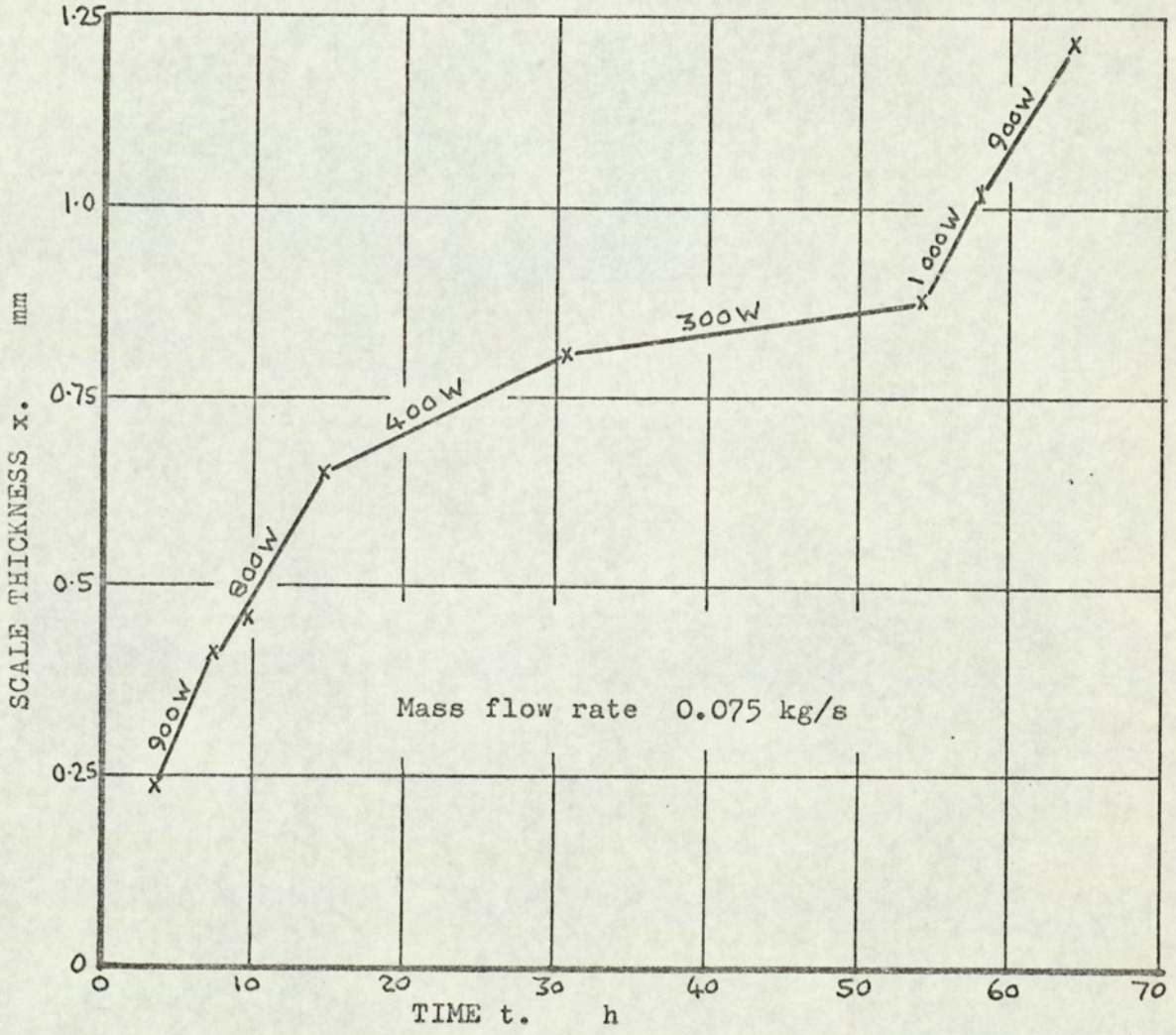

FIG.C6.5

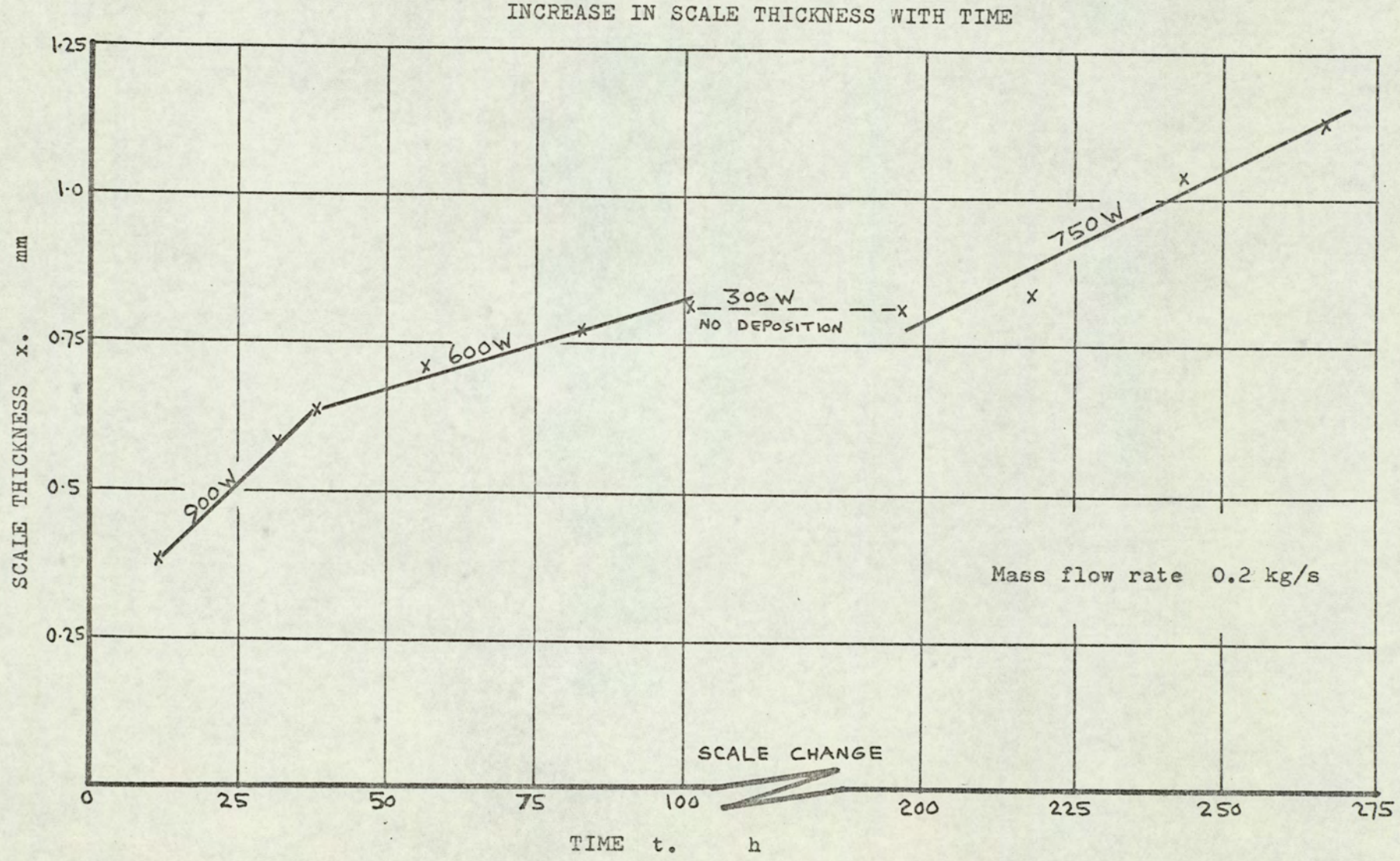
INCREASE IN SCALE THICKNESS WITH TIME
SCALE THICKNESS x. mm
1·25
1·0
0·75
0·5
0·25
0
25
50
75
100
200
225
250
275
TIME t. h
900W
600W
300W
NO DEPOSITION
750W
SCALE CHANGE
Mass flow rate 0.2 kg/s

FIG.C6.6

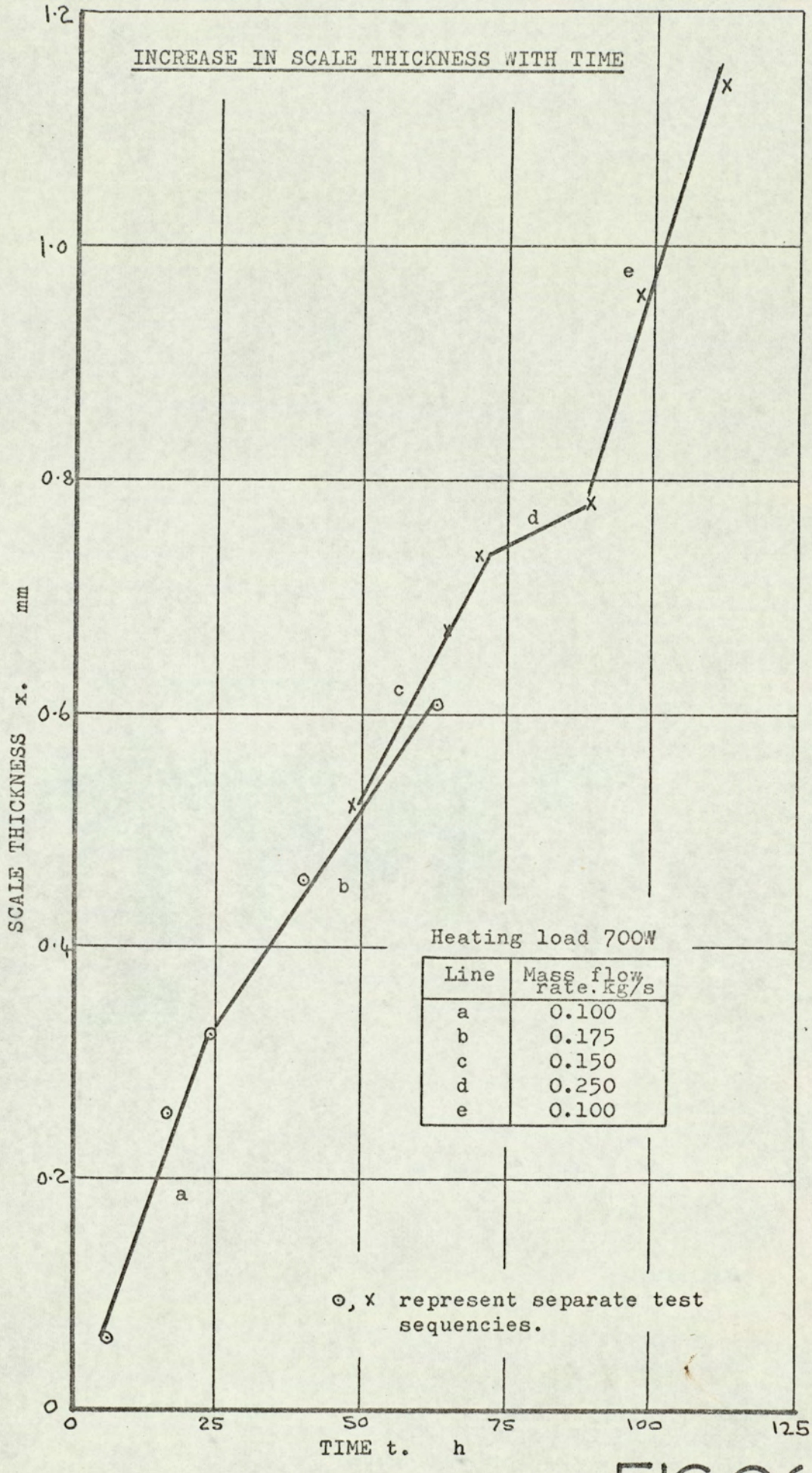
INCREASE IN SCALE THICKNESS WITH TIME
SCALE THICKNESS x. mm
TIME t. h
1·2
1·0
0·8
0·6
0·4
0·2
0
0
25
50
75
100
125
a
b
c
d
e
Heating load 700W
Line | Mass flow rate.kg/s
a | 0.100
b | 0.175
c | 0.150
d | 0.250
e | 0.100
⊙, X represent separate test sequencies.

FIG.C6.7

INCREASE IN SCALE THICKNESS WITH TIME

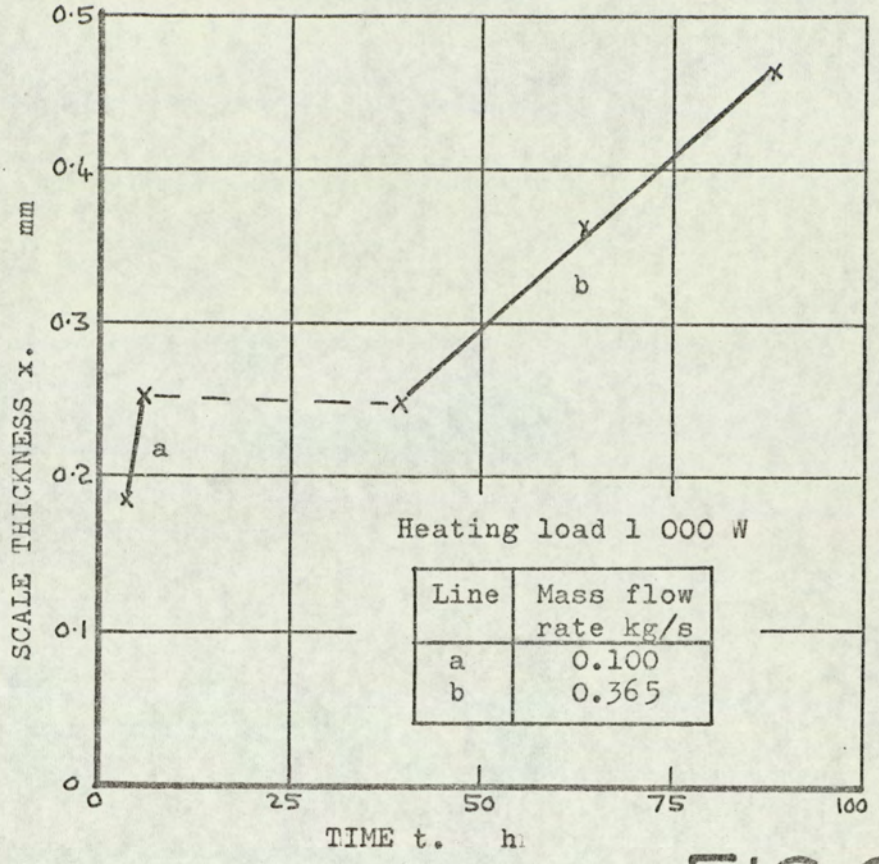

FIG.C6.8

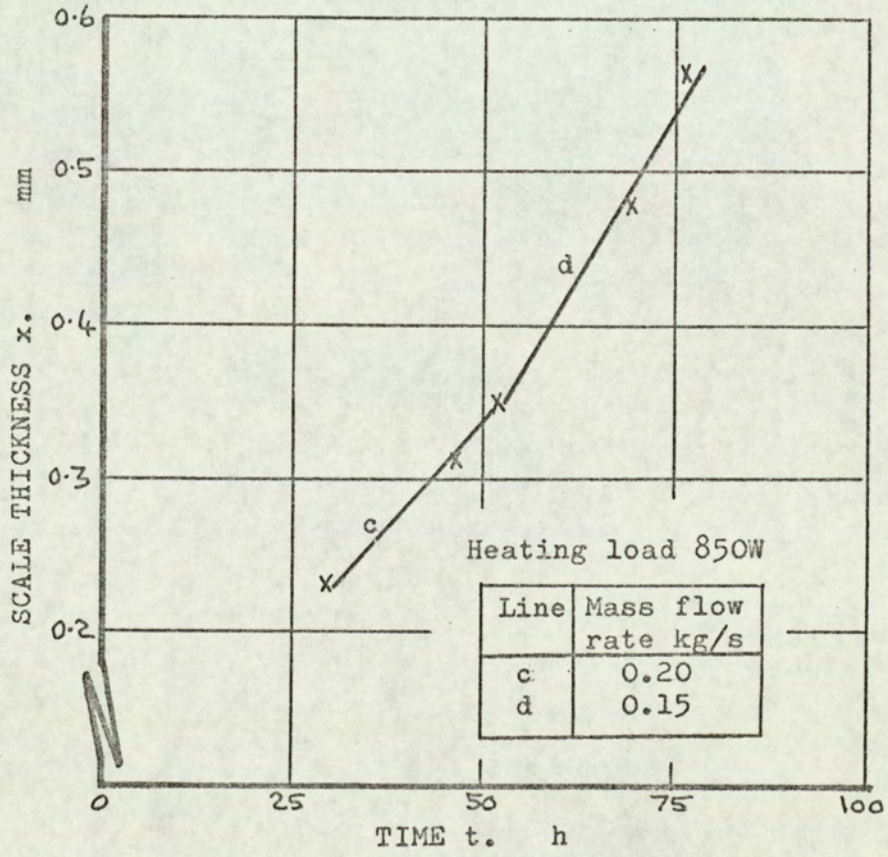

FIG.C6.9

INCREASE IN SCALE THICKNESS WITH TIME

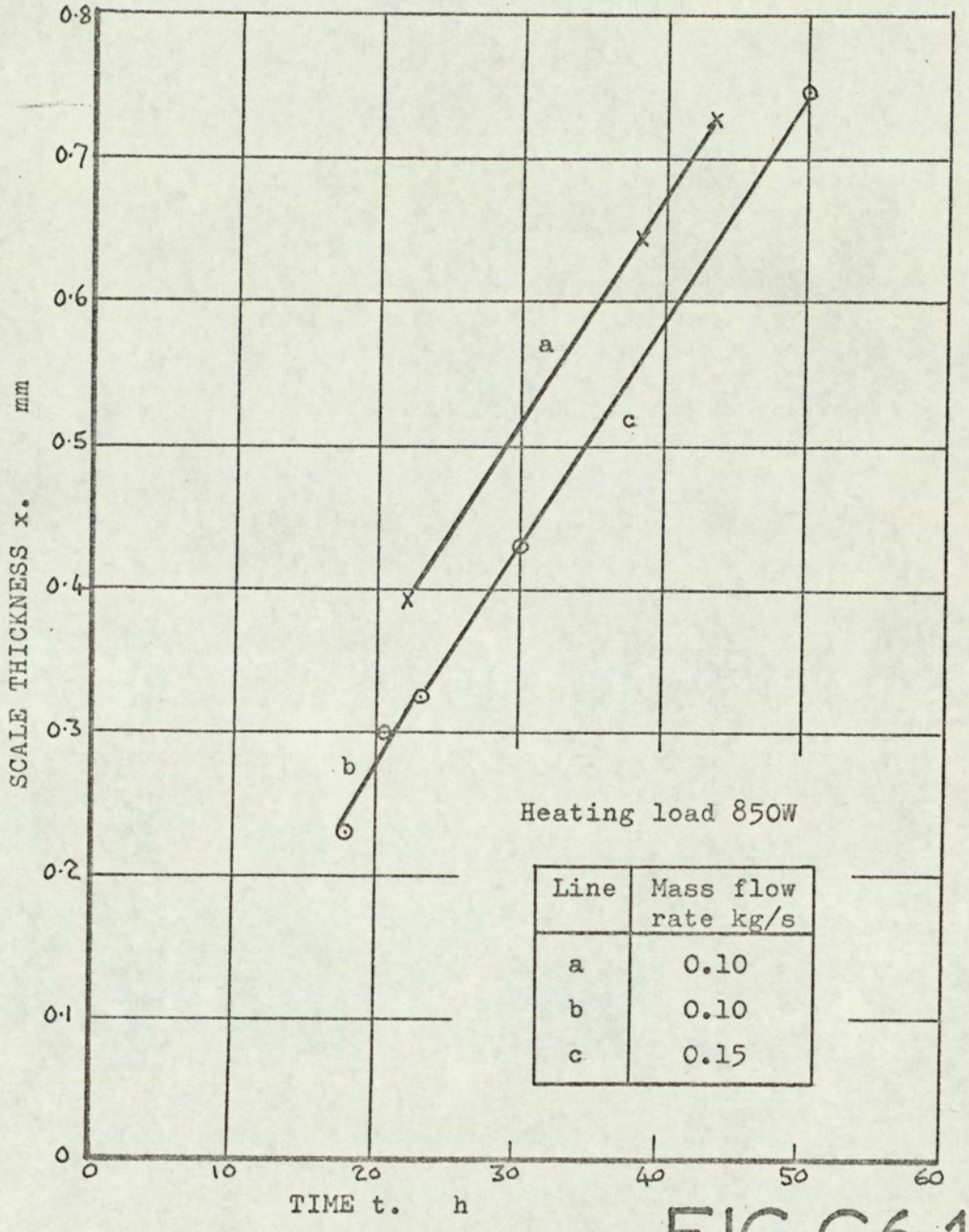

FIG.C6.10

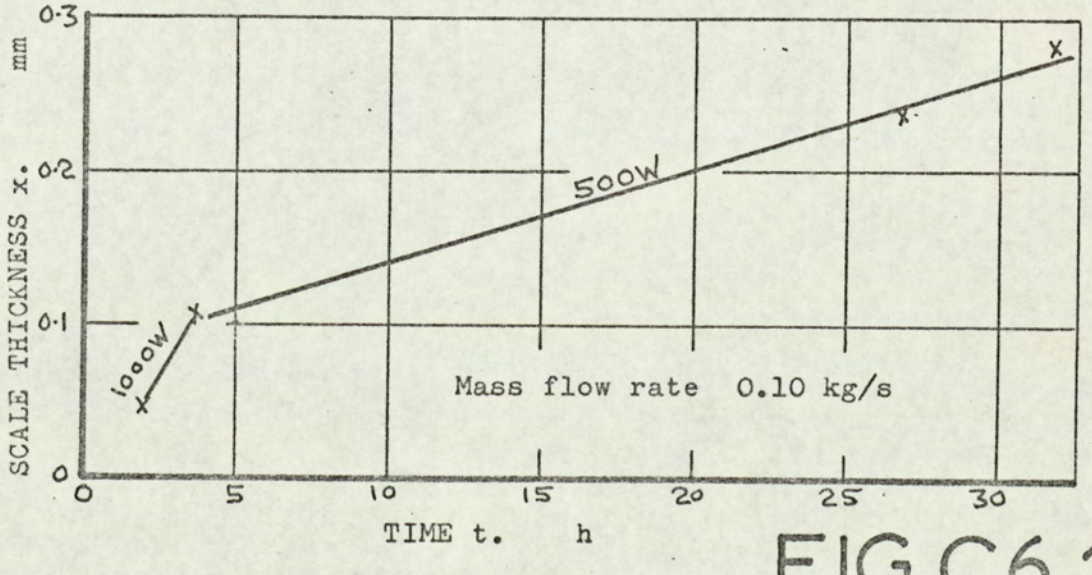

FIG.C6.11

INCREASE IN SCALE THICKNESS WITH TIME

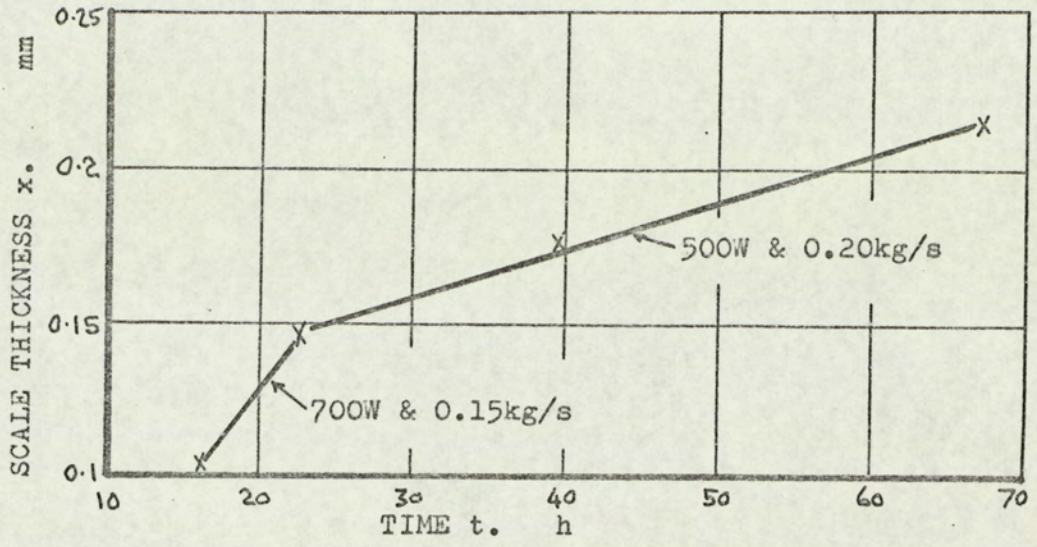

FIG.C6.12

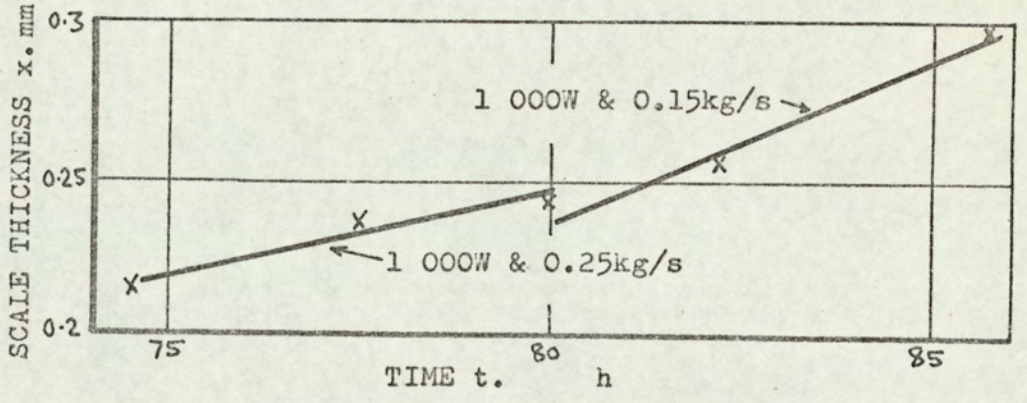

FIG.C6.13

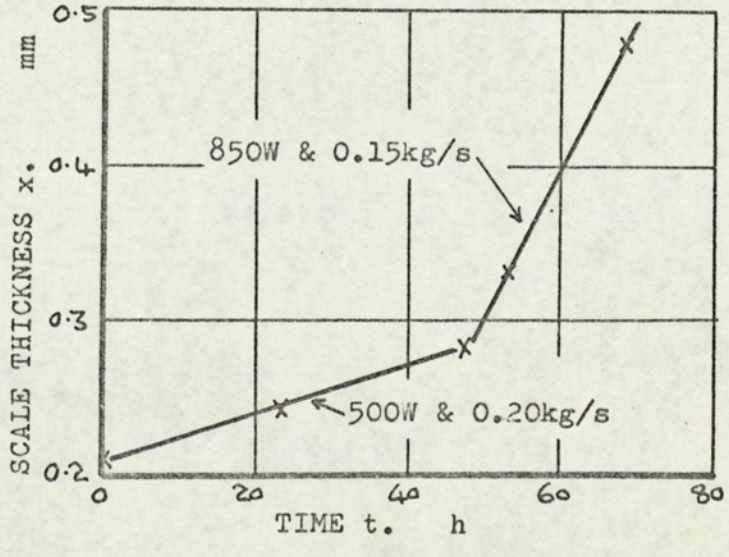

FIG.C6.14

RESULTS SUMMARY

MASS FLOW $\dot{m}$ (kg/s)	HEAT INPUT q (W)	AVERAGE RADIUS (mm)	HEAT FLUX q" (kW/m^2)	DEPOSITION RATE $\frac{dx}{dt}$ (mm/h)	$\frac{dx}{dt}$ SCALED TO $q''=100\,kW/m^2$ (mm/h)
0.075	500	11.0	40.2	0.0086	0.0533
"	600	11.3	46.9	0.0153	0.0694
"	650	11.6	49.4	0.0140	0.0573
"	650	11.0	52.2	0.0129	0.0474
"	500	11.45	38.6	0.0102	0.0685
"	900	10.63	74.8	0.0460	0.0822
"	800	10.825	65.3	0.0330	0.0774
"	400	11.025	32.1	0.0098	0.0952
"	300	11.14	23.8	0.0030	0.0534
"	1 000	11.25	78.5	0.0379	0.0616
"	900	11.41	69.7	0.0325	0.0669
"	700	11.10	55.8	0.0196	0.0629
0.200	600	11.034	48.1	0.0031	0.0133
"	750	11.30	58.7	0.0051	0.0147
"	900	10.80	73.7	0.0097	0.0178
"	850	10.585	71.0	0.0057	0.0113
"	500	10.55	41.9	0.0016	0.0091
"	500	10.49	42.2	0.0015	0.0084

continued over...

FIG.C6.15

RESULTS SUMMARY (continued)

MASS FLOW $\dot{m}$ (kg/s)	HEAT INPUT q (W)	AVERAGE RADIUS (mm)	HEAT FLUX q" (kW/m^2)	DEPOSITION RATE $\frac{dx}{dt}$ (mm/h)	$\frac{dx}{dt}$ SCALED TO q"=100 kW/m^2 (mm/h)
0.10	700	10.45	59.2	0.0143	0.0408
0.10	"	11.25	55.0	0.0164	0.0543
0.15	"	10.925	56.6	0.0097	0.0300
0.175	"	10.80	57.3	0.0075	0.0228
0.25	"	11.05	56.0	0.0024	0.0076
0.15	"	10.375	59.7	0.0064	0.0180
0.15	850	10.75	69.9	0.0085	0.0174
0.10	"	10.85	69.3	0.0158	0.0329
0.15	"	10.85	69.3	0.0156	0.0325
0.10	"	10.575	71.2	0.0168	0.0331
0.15	"	10.70	70.3	0.0096	0.0195
0.10	1 000	10.525	84.0	0.0338	0.0479
0.365	"	10.675	83.0	0.0045	0.0065
0.10(S.S.)	"	10.88	81.3	0.0343	0.0518
0.25	"	10.53	84.0	0.0054	0.0076
0.15	"	10.565	83.8	0.0105	0.0149
0.10	500	10.99	40.2	0.0060	0.0371

FIG.C6.15

TYPICAL DIAMETER MEASUREMENTS

Test No. T/27

HEATING LOAD 500 W FLOW RATE 0.2 kg/s TIME 23.5 h

LOCATION	CATHETOMETER READINGS		AVERAGE DIAMETER mm
	VERTICAL DIAMETER	HORIZONTAL DIAMETER	
A	SCALING STARTS ABOUT 5 mm BEYOND A		CLEAN TUBE 20.6
B	74.85 53.55 21.30	72.75 51.55 21.20	21.25
C	74.75 53.10 21.65	73.10 51.70 21.40	21.525
D	74.80 53.15 21.65	73.20 51.65 21.55	21.60
E	74.55 53.00 21.55	73.35 52.00 21.35	21.45
F	74.50 53.15 21.35	73.50 52.40 21.10	21.225
G	74.45 53.35 21.10	73.25 52.65 20.60	20.85
H	END OF SCALING ABOUT 3 mm BEYOND H		

PLANIMETER 5.416 - 4.745 = 0.671

MEAN SCALE THICKNESS x_m = 0.241 mm

FIG.C6.16

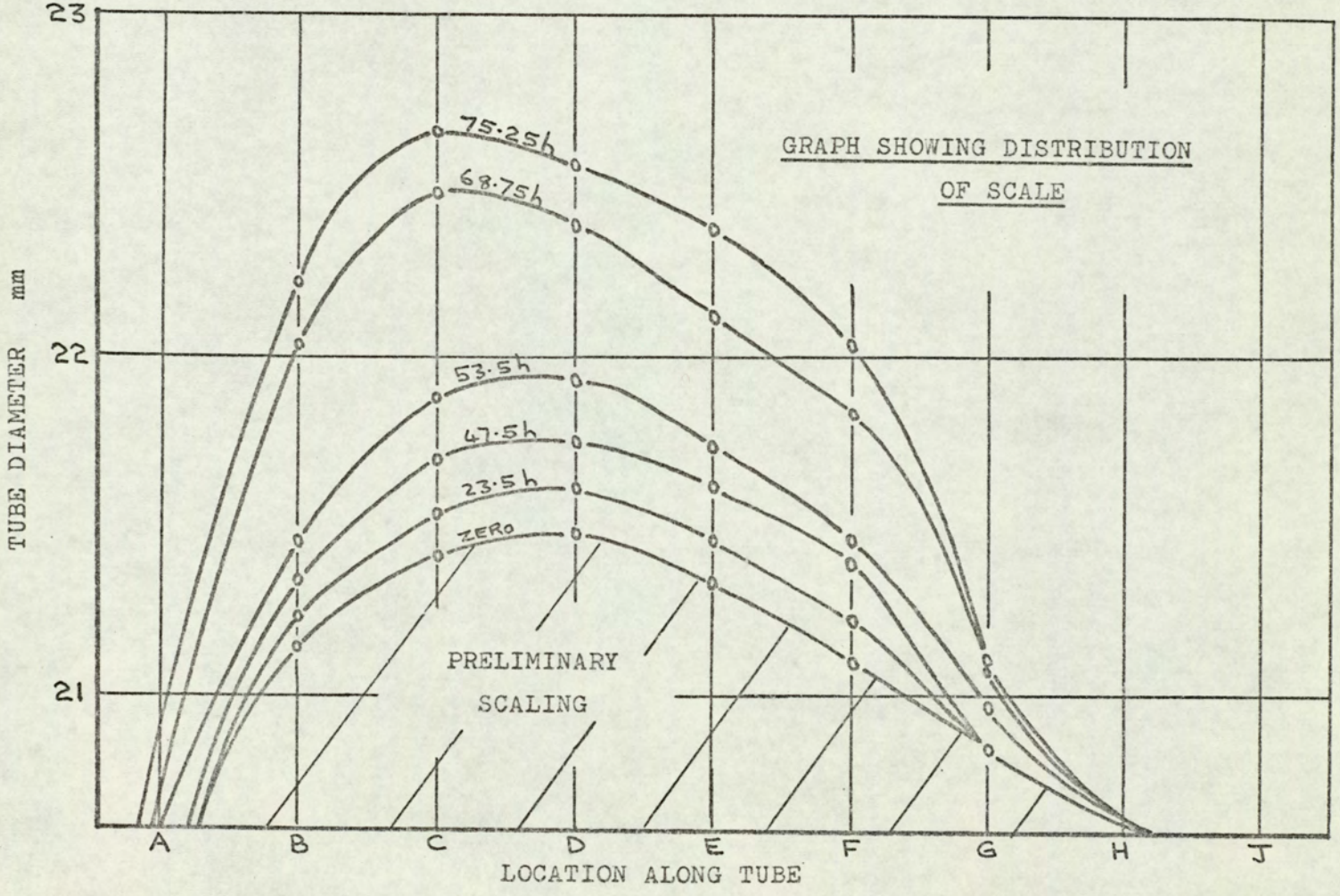
GRAPH SHOWING DISTRIBUTION
OF SCALE
TUBE DIAMETER mm
23
22
21
75·25h
68·75h
53·5h
47·5h
23·5h
ZERO
PRELIMINARY
SCALING
A
B
C
D
E
F
G
H
J
LOCATION ALONG TUBE

FIG.C6.17

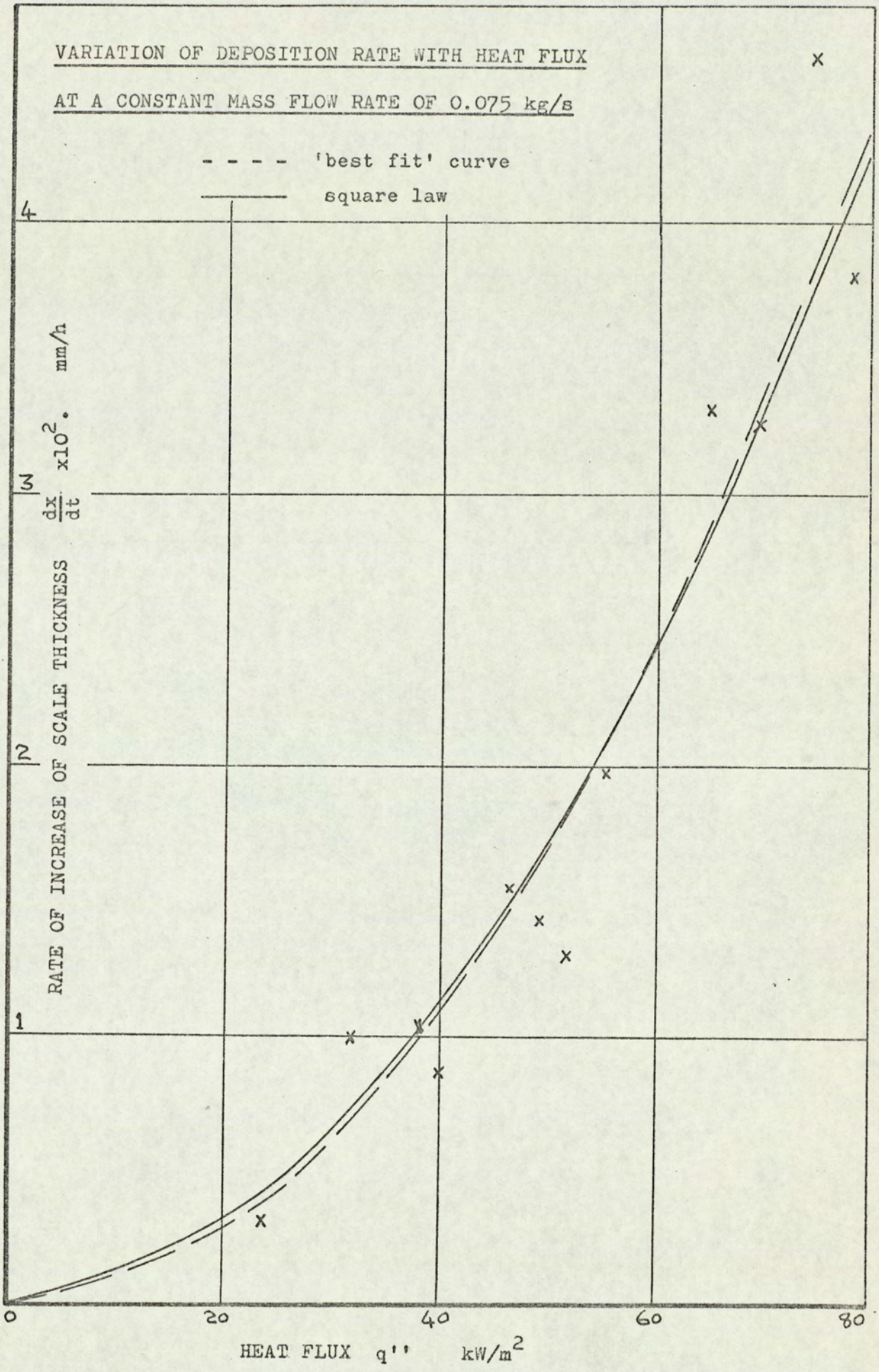
VARIATION OF DEPOSITION RATE WITH HEAT FLUX
AT A CONSTANT MASS FLOW RATE OF 0.075 kg/s
- - - - 'best fit' curve
——— square law
RATE OF INCREASE OF SCALE THICKNESS dx/dt x10^2. mm/h
HEAT FLUX q'' kW/m^2
0
20
40
60
80
1
2
3
4

FIG.C6.18

EFFECT OF MASS FLOW RATE ON DEPOSITION RATE

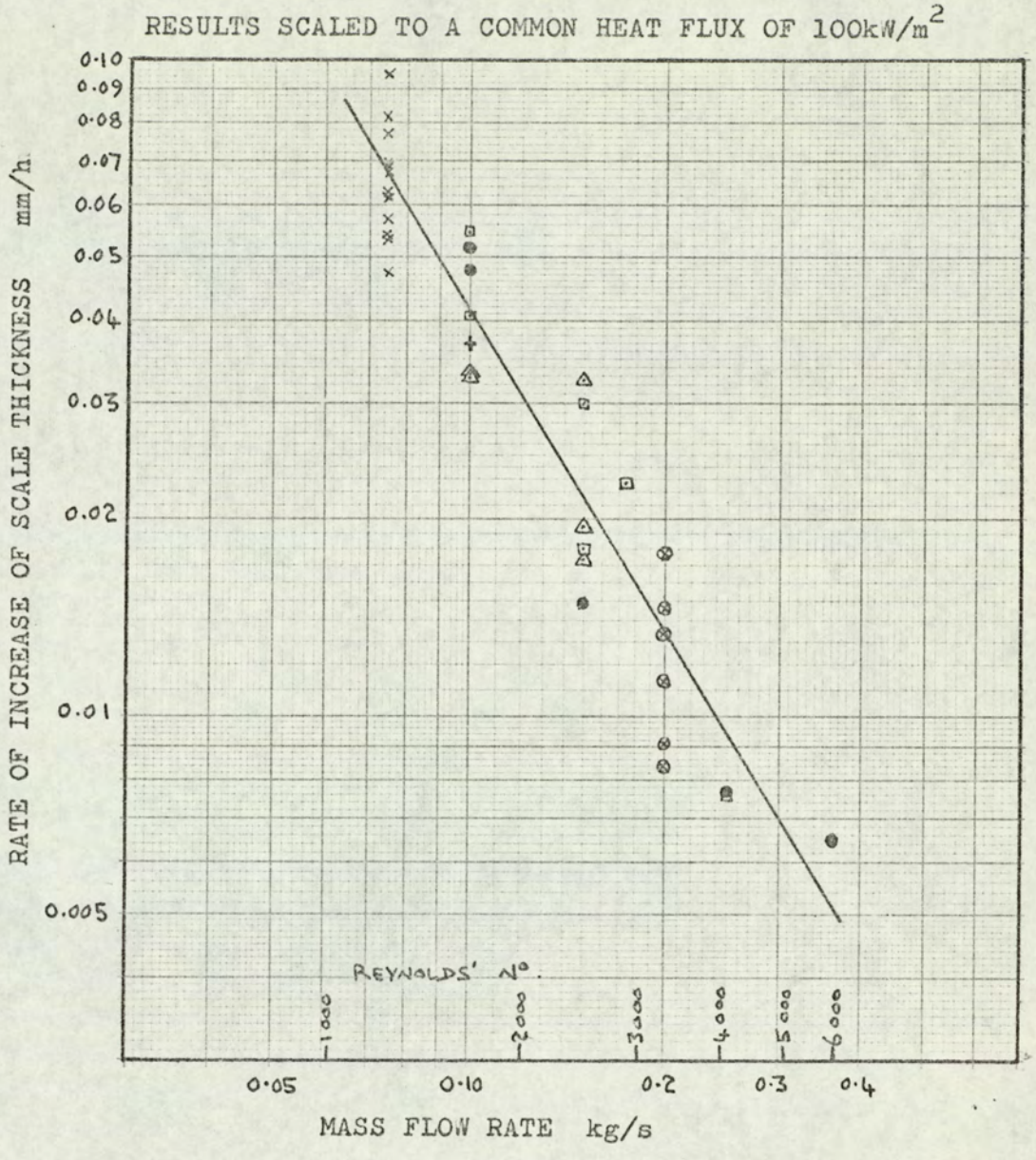

× Tests at 0.075 kg/s
⊗ Tests at 0.200 kg/s
— Varying heating load

\+ Tests at 500W
⊡ Tests at 700W
△ Tests at 850W
● Tests at 1 000W
— Varying mass flow rate

FIG.C6.19

VARIATION OF DEPOSITION RATE WITH HEAT FLUX AT VARIOUS MASS FLOW RATES

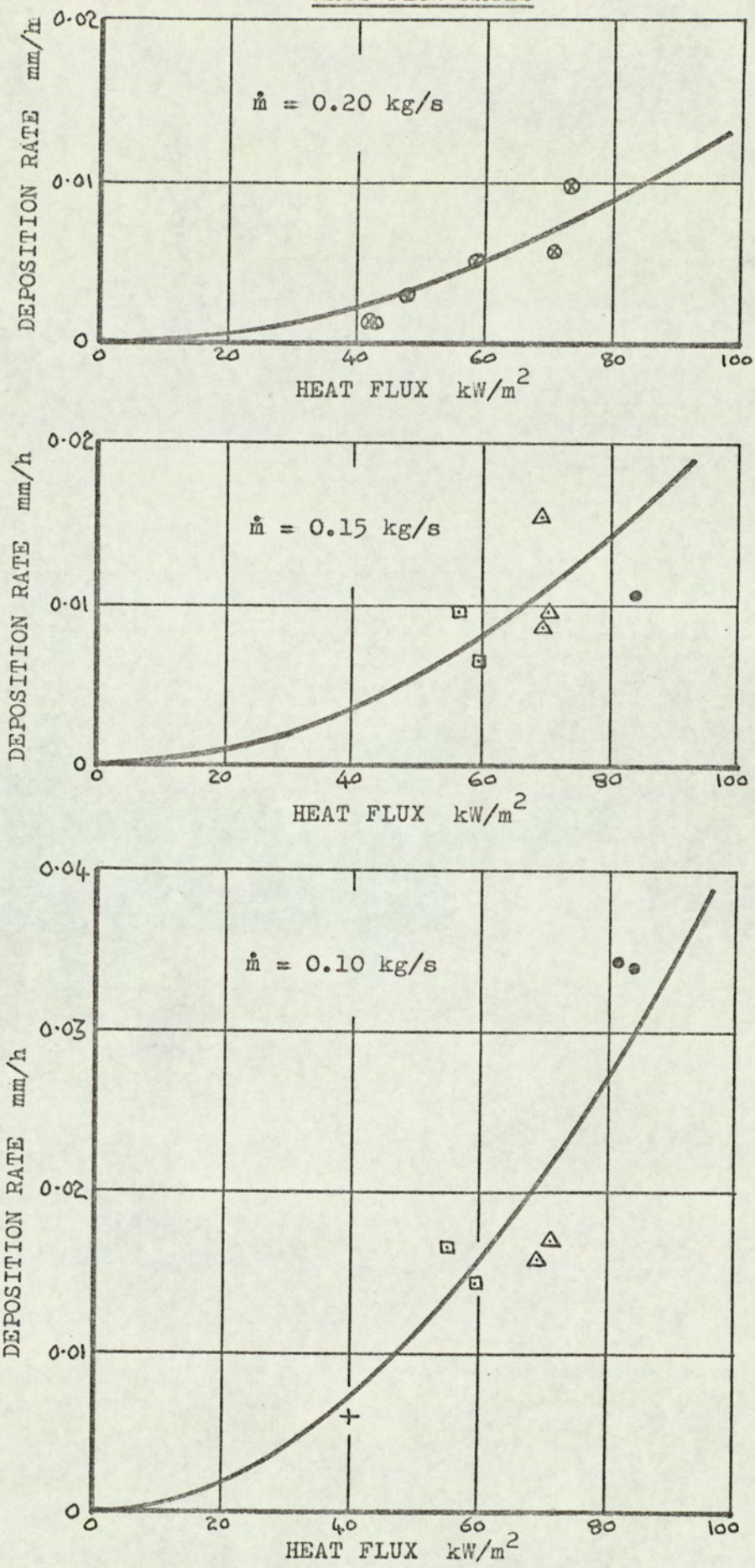

FIG.C6.20

VARIATION OF DEPOSITION RATE WITH HEAT FLUX AT VARIOUS MASS FLOW RATES

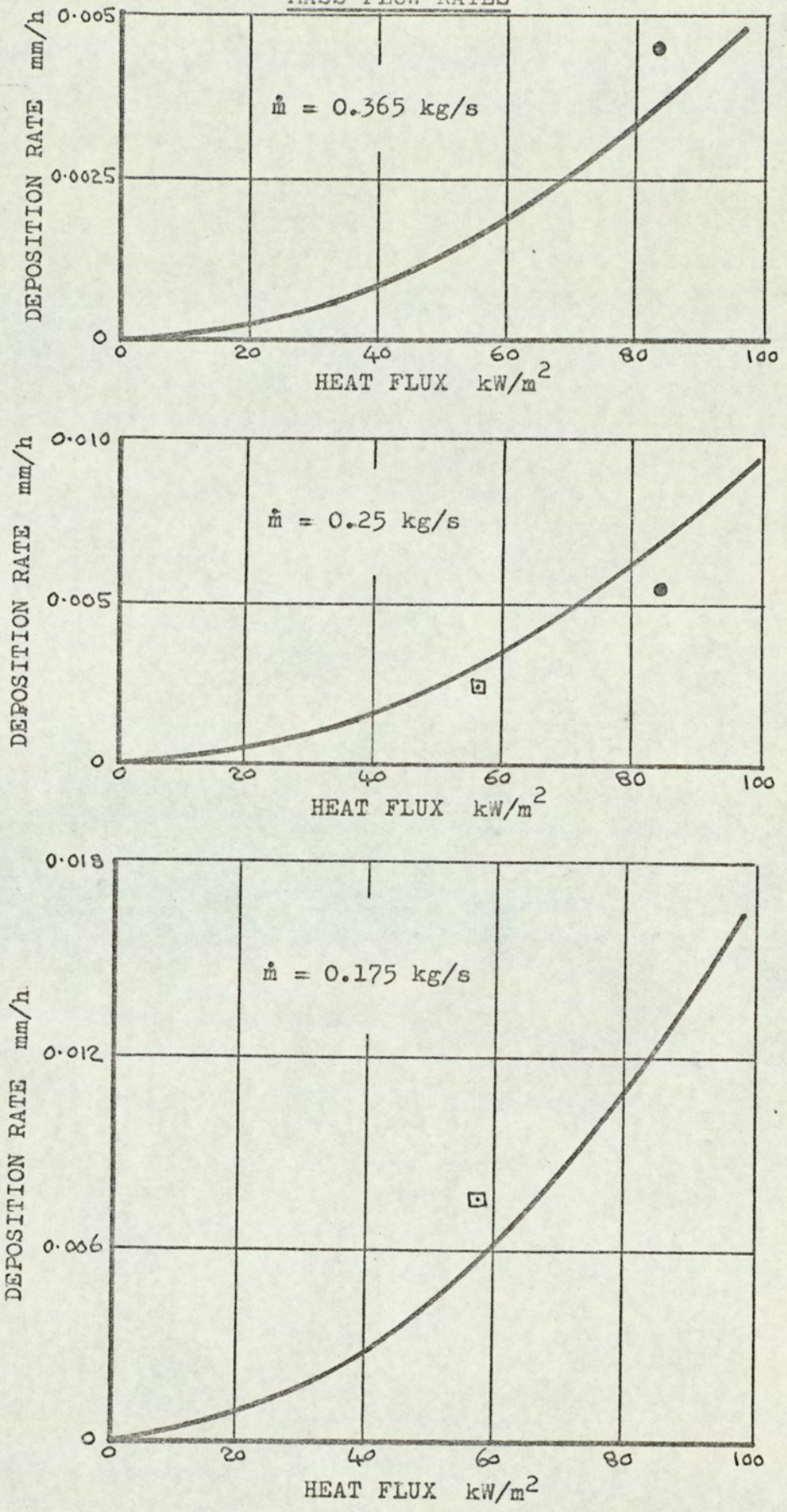

FIG.C6.21

RESULTS SUMMARY

MASS FLOW $\dot{m}$ (kg/s)	HEAT FLUX q'' (kW/m^2)	DEPOSITION RATE $\frac{dx}{dt}$ SCALED TO $\begin{cases} q''=100\ kW/m^2 \\ \dot{m}=0.1\ kg/s \end{cases}$ (mm/h)	RESERVOIR TEMPERATURE (°C)
0.075	40.2	0.0335	18.9
"	46.9	0.0436	20.3
"	49.4	0.0360	19.8
"	52.2	0.0298	20.1
"	38.6	0.0430	20.8
"	74.8	0.0516	23.6
"	65.3	0.0486	22.5
"	32.1	0.0598	21.3
"	23.8	0.0336	19.9
"	78.5	0.0387	21.3
"	69.7	0.0420	22.6
"	55.8	0.0395	20.6
0.2	48.1	0.0410	18.5
"	58.7	0.0453	18.5
"	73.7	0.0548	18.5
"	71.0	0.0348	23.2
"	41.9	0.0280	22.0
"	42.2	0.0259	20.8

continued over...

FIG.C6.22

RESULTS SUMMARY FIG. C6.22 continued

MASS FLOW $\dot{m}$ (kg/s)	HEAT FLUX q'' (kW/m^2)	DEPOSITION RATE $\frac{dx}{dt}$ SCALED TO ($q''=100\ kW/m^2$, $\dot{m}=0.1\ kg/s$) (mm/h)	RESERVOIR TEMPERATURE (^oC)
0.10	59.2	0.0408	21.5
0.10	55.0	0.0543	21.5
0.15	56.6	0.0578	21.5
0.175	57.3	0.0564	21.5
0.25	56.0	0.0336	21.5
0.15	59.7	0.0348	22
0.15	69.9	0.0336	22
0.10	69.3	0.0329	22
0.15	69.3	0.0627	22
0.10	71.2	0.0331	22
0.15	70.3	0.0376	22.5
0.10	84.0	0.0479	23
0.365	83.0	0.0531	21
0.10	81.3	0.0518	22
0.25	84.0	0.0336	22
0.15	83.8	0.0288	22
0.10	40.2	0.0371	22

FIG.C6.22

GRAPH TO OBSERVE THE EFFECT OF RESERVOIR TEMPERATURE

ON SCALING RATE

RESULTS ADJUSTED TO AN EFFECTIVE 100 kW/m^2 & 0.1 kg/s

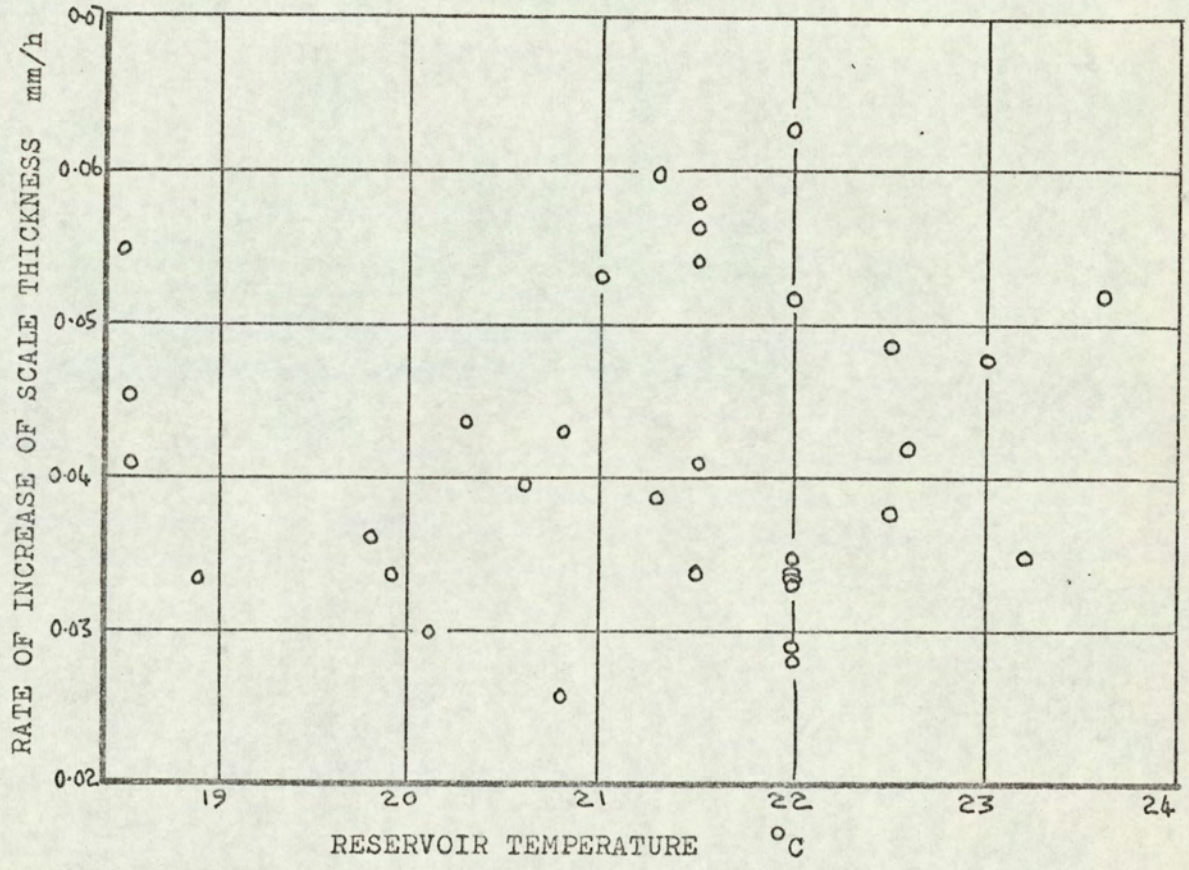

FIG.C6.23

DEPOSITION SEQUENCE

Heating load 1 000W. Mass flow rate 0.1 kg/s.

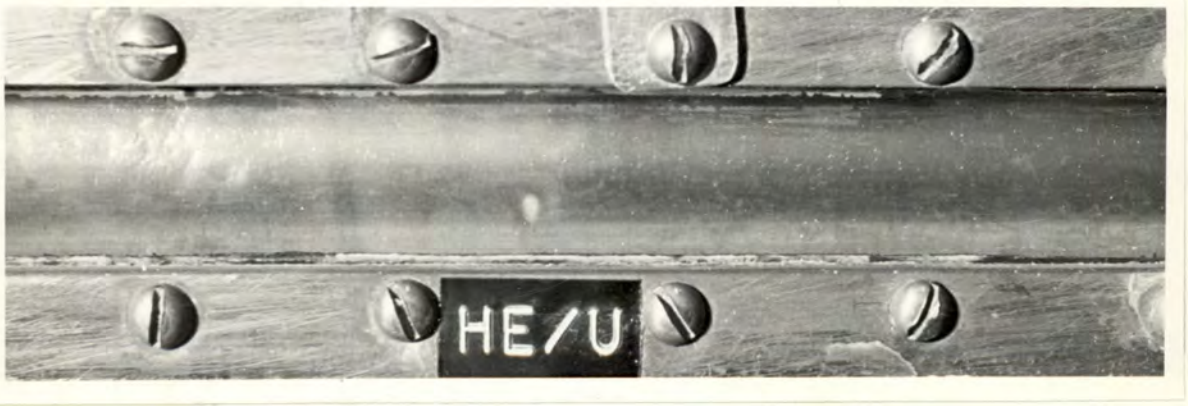

Clean tube

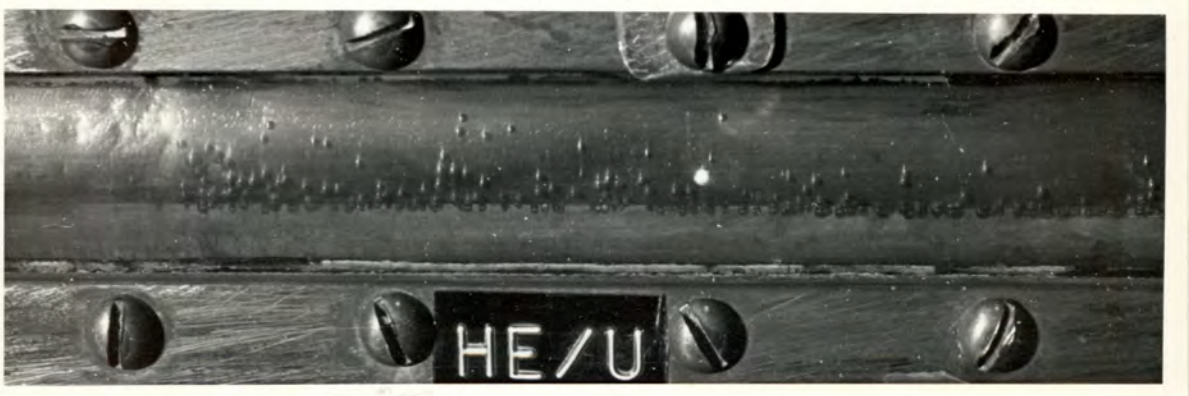

After 0.5 hours

After 1.0 hour

FIG.C6.24

DEPOSITION SEQUENCE

Heating load 1 000W. Mass flow rate 0.1 kg/s.

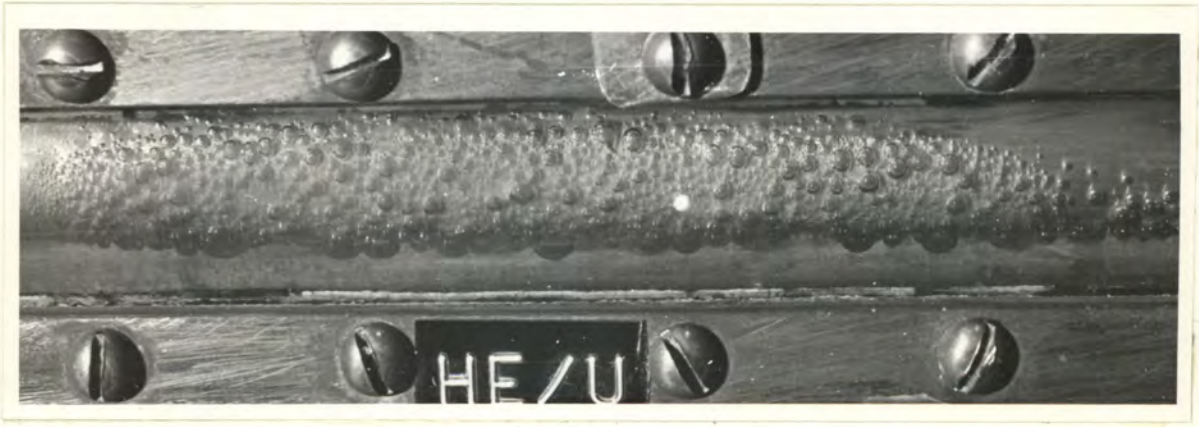

After 1.5 hours

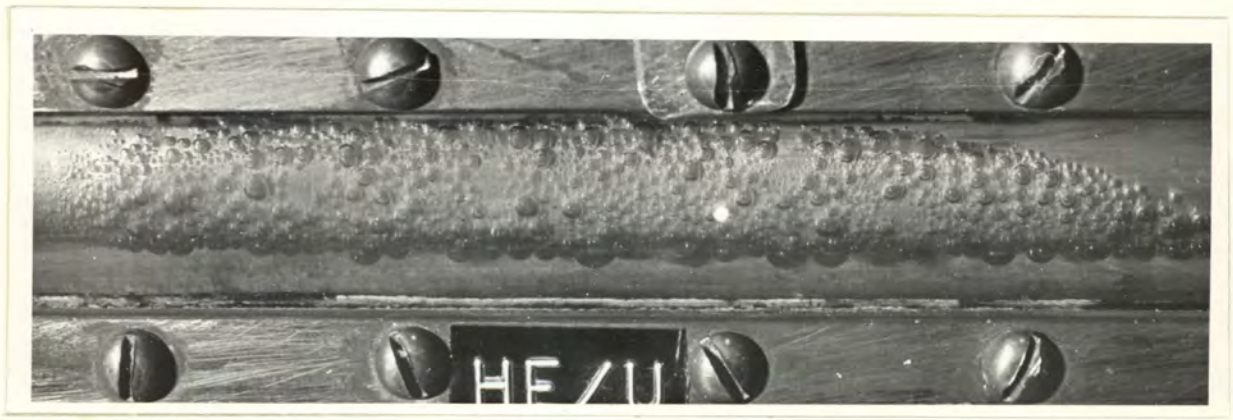

After 2 hours

After 3 hours

FIG.C6.25

DEPOSITION SEQUENCE

Heating load 1 000W. Mass flow rate 0.1 kg/s.

After 4 hours

After 5 hours

After 6 hours

FIG.C6.26

TEMPERATURE RECORDING

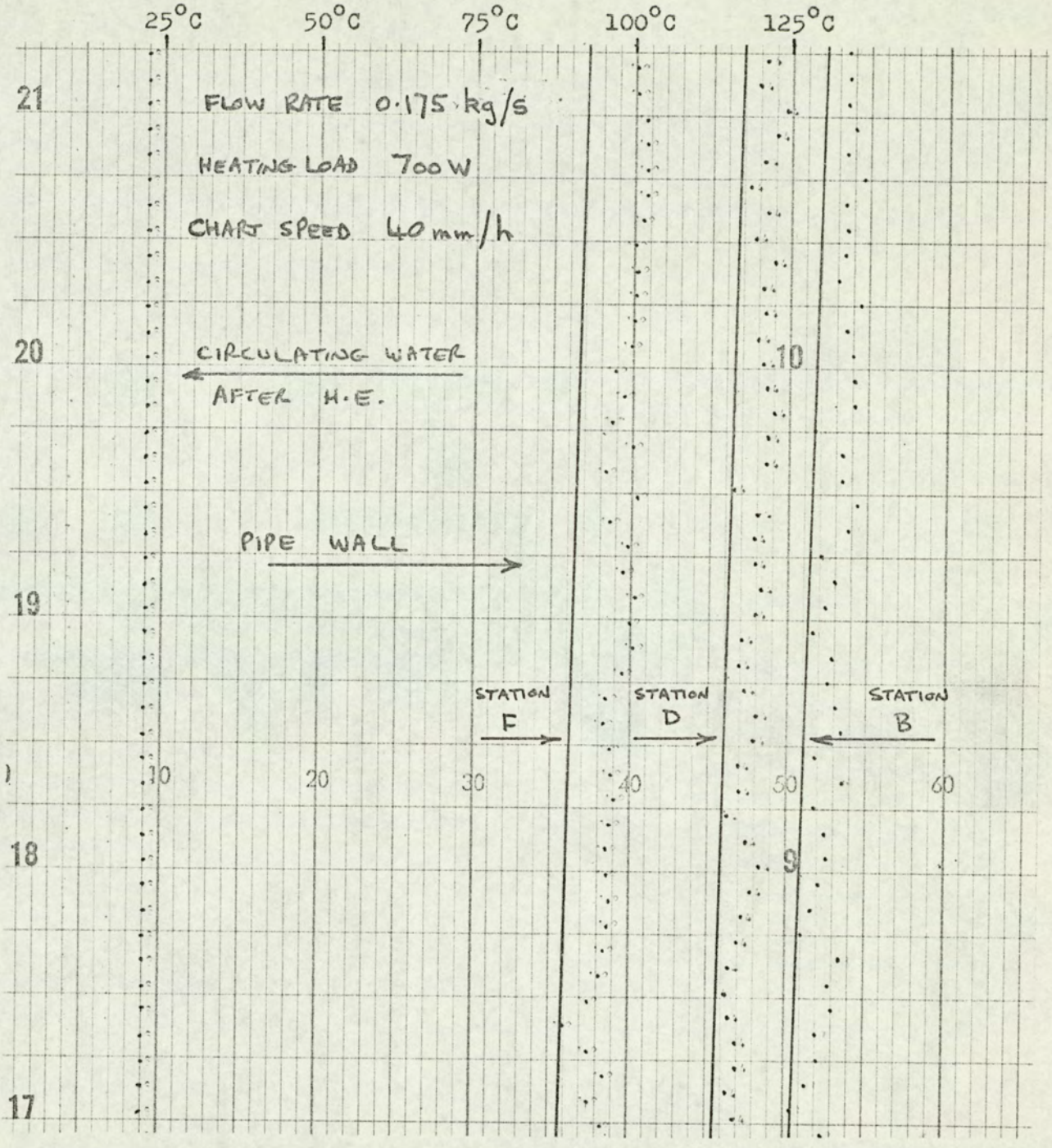

FIG.C6.27

TEMPERATURE RECORDING

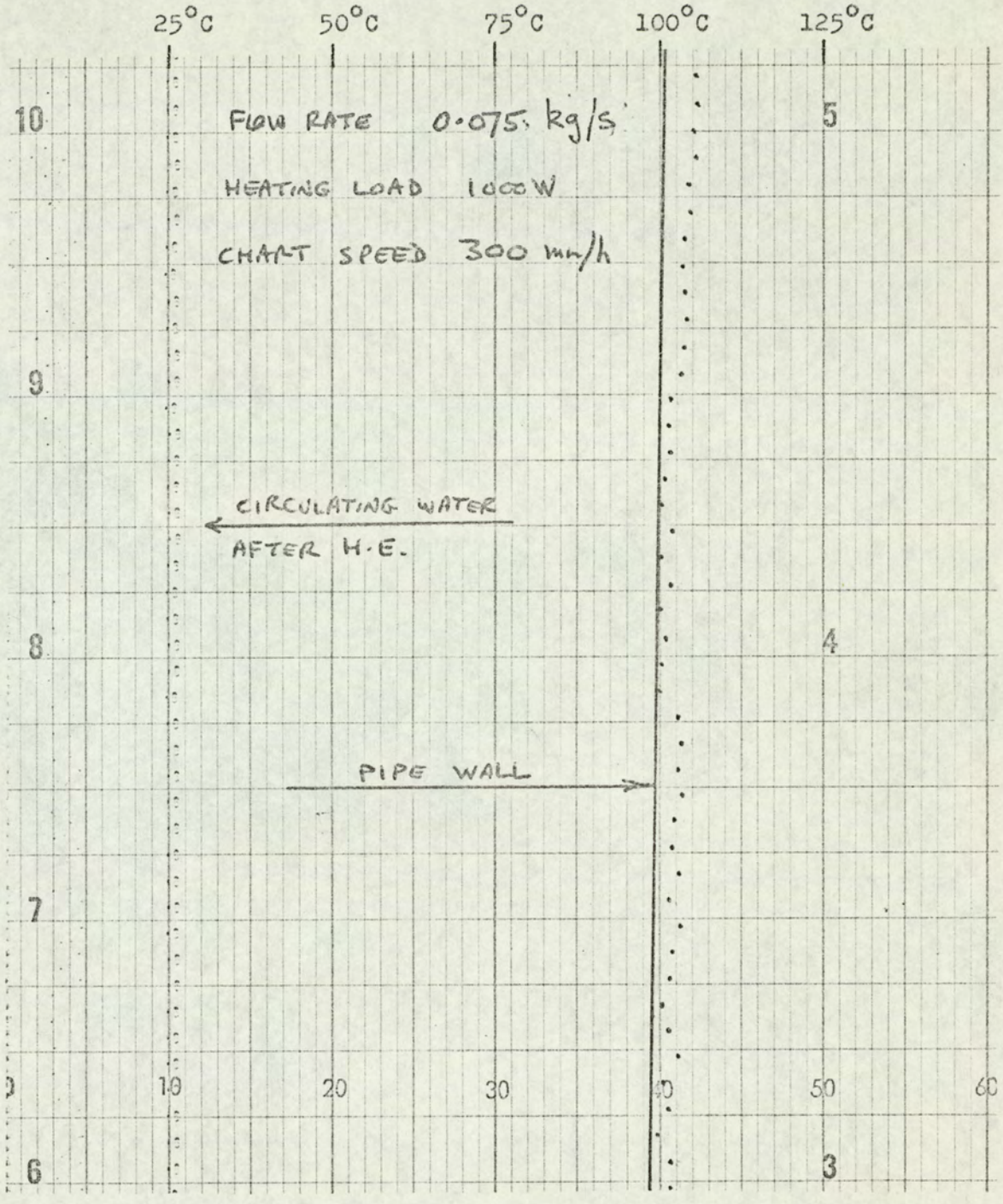

FIG.C6.28

TUBE WITH SCALE PARTIALLY REMOVED SHOWING RELATIVE THICKNESS OF DEPOSITS AND AREAS OF ADHESION TO TUBE

UNDERSIDE (TUBE SIDE) AND EDGE OF SCALE SAMPLE

WATERSIDE OF SCALE SAMPLE

FIG.C6.29

SECTION D

HEAT EXCHANGER ANALYSIS WITH SCALING ON THE TUBE SIDE

CONTENTS

SYMBOLS USED IN SECTION D

B	gradient, equation D2.1
LMTD	logarithmic mean temperature difference
$\dot{m}_c$	mass flow rate of 'cold' liquid
p	exponent in scaling rate law
R_o	initial overall thermal resistance
R_T	overall thermal resistance
t	time
ΔT_{inlet}	temperature difference between incoming liquid streams
y	constant in equation D2.3
z	constant in equation D2.3
n	exponent

CHAPTER D1

Formulation of the problem

In the conventional analysis of the simple double-pipe heat exchanger it is customary to derive an expression for the quantity of heat transmitted which defines the logarithmic mean temperature difference (LMTD).

The LMTD is a function of the 'hot' and 'cold' liquid inlet and outlet temperatures, and its derivation and definition imply a constant thermal resistance throughout the length of the heat exchanger.

Only if the flow passages are of such length that variations in the local heat transfer coefficients in the entry or exit regions or near to bends are small compared with the nearly constant coefficients along the length of the tube is this assumption approached in practice.

Once fouling is present the concept of a constant coefficient of heat transfer with respect to length or time no longer applies. It may be, for example, that a deposition of dirt (as opposed to scale) occurs at some time during the operation of a heat exchanger. Since the thickness of the deposit is unlikely to be uniform along the length of the heat exchanger, the thermal resistance will also vary along the tube.

It is even more likely that a continuous deposition of dirt would occur. In this case the thickness of the deposit becomes dependent on both length and time.

From the literature survey (section B) it is apparent that there is no published information on dirt deposition. (Kern (3)

develops his theory on an assumed constant rate of deposition.)

Until a deposition rate law can be formulated it is impossible to develop a thermal resistance analysis for a heat exchanger.

However, in the case of the deposition of insoluble salts, a scaling rate law relating the rate of increase of scale thickness to the temperature difference between the deposition surface and the bulk liquid (Equations C3.1 and C3.7) can be applied.

It is then possible to determine numerically the relationship between the overall average thermal resistance of the heat exchanger and time. This has been done for both the parallel flow and counterflow arrangements, resulting in a law of the form

$$R_T^{p+1} = R_o^{p+1} + y\left[\frac{z\,\Delta T_{inlet}}{\dot{m}_c^{0.8}}\right]^p t$$

in which y and z are constants, and p is the exponent in the assumed scaling rate law. The analysis leading to this law is described in the following chapter.

CHAPTER D2

THE ANALYSIS

The problem of a variable thermal resistance along the tube is mentioned by Kern (33) in his book on Process Heat Transfer. If a simple relationship between the thermal resistance and tube length is known then an analytical solution may be possible. Otherwise a step by step procedure would be adopted.

In this application where the thermal resistance varies with both length and time the equations have been solved using a numerical step by step calculation with a variety of initial conditions.

The method of calculation is given in paragraph D2.1 below, and the numerical data used in the analysis is specified in paragraph D2.2.

D2.1 Calculation procedures

To simplify the problem scaling on the tubeside only has been considered.

Appendix F2 details the formulae used in the calculations and shows the computer programs used to obtain the results.

A general description of the calculation procedure is as follows.

Firstly, at zero time, having fixed the inlet temperatures and flow rates of the two fluids and specified the size of the heat exchanger the variations in fluid temperature with length are calculated by incrementing along the tube in steps of tube

length/100. For each increment the thermal resistance is found and so the elemental heat flow is known. The total heat flow is, of course, the summation of the elemental values along the tube. Once the temperature profiles are known the LMTD is readily found, and combining this with the total quantity of heat transferred determines the effective overall thermal resistance.

Alongside these calculations the temperature of the tube surface on the 'cold' scaling liquid side is determined for each element of length. This enables a scaling rate to be determined based on the difference in temperatures of the tube surface and the bulk liquid. Therefore for a specified time increment an average thickness of scale deposit is known for each element of length.

So the calculation is repeated for the next increment of time for which the thermal resistances and hence the heat flow values for each element will be changed due to the scale deposit.

Although essentially the same procedure, the analysis of the counterflow heat exchanger has to be modified slightly because the initial specified inlet temperatures are at opposite ends of the exchanger. In order to start the calculation it is necessary to know the liquid temperatures applicable to the first length element.

This difficulty has been solved by adopting an iterative procedure whereby the calculation starts at the 'cold' liquid inlet by guessing a temperature of the 'hot' liquid outlet at that point. The temperature profiles are developed along the tube to the 'hot' liquid inlet where the calculated temperature is compared with the specified temperature. If these

temperatures are not in sufficiently close agreement the guessed 'hot' liquid outlet temperature is modified by the ratio of the required 'hot' liquid inlet temperature to the calculated 'hot' liquid inlet temperature. New temperature profiles are calculated and the cycle repeats until the desired level of agreement is achieved. In the program the calculated temperature had to be within 1% of the specified temperature before the temperature profiles would be accepted for the completion of the calculations.

The iteration procedure had to be carried out at each successive interval of time due to the changing thermal resistance along the tube.

D2.2 Selection of data for the example

The calculations are based on water as the 'hot' and the 'cold' liquid and the same sets of data apply to both the parallel flow and the counterflow analyses.

The following list shows that part of the data common to all calculations:

tube length	1 m
tube radius	0.0127 m
specific heat of water	4.18×10^3 J/kg deg C
surface coefficient of heat transfer on 'hot' side	4.44×10^3 W/m^2 deg C
flow rate of 'hot' water	1.5 kg/s
thermal conductivity of 'cold' water	0.6 W/m deg C
dynamic viscosity of 'cold' water	10.1×10^{-4} kg/ms
inlet temperature of 'cold' water	20°C
scaling rate constant	1.25×10^{-7}
scale material density	1600 kg/m^3
scale material thermal conductivity	1.5 W/m deg C

With this basic data, three variables were introduced. These are the mass flow rate of the 'cold' water, the exponent in the scaling rate law, and the 'hot' water inlet temperature. The 'hot' water inlet temperature in conjunction with the 'cold' water inlet temperature is more usefully interpreted as the inlet temperature difference between the two streams.

Fig. D2.1 tabulates values of these variables together with their data reference numbers D12.0 to D16.1

D2.3 Presentation and analysis of results

The results of trial data used to check the parallel flow program P12B suggested that the form of the thermal resistance - time law was likely to be:

$$R_T^{p+1} = R_o^{p+1} + B\,t \qquad \text{(D2.1)}$$

This relates the thermal resistance R_T at time t to the initial thermal resistance R_o. Therefore the programs for the parallel flow and the counterflow heat exchangers had the calculation R_T^{p+1} written in to them.

All sets of data were applied to the simpler parallel flow program P12B and the results analysed in a series of graphs.

The following equation agrees with the computed results to within ± 3%.

$$R_T^{p+1} = R_o^{p+1} + \frac{2.5}{10^7}\left[\frac{2.18}{10^4}\,\frac{\Delta T_{inlet}}{\dot{m}^{0.8}}\right]^p t \qquad \text{(D2.2)}$$

Three sets of data comparing different values of p (D12.1, D14.1, D16.1) were used with the counterflow program P13 and the results also agreed with equation D2.2 therefore, bearing in mind the extra computing time involved in P13, it was not considered necessary to work through the remaining data.

The verification of equation D2.2 was as follows:

(i) For all data, plotting (thermal resistance)$^{p+1}$ against time gave straight lines of the form

$$R_T^{p+1} = R_o^{p+1} + Bt$$

The gradient B was given the form

$$B = y\left[z\,\frac{\Delta T_{inlet}}{\dot{m}_c^{\,n}}\right]^p \qquad (D2.3)$$

where y and z are constants, and checked by

(ii) Using data D12.0, 12.1, 12.2, and 12.3, for which $\dot{m}_c$ varied, plotting log B against log $\dot{m}_c$ to give a straight line.

(iii) Using data D12.2, 12.4, 12.5 and 12.6 for which ΔT_{inlet} varied, plotting log B against log ΔT_{inlet} to give a straight line.

(iv) Using data D12.1, 13.1, 14.1, 15.1, 16.1 for which p varied, plotting log B against p to give a straight line.

The equations of the lines resulting from (ii), (iii) and (iv) led to the value of B quoted in equation D2.2.

A typical set of output figures for program P12B is shown on Fig. D2.2 in which the thermal resistance is designated 1/U. The output from program P13 follows the same form with the additional printing of the 'hot' liquid inlet temperature calculated by the iterative procedure. This gave a visible check against the specified inlet temperature of 85°C.

Fig. D2.3 shows the effect of varying mass flow rate on the thermal resistance characteristic and Fig. D2.4 shows the effect of varying the inlet temperature difference.

These results are from the parallel flow analysis. A typical comparison between the parallel flow and counterflow

arrangements for the same input data is shown on Fig. D2.5.

A set of thermal resistance - time characteristics is shown in Fig. D2.6 for various values of the exponent p in the scaling rate law.

HEAT EXCHANGER ANALYSIS

TABLE SHOWING COMBINATIONS OF VARIABLES USED IN DATA

DATA REFERENCE NUMBER	D12.0	D12.1	D12.2	D12.3	D12.4	D12.5	D12.6	D13.1	D14.1	D15.1	D16.1
MASS FLOW RATE OF 'COLD' WATER $\dot{m}_c$ kg/s	0.5	1.5	1.0	2.0	1.0			1.5			
'HOT' WATER INLET TEMPERATURE T_{hi} °C	85				95	90	80	85			
INLET TEMPERATURE DIFFERENCE T_{inlet} deg C	65				75	70	60	65			
EXPONENT IN SCALING RATE LAW p	1.00							1.25	1.50	1.75	2.00
DATA COMMON TO ALL CASES IS LISTED IN CHAPTER D2 PARAGRAPH D2.2											

FIG.D2.1

TYPICAL OUTPUT FOR PROGRAM P12B

(PARALLEL-FLOW HEAT EXCHANGER)

DATA D 13.1

```
P=
 1.2500000
T= .00000000    1/U= .00033189    1/U TO (P+1)= .01486749
T= 8.0000000    1/U= .00039203    1/U TO (P+1)= .02162508
T= 16.000000    1/U= .00044197    1/U TO (P+1)= .02832196
T= 24.000000    1/U= .00048551    1/U TO (P+1)= .03498992
T= 32.000000    1/U= .00052456    1/U TO (P+1)= .04164184
T= 40.000000    1/U= .00056022    1/U TO (P+1)= .04828408
T= 48.000000    1/U= .00059322    1/U TO (P+1)= .05492015
```

DATA D 14.1

```
P=
 1.5000000
T= .00000000    1/U= .00033189    1/U TO (P+1)= .00200672
T= 6.0000000    1/U= .00042338    1/U TO (P+1)= .00368836
T= 12.000000    1/U= .00049013    1/U TO (P+1)= .00531850
T= 18.000000    1/U= .00054484    1/U TO (P+1)= .00692896
T= 24.000000    1/U= .00059205    1/U TO (P+1)= .00852883
T= 30.000000    1/U= .00063403    1/U TO (P+1)= .01012200
T= 36.000000    1/U= .00067209    1/U TO (P+1)= .01171052
```

DATA D 15.1

```
P=
 1.7500000
T= .00000000    1/U= .00033189    1/U TO (P+1)= .00027085
T= 4.0000000    1/U= .00045433    1/U TO (P+1)= .00064236
T= 8.0000000    1/U= .00053169    1/U TO (P+1)= .00098982
T= 12.000000    1/U= .00059203    1/U TO (P+1)= .00133030
T= 16.000000    1/U= .00064268    1/U TO (P+1)= .00166719
T= 20.000000    1/U= .00068688    1/U TO (P+1)= .00200184
T= 24.000000    1/U= .00072642    1/U TO (P+1)= .00233491
T= 28.00000     1/U= .00076239    1/U TO (P+1)= .00266676
```

COLUMN	QUANTITY	UNITS
T	Time t	h
1/U	Thermal resistance R_T	m^2degC/W
1/U to (p+1)	(Thermal resistance)$^{p+1}$	$10^6(m^2\text{degC/W})^{p+1}$

FIG.D2.2

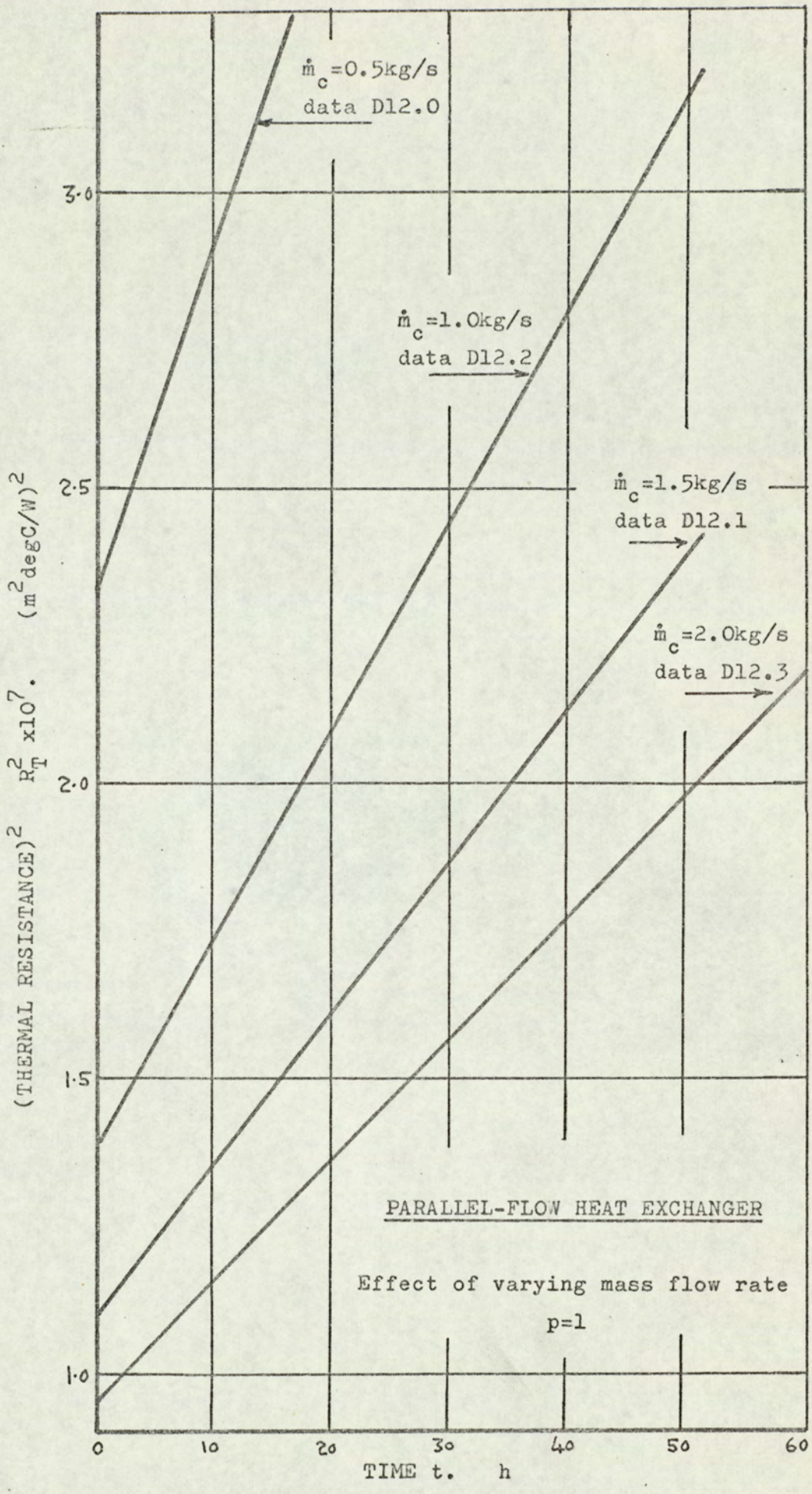
$\dot{m}_c$=0.5kg/s
data D12.0
$\dot{m}_c$=1.0kg/s
data D12.2
$\dot{m}_c$=1.5kg/s
data D12.1
$\dot{m}_c$=2.0kg/s
data D12.3
PARALLEL-FLOW HEAT EXCHANGER
Effect of varying mass flow rate
p=1
(THERMAL RESISTANCE)^2 R_T^2 x10^7. (m^{2}degC/W)^2
3·0
2·5
2·0
1·5
1·0
0
10
20
30
40
50
60
TIME t. h

FIG.D2.3

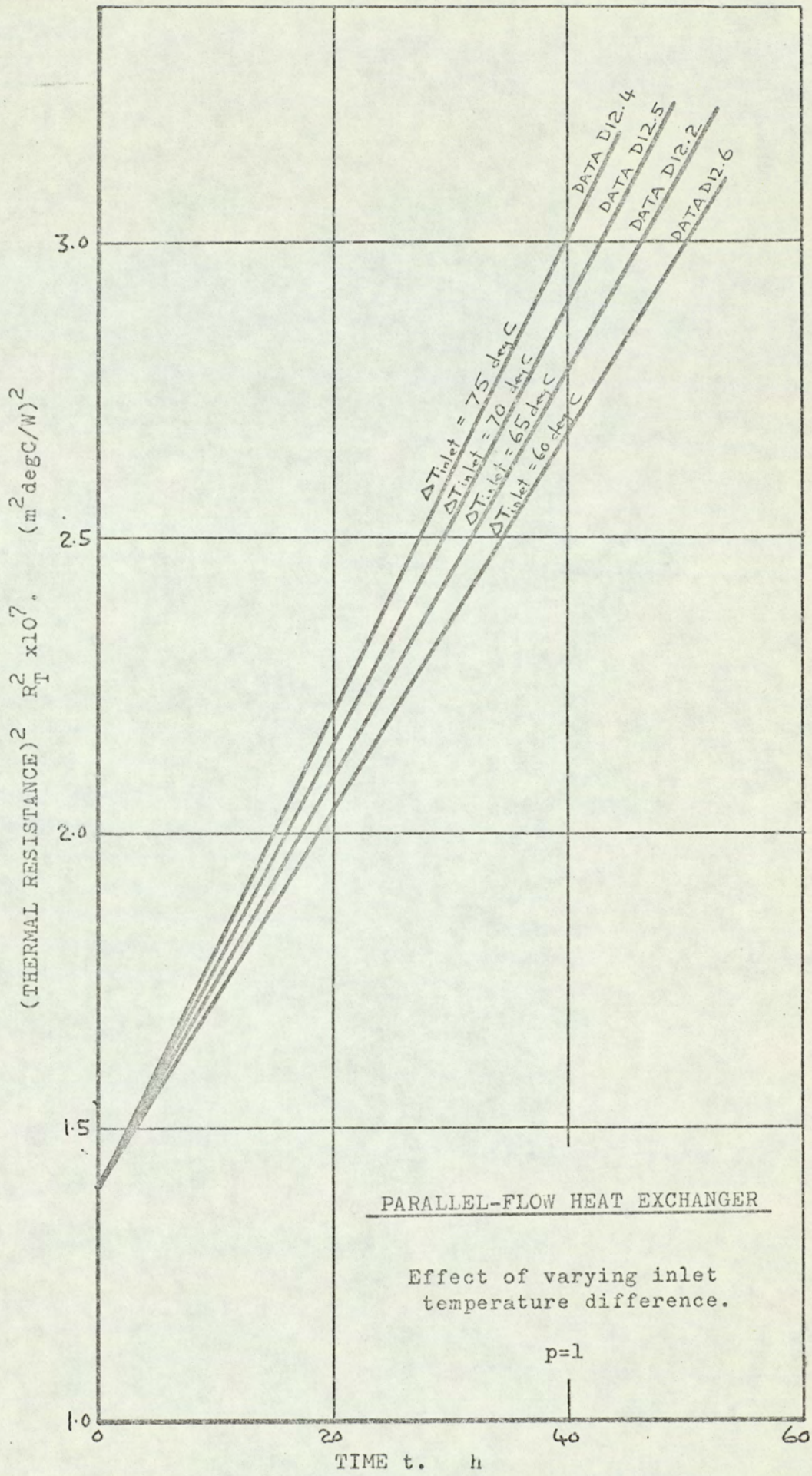
DATA D12.4
DATA D12.5
DATA D12.2
DATA D12.6
ΔTinlet = 75 deg C
ΔTinlet = 70 deg C
ΔTinlet = 65 deg C
ΔTinlet = 60 deg C
3.0
2.5
2.0
1.5
1.0
0
20
40
60
TIME t. h
(THERMAL RESISTANCE)² R²T x10⁷. (m² degC/W)²
PARALLEL-FLOW HEAT EXCHANGER
Effect of varying inlet temperature difference.
p=1

FIG. D2.4

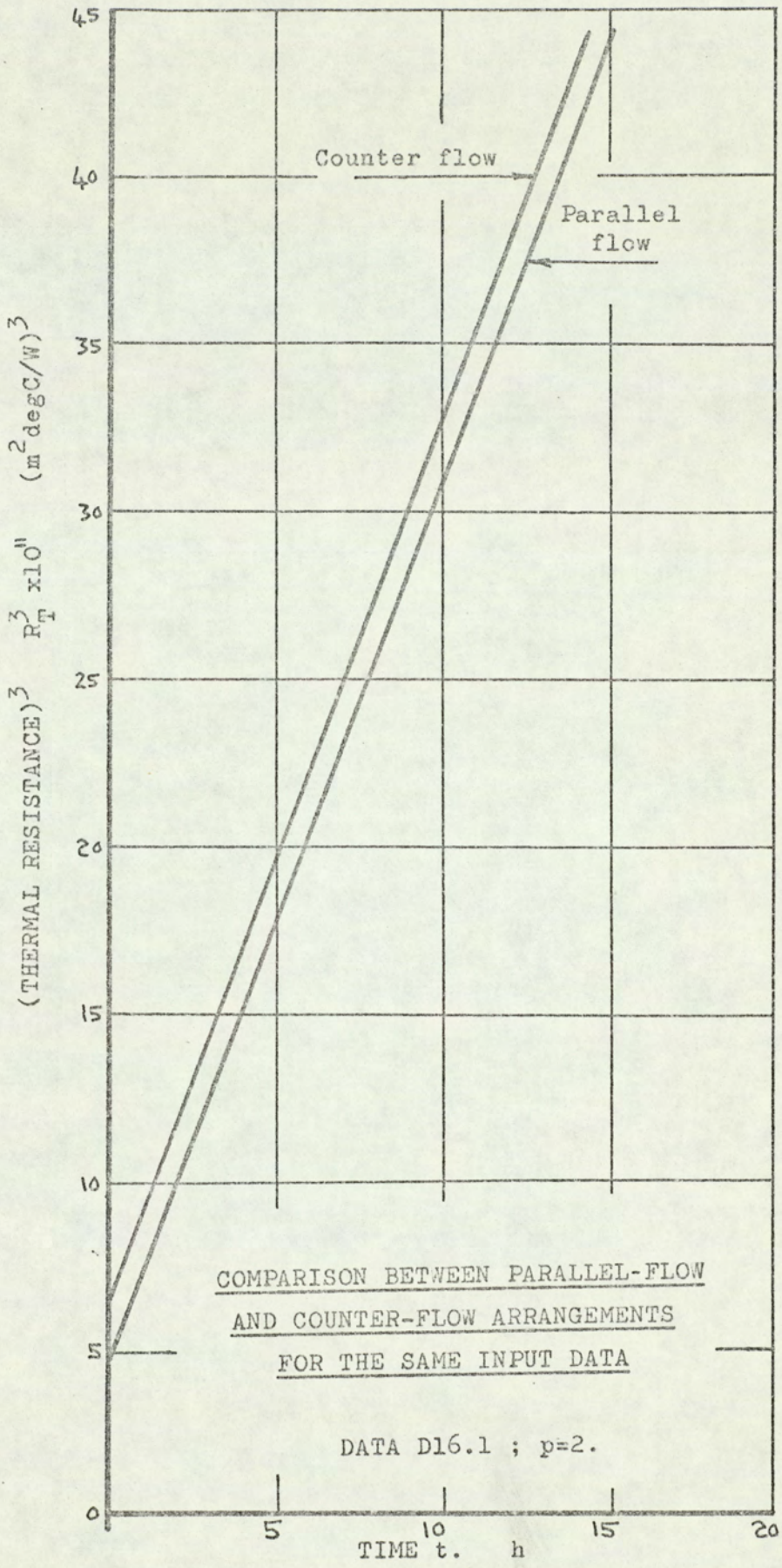
45
40
35
30
25
20
15
10
5
0
Counter flow
Parallel flow
(THERMAL RESISTANCE)^3 R_T^3 x10^{11} (m^{2}degC/W)^3
COMPARISON BETWEEN PARALLEL-FLOW
AND COUNTER-FLOW ARRANGEMENTS
FOR THE SAME INPUT DATA
DATA D16.1 ; p=2.
5
10
15
20
TIME t. h

FIG. D2.5

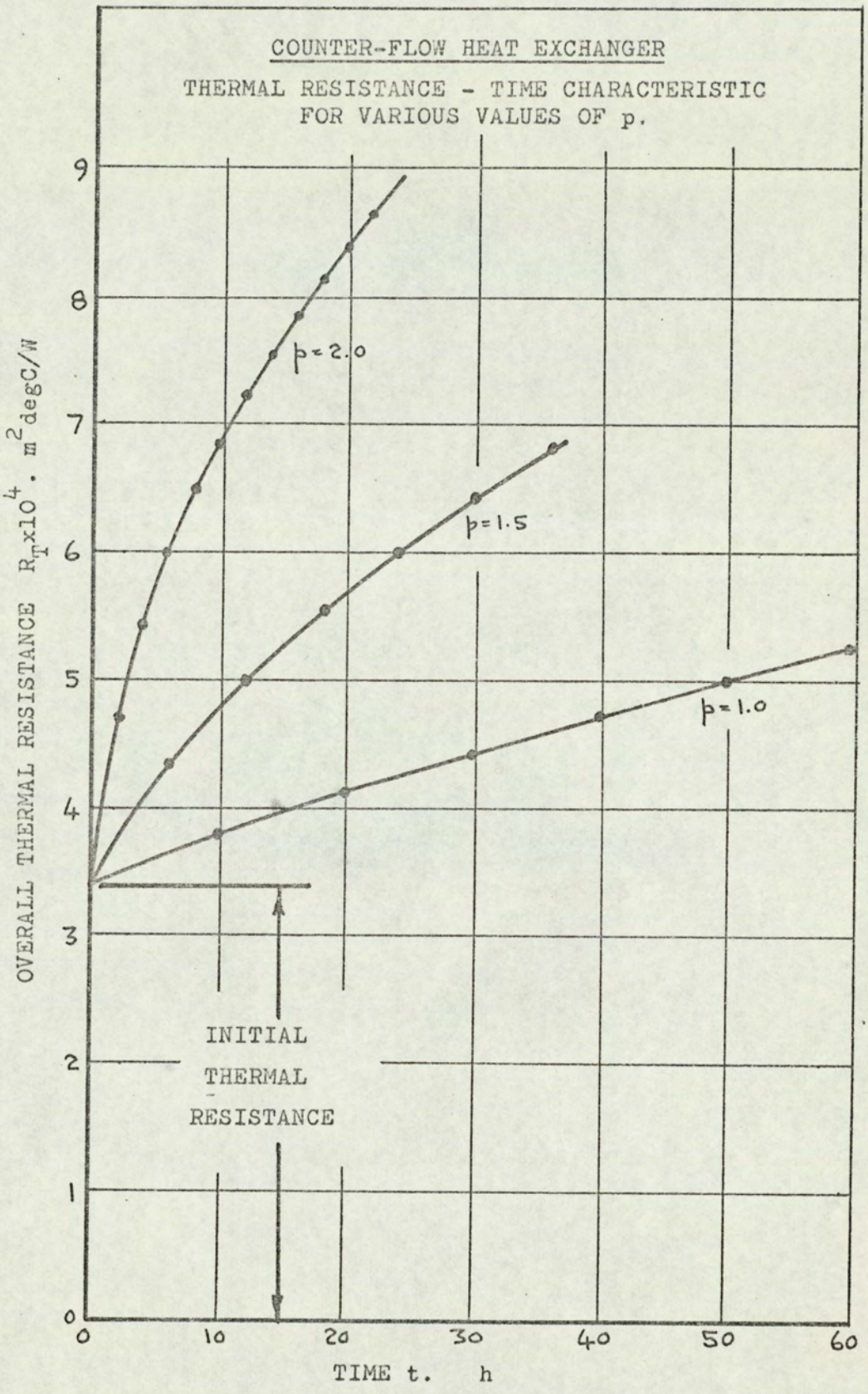
COUNTER-FLOW HEAT EXCHANGER
THERMAL RESISTANCE - TIME CHARACTERISTIC
FOR VARIOUS VALUES OF p.
OVERALL THERMAL RESISTANCE $R_T \times 10^4$. $m^2 degC/W$
TIME t. h
p = 2.0
p = 1.5
p = 1.0
INITIAL
THERMAL
RESISTANCE
0
1
2
3
4
5
6
7
8
9
0
10
20
30
40
50
60

FIG D2.6

CHAPTER D3

DISCUSSION

The foregoing analysis shows that an expression can be derived for the thermal resistance - time characteristic for the simple parallel flow or counterflow heat exchanger subject to scaling by insoluble salts.

In fact the analysis shows the same type of law for both cases, the only difference being in the initial thermal resistance of the clean heat exchanger (Fig. D2.5).

The term $\dot{m}_c^{0.8}$ in equation D2.2 clearly originates from the heat transfer coefficient applied to the scale surface - liquid interface on the tube side, and shows that an increased mass flow rate will diminish the rate of fouling. This is to be expected since the resulting improved heat transfer coefficient at the scale surface would reduce the temperature of the surface and so reduce the rate of deposition (Equation F2.9).

One of the difficulties in predicting the thermal resistance of a heat exchanger from operating data at an early stage in its history is to know what type of law to fit through the available points. In practice, considerable scatter may be experienced (Section B3.4) and a variety of laws could reasonably be drawn through the points. This analysis shows that, for the type of deposition analysed, the basic scaling rate law suggests the general form of the thermal resistance characteristic in specifying the exponent p.

Although the analysis has been based on a specific set of data this data was chosen as being fairly representative of a practical situation. There is no reason to suspect a different result from the analysis had the data been changed. Also the similarity between the derived formula (Equation D2.2) and the result of the theoretical analysis of a simpler arrangement described by Reitzer (18) supports the view that the numerical solution applies outside the range of the example described.

SECTION E

CLOSING DISCUSSION

CONTENTS

SYMBOLS USED IN SECTION E

B_n	a coefficient
n	exponent
p	exponent
R_o	initial thermal resistance
R_T	thermal resistance at time t
T_s	temperature at scale - liquid interface
T_b	temperature of bulk liquid
t	time

SECTION E

DISCUSSION

Fouling has been a problem to the designer, manufacturer, and user of heat exchanger equipment for many years.

The history of published work began in 1924 with the paper by McCabe and Robinson (9) on scaling in evaporators. For the next thirty years there were no further theoretical developments, and then in 1959, Kern and Seaton (2) published their theoretical analysis of fouling, in which they first introduced their shear removal theory. In the last decade, more work has been published with varying degrees of theoretical and practical content (Table A2.1 and Section B).

The literature, with its variety of comment, indicates the complex nature of fouling and the need for a better understanding of the problem.

Calculations (paragraph A1.3) show that even after a small amount of deposition the foulant can become the principal resistance to heat transfer. Therefore sophisticated calculations of surface coefficients become almost meaningless once a tube is fouled. The use of the fouling factor results in oversurfacing and this, in turn, could increase the areas of stagnant fluid within a heat exchanger, resulting in more rather than less fouling.

Again, the fouling factor is not time-dependent, and so it gives no indication as to when the minimum acceptable performance will be achieved. Consequently heat exchanger equipment is frequently overdesigned.

Accepting all this, there is clearly an urgent need for the

collection and publication of performance data on heat exchangers so that patterns of behaviour can be investigated. Hudson (1) suggests a classification of fouling (chapter A1) and it would be useful to know if any one type of fouling predominates. A knowledge of this would suggest the most beneficial area for research.

Again, collective information might also reveal if any particular design of heat exchanger was unusually prone to fouling.

The difficulty of postulating questions which would lead to fruitful researches has undoubtedly been one of the factors responsible for the relatively small amount of published work.

It seems, from the literature survey, that fouling is widely accepted as inevitable, and therefore the emphasis is on trying to determine its effect on the thermal performance of heat exchanger equipment. To this end, the interesting characteristic is the thermal resistance - time relationship, an understanding of which would allow a prediction of the variation of the thermal resistance of a heat exchanger with time to be made. Some theoretical and practical work has been concerned with this thermal resistance characteristic (Section B). This work shows that the performance data can generally be satisfied by

$$R_T^n = R_o^n + B_n t$$

There are practical difficulties in establishing the law through test data. These difficulties arise partly due to the overall scatter of results and partly due to inconsistencies in the trend of results. If a wide scatter band is apparent but the trend is towards a steadily increasing thermal resistance then the more data that can be collected in a given time, the

more reliable will be the prediction based on that data.

It must also be appreciated that the slower the scaling rate the more difficult it becomes to predict the time at which a specified maximum allowable thermal resistance would occur. Under these circumstances a slight change to the predicted characteristic could make a difference in the anticipated service time of several weeks.

Before attempting to fit a law to observed data it is better to be able to anticipate the type of law rather than being guided solely by the trend of results.

It is this point which underlies the research reported in this thesis.

Fouling can manifest itself in various forms and it was decided to base the work on that aspect concerned with the deposition of insoluble salts on heated surfaces.

The analysis of the thermal resistance characteristic of a simple scaling configuration by Reitzer (18) suggests a connection between the scaling rate law for an 'inverse solubility' salt, and the form of the thermal resistance - time law.

The research was directed towards verifying the nature of the scaling rate law for calcium sulphate, and subsequently analysing the performance of a simple heat exchanger with scaling on the tube side. Calcium sulphate was chosen because of its reputation as a troublesome scaling salt, and it possesses the necessary inverse solubility characteristic. The experimental work (Section C) established a scaling rate law (equation C6.3) for the range of tests conducted and this law is in agreement with the general form,

$$\frac{dx}{dt} \propto (T_s - T_b)^p$$

This law was applied to the analysis of a simple heat exchanger (Section D) with a view to deriving a relationship between the overall thermal resistance, and time.

For both parallel flow and counterflow arrangements, the result takes the general form:

$$R_T^n = R_o^n + B_n t$$

Whilst the dependence of the coefficient B_n on liquid mass flow rate and the overall inlet temperature difference was investigated, of primary interest was the index n. It was found that $n = p + 1$ where p is the exponent in the scaling rate law. This suggests that a knowledge of the deposition rate law for a particular scaling salt can suggest the form of the thermal resistance characteristic to be expected for a heat exchanger subject to that type of scaling.

The work reported in this thesis can only be a small contribution towards an appreciation of the complex problem of fouling. Time has limited the research to just one aspect of the subject. Undoubtedly the time factor involved in test programmes is responsible for the scarcity of practical data. Bearing in mind the estimated cost of fouling to the heat exchanger industry (Chapter A2), even a lengthy test programme might well be justified.

That aspect of fouling concerned with dirt deposition represents an unexplored area and offers considerable scope for future researches. How can one classify dirt? Why does dirt adhere to the tube surface? Is the deposition affected by the flow pattern, temperature, or tube surface condition? These are some of the questions which could be the basis of further investigations into the fouling of heat exchanger equipment.

SECTION F

APPENDICES

CONTENTS

APPENDIX F1

SCALING INSIDE A CIRCULAR TUBE (ISOTHERMAL BOUNDARIES)

F1.1 Symbols

C	specific heat of liquid
c_b	saturation concentration of scaling salt at T_b
c_s	saturation concentration of scaling salt at T_s
h	surface coefficient of heat transfer
k	thermal conductivity of liquid
k_s	thermal conductivity of scale material
K_1	a constant
K_2	rate coefficient
$\dot{m}$	mass flow rate of liquid
m_s	mass of scale
p	index in scaling rate equation
q'	heat flow per unit length
R	inside radius of tube
R_T	overall thermal resistance
t	time
T_b	bulk liquid temperature
T_s	scale - liquid interface temperature
T_w	tube wall temperature
x	scale thickness
ρ_s	density of scale material
μ	dynamic viscosity of liquid

F1.2 Interface temperature

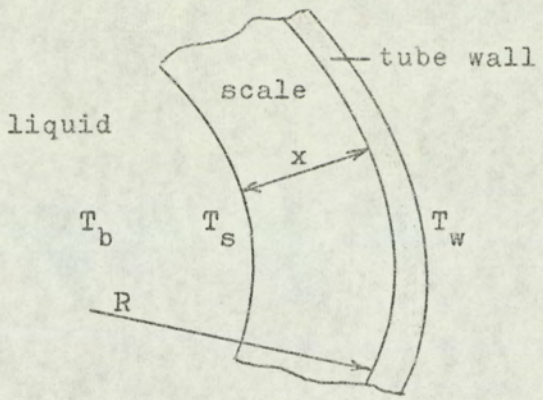

Suppose the tube wall temperature T_w, and the bulk liquid temperature T_b are held constant, then the scale - liquid interface temperature T_s will vary as the scale thickness x increases.

The heat flow per unit length of tube of inside radius R, based on the thermal resistance of the scale layer at any instant is given by:

$$q' = \frac{2\pi k_s (T_w - T_s)}{\ln\left[\frac{R}{R - x}\right]} \qquad (F1.1)$$

or, based on the surface coefficient of heat transfer h, at the scale - liquid interface:

$$q' = h \cdot 2\pi (R - x)(T_s - T_b) \qquad (F1.2)$$

The Dittus - Boelter equation gives:

$$h = 0.023 \frac{k}{(2R - 2x)} \left[\frac{4\dot{m}}{\pi(2R - 2x)\mu}\right]^{0.8} \left[\frac{C\mu}{k}\right]^{0.4}$$

which rearranges into:

$$h(R - x) = \frac{K_1}{(R - x)^{0.8}} \qquad (F1.3)$$

where $K_1 = 0.0115k\left[\frac{2\dot{m}}{\pi\rho}\right]^{0.8} \left[\frac{\mu C}{k}\right]^{0.4}$

Equations (F1.1), (F1.2) and (F1.3) can be combined to eliminate q', and h and the result presented as an equation for

the interface temperature to give:

$$T_s = \frac{k_s T_w (R - x)^{0.8} + K_1 T_b \ln\left[\frac{R}{R - x}\right]}{k_s (R - x)^{0.8} + K_1 \ln\left[\frac{R}{R - x}\right]} \qquad (F1.4)$$

F1.3 Rate of deposition

To complete this analysis it is necessary to specify a law governing the rate of deposition. The literature (18) suggests:

$$\frac{dm_s}{dt} \propto 2\pi (R - x)(c_b - c_s)^p$$

in which the concentration difference is the driving force causing scale deposition. The value of the index p depends on the relative extent to which mass transfer or crystal surface reaction predominates. For this analysis a value p = 1 has been chosen.

With a salt having an inverse solubility characteristic, this concentration difference would arise from the temperature gradient which would occur in a solution flowing past a heated surface.

The equation then becomes, for unit length of heated tube:

$$\frac{dm_s}{dt} = 2\pi (R - x) K_2 (T_s - T_b) \qquad (F1.5)$$

The constant K_2 is called the rate coefficient. Whilst K_2 is dependent both upon the temperature at the scale surface and also upon the Reynolds' number in a particular application it may be regarded as sensibly constant.

From the geometry of the scale build-up the rate of mass deposition is related to the rate of increase of scale thickness by:

$$\frac{dm_s}{dt} = 2\pi (R - x) \rho_s \frac{dx}{dt}$$

and eliminating $\frac{dm_s}{dt}$ we have:

$$\frac{dx}{dt} = \frac{K_2}{\rho_s}(T_s - T_b) \qquad \text{(Fl.6)}$$

Fl.4 Thermal resistance

The overall thermal resistance based on the inside of the tube is given by

$$R_T = \frac{R}{k_s} \ln\left(\frac{R}{R - x}\right) + \left(\frac{R}{R - x}\right) \frac{1}{h}$$

$$= \frac{R}{k_s} \ln\left(\frac{R}{R - x}\right) + \frac{R}{K_1}(R - x)^{0.8}$$

so that

$$\frac{dR_T}{dx} = \frac{R}{k_s(R - x)} - \frac{0.8R}{K_1(R - x)^{0.2}} \qquad \text{(Fl.7)}$$

Equations Fl.4, Fl.6 and Fl.7 now describe the variation in scale thickness and overall thermal resistance with time.

A numerical solution was considered to be the most expedient in which the differentials are expressed as finite differences. A computer program was written in Elliot-Algol language to perform a step by step calculation from zero time (with no scale) through regular time increments until the scale thickness built up to one quarter of the clean tube radius.

Fig. Fl.1 summarises corresponding text and program symbols together with the units used. A copy of the program appears as Fig. Fl.2 and its associated data list is shown on Fig. Fl.3. The output is tabulated in Figs. Fl.4 (a) to (d).

Fl.5 Comment on data used

Various bulk water temperatures are specified, the lowest

(20°C) being representative of a town's mains supply. Fluid properties are specified according to the bulk water temperature, and the range of mass flow rates corresponds to a range of Reynolds' numbers from 10 000 to 50 000. For the tube size chosen this means that velocities vary from approximately 0.4 to 2 m/s typifying many heat exchanger applications.

The rate coefficient value is representative of the results obtained in the test programme described in Section C.

ISOTHERMAL BOUNDARIES PROGRAM

SYMBOLS AND UNITS

TEXT SYMBOL	PROGRAM SYMBOL	UNITS
R	R	m
k	K	W/m deg C
K_1	K1	-
K_2	K2	kg/m^2 s deg C
k_s	KS	W/m deg C
c	C	J/kg deg C
ρ	MU	kg/m s
$\dot{m}$	M	kg/s
ρ_s	RHOS	kg/m^3
q'	Q	W/m
t	T	s
x	X	m
T_w	TW	^oC
T_b	TB	^oC
T_s	TS	^oC
R_T	RT	m^2 deg C/W
Y	Y	-
Δx	DELX	m
Δt	DELT	s
ΔR_T	DELRT	m^2 deg C/W
-	N	PROGRAM SWITCHING PARAMETERS
-	B	
-	J	

FIG.F1.1

'ISOTHERMAL BOUNDARIES' PROGRAM

```
'ISOTHERMAL BOUNDARIES'

BEGIN REAL J, R,K,K1,K2,KS,C,MU,M,RHOS,Q,T,X,Y,TW,TB,TS,RT,DELX,
                DELT,DELRT'
        INTEGER N,B'
        SWITCH S:=REPEAT,AGAIN,START'
START:      B:=0'
                      READ N,R,K,K2,KS,C,RHOS'
   REPEAT:    READ TW,TB,M,MU'
  PRINT TW,ΣΣS8??,SAMELINE,TB,ΣΣS8??,M'
   X:=R/1000'      T:=0'
    DELX:=R/50'
     K1:=0.0115*K*(2*M/3.1416/MU)**0.8*(MU*C/K)**0.4'
   RT:=R/KS*LN(R/(R-X))+R/K1*(R-X)**0.8'
    AGAIN:BEGIN
       TS:=(KS*TW*(R-X)**0.8+K1*TB*LN(R/(R-X)))/(KS*(R-X)**0.8
                                +K1*LN(R/(R-X)))'
         Q:=6.2832*K1*(TS-TB)/(R-X)**0.8'
      PRINT T,PREFIX(ΣΣS2??),X,Q,RT'


     Y:=R/KS/(R-X)-0.8*R/K1/(R-X)**0.2'
        DELRT:=Y*DELX'
       RT:=RT+DELRT'
      DELT:=RHOS*DELX/K2/(TS-TB)'
       T:=T+DELT'
      X:=X+DELX'
     END'
IF X LESSEQ R/4 THEN GOTO AGAIN'
    B:=B+1'
IF B LESS N THEN GOTO REPEAT'
READ J'
IF J LESS 100 THEN GOTO START'
END'
```

FIG.F1.2

DATA FOR 'ISOTHERMAL BOUNDARIES' PROGRAM

Program symbol	Value
N	4
R	0.0127
K	0.62
K2	1.25@-7
KS	1
C	4.18@3
RHOS	1600
TW	80
TB	20
M	0.5
MU	10.1@-4
TW	80
TB	30
M	0.5
MU	8@-4
TW	80
TB	40
M	0.5
MU	6.5@-4
TW	80
TB	50
M	0.5
MU	5.4@-4
J	10
N	1
R	0.0127
K	0.62
K2	1.25@-7
KS	0.5
C	4.18@3
RHOS	1600
TW	80
TB	30
M	0.5
MU	8@-4
J	10
N	1
R	0.0127

(continued)

K	0.62
K2	1.25@-7
KS	1.5
C	4.18@3
RHOS	1600
TW	80
TB	30
M	0.5
MU	8@-4
J	10
N	5
R	0.0127
K	0.62
K2	1.25@-7
KS	1
C	4.18@3
RHOS	1600
TW	80
TB	30
M	0.2
MU	8@-4
TW	80
TB	30
M	0.4
MU	8@-4
TW	80
TB	30
M	0.6
MU	8@-4
TW	80
TB	30
M	0.8
MU	8@-4
TW	80
TB	30
M	1
MU	8@-4
J	150

FIG.F1.3

ISOTHERMAL BOUNDARIES - RESULTS

T	X	Q	RT
TW= 80.000000	TB= 20.000000		M= .50000000
.00000000	.00001270	18089.409	.00026467
56919.215	.00026670	9252.4251	.00051489
170016.96	.00052070	6173.5090	.00077029
342342.13	.00077470	4607.5415	.00103108
577161.53	.00102870	3659.1365	.00129749
877980.12	.00128270	3023.0253	.00156978
1248563.7	.00153670	2566.6712	.00184819
1692964.0	.00179070	2223.2370	.00213302
2215547.1	.00204470	1955.3638	.00242455
2821025.4	.00229870	1740.5332	.00272311
3514493.1	.00255270	1564.3641	.00302905
4301467.1	.00280670	1417.2409	.00334273
5187933.1	.00306070	1292.4911	.00366454
TW= 80.000000	TB= 30.000000		M= .50000000
.00000000	.00001270	16470.357	.00024224
68623.497	.00026670	8053.8686	.00049282
211249.12	.00052070	5292.7495	.00074858
431893.08	.00077470	3920.1489	.00100973
734858.61	.00102870	3098.9747	.00127651
1124762.7	.00128270	2552.4123	.00154916
1606565.9	.00153670	2162.3647	.00182794
2185605.5	.00179070	1869.9587	.00211313
2867632.7	.00204470	1642.5561	.00240504
3658854.9	.00229870	1460.6045	.00270397
4565982.7	.00255270	1311.6769	.00301028
5596283.3	.00280670	1187.4961	.00332433
6757641.3	.00306070	1082.3366	.00364653
TW= 80.000000	TB= 40.000000		M= .50000000
.00000000	.00001270	14252.640	.00022395
86169.028	.00026670	6686.0377	.00047482
272851.66	.00052070	4336.0433	.00073087
565502.92	.00077470	3190.6980	.00099232
969967.71	.00102870	2512.5759	.00125939
1492517.0	.00128270	2064.1323	.00153234
2139888.6	.00153670	1745.5141	.00181142
2919331.7	.00179070	1507.4212	.00209692
3838658.2	.00204470	1322.7084	.00238912
4906299.1	.00229870	1175.1976	.00268836
6131369.0	.00255270	1054.6463	.00299497
7523738.9	.00280670	954.25517	.00330933
9094117.7	.00306070	869.33217	.00363184

FIG.F1.4.a

ISOTHERMAL BOUNDARIES - RESULTS (Continued)

T	X	Q	RT
TW = 80.000000	TB = 50.000000		M = .50000000
.00000000	.00001270	11462.298	.00020885
115393.85	.00026670	5175.5978	.00045996
375122.62	.00052070	3317.8996	.00071626
787019.60	.00077470	2427.8978	.00097795
1359477.9	.00102870	1905.6185	.00124527
2101502.6	.00128270	1562.1183	.00151846
3022768.6	.00153670	1318.9670	.00179779
4133685.9	.00179070	1137.7560	.00208353
5445472.1	.00204470	997.45909	.00237599
6970234.2	.00229870	885.59798	.00267547
8721060.2	.00255270	794.29903	.00298234
10712124	.00280670	718.34890	.00329695
12958805	.00306070	654.15841	.00361971
TW = 80.000000	TB = 30.000000		M = .50000000
.00000000	.00001270	15649.497	.00025495
72222.993	.00026670	5215.9215	.00075978
292450.24	.00052070	3103.7078	.00127499
668714.14	.00077470	2195.7007	.00180100
1209621.2	.00102870	1690.4445	.00233828
1924405.4	.00128270	1368.5561	.00288732
2822987.8	.00153670	1145.5001	.00344863
3916042.8	.00179070	981.78046	.00402279
5215073.3	.00204470	856.47128	.00461039
6732493.6	.00229870	757.44968	.00521206
8481725.3	.00255270	677.20832	.00582851
10477303	.00280670	610.84857	.00646046
12734995	.00306070	555.03886	.00710871
TW = 80.000000	TB = 30.000000		M = .50000000
.00000000	.00001270	16763.454	.00023801
67423.664	.00026670	9838.1606	.00040383
184182.08	.00052070	6919.5282	.00057311
352952.72	.00077470	5310.3556	.00074598
576604.41	.00102870	4290.6851	.00092259
858215.14	.00128270	3586.5956	.00110311
1201091.9	.00153670	3071.1099	.00128771
1608793.0	.00179070	2677.3115	.00147658
2085152.4	.00204470	2366.5890	.00166992
2634308.6	.00229870	2115.1003	.00186794
3260735.2	.00255270	1907.3279	.00207087
3969276.9	.00280670	1732.7365	.00227896
4765190.3	.00306070	1583.9222	.00249247

FIG.F1.4.b

ISOTHERMAL BOUNDARIES - RESULTS (Continued)

T	X	Q	RT
TW= 80.000000	TB= 30.000000		M= .20000000
.00000000	.00001270	8134.8696	.00049046
66753.377	.00026670	5394.3837	.00073706
169061.06	.00052070	4013.6581	.00098883
308852.63	.00077470	3181.7016	.00124597
488195.58	.00102870	2625.4902	.00150873
709308.14	.00128270	2227.3465	.00177733
974573.60	.00153670	1928.2116	.00205206
1286556.2	.00179070	1695.1877	.00233317
1648019.3	.00204470	1508.4962	.00262098
2061945.1	.00229870	1355.5308	.00291579
2531557.6	.00255270	1227.8768	.00321797
3060348.6	.00280670	1119.7023	.00352786
3652105.9	.00306070	1026.8379	.00384588
TW= 80.000000	TB= 30.000000		M= .40000000
.00000000	.00001270	13896.816	.00028710
68035.021	.00026670	7394.9576	.00053696
197973.68	.00052070	5004.5071	.00079200
393175.58	.00077470	3762.3324	.00105243
657240.43	.00102870	3001.1566	.00131848
994030.42	.00128270	2486.8185	.00159040
1407695.0	.00153670	2115.9258	.00186845
1902699.0	.00179070	1835.7528	.00215290
2483853.4	.00204470	1616.5910	.00244406
3156350.7	.00229870	1440.4251	.00274225
3925804.3	.00255270	1295.6950	.00304782
4798293.4	.00280670	1174.6424	.00336112
5780413.5	.00306070	1071.8663	.00368256
TW= 80.000000	TB= 30.000000		M= .60000000
.00000000	.00001270	18901.030	.00021109
69188.729	.00026670	8585.0716	.00046217
224000.21	.00052070	5513.2606	.00071843
469081.31	.00077470	4037.7636	.00098008
809411.03	.00102870	3170.7404	.00124737
1250331.4	.00128270	2600.0362	.00152052
1797581.8	.00153670	2195.8307	.00179981
2457337.7	.00179070	1894.4719	.00208552
3236253.5	.00204470	1661.0831	.00237794
4141511.3	.00229870	1474.9536	.00267739
5180875.5	.00255270	1323.0090	.00298422
6362754.4	.00280670	1196.5887	.00329879
7696270.9	.00306070	1089.7285	.00362151

FIG.F1.4.c

ISOTHERMAL BOUNDARIES - RESULTS (Continued)

T	X	Q	RT
TW= 80.000000	TB= 30.000000		M= .80000000
.00000000	.00001270	23427.371	.00017031
70266.491	.00026670	9396.4422	.00042204
248313.48	.00052070	5831.3260	.00067895
539990.37	.00077470	4202.8467	.00094127
951564.64	.00102870	3269.8763	.00120921
1489760.7	.00128270	2665.1378	.00148303
2161803.3	.00153670	2241.2421	.00176299
2975465.9	.00179070	1927.5527	.00204936
3939125.0	.00204470	1685.9796	.00234246
5061821.5	.00229870	1494.1709	.00264258
6353328.7	.00255270	1338.1442	.00295009
7824231.1	.00280670	1208.7054	.00326535
9486012.2	.00306070	1099.5600	.00358875
TW= 80.000000	TB= 30.000000		M= 1.0000000
.00000000	.00001270	27603.530	.00014454
71291.088	.00026670	9993.1013	.00039668
271427.36	.00052070	6051.8980	.00065401
607401.44	.00077470	4314.2816	.00091674
1086705.7	.00102870	3335.7655	.00118511
1717378.9	.00128270	2707.9739	.00145935
2508057.6	.00153670	2270.9121	.00173973
3468034.6	.00179070	1949.0537	.00202652
4607323.6	.00204470	1702.0968	.00232004
5936732.0	.00229870	1506.5718	.00262059
7467944.0	.00255270	1347.8857	.00292853
9213612.4	.00280670	1216.4874	.00324422
11187465	.00306070	1105.8630	.00356806

FIG.F1.4.d

APPENDIX F2

HEAT EXCHANGER ANALYSIS WITH SCALING ON THE TUBE SIDE

F2.1 Symbols

	c	specific heat capacity
	h	surface coefficient of heat transfer
	k	thermal conductivity
	l	distance along tube
	L	tube length
	LMTD	logarithmic mean temperature difference
	$\dot{m}$	mass flow rate
	p	exponent in equation F2.9
	q	heat flow rate
	R	tube radius
	R_{th}	thermal resistance for an element of length
	R_T	overall thermal resistance
	t	time
	T	temperature
	x	scale thickness
	ρ	density
	μ	dynamic viscosity
Suffixes:	h	'hot' shell-side liquid
	c	'cold' tube-side liquid
	s	scale - liquid interface
	sc	scale material
	i	inlet
	o	outlet

F2.2 The analysis

As in Appendix F1 the equations are based on finite elements which allows a numerical solution for a given set of data.

Consider first an element of tube length, Δl, as shown in the diagram below.

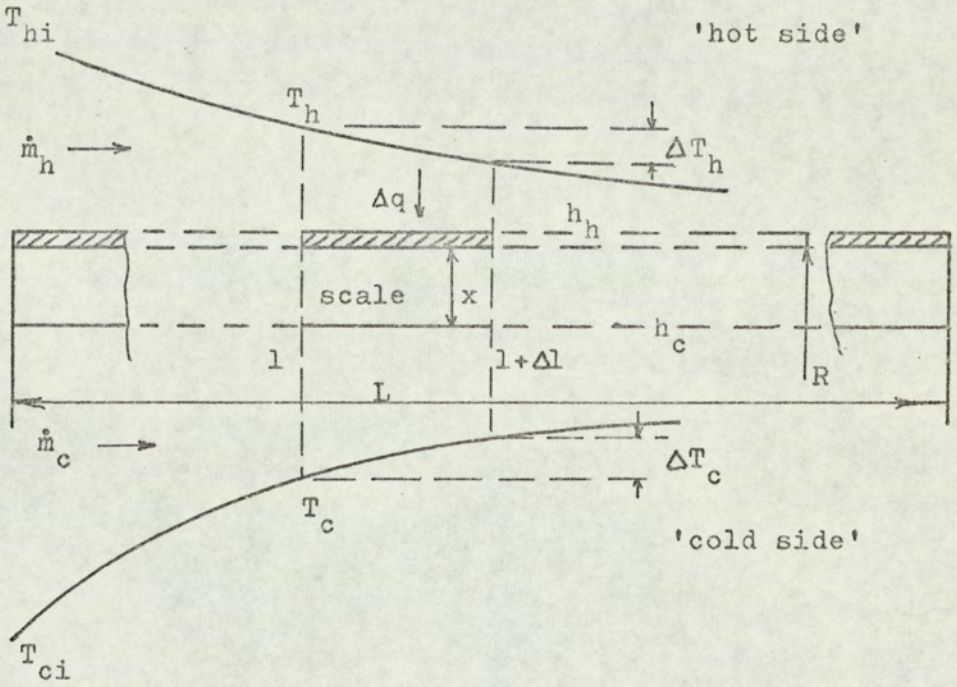

At time t the scale is assumed to have a thickness x and so the thermal resistance for the section is given by:

$$R_{th} = \frac{1}{h_h} + \frac{R}{k_{sc}} \ln\left[\frac{R}{R - x}\right] + \left[\frac{R}{R - x}\right] \frac{1}{h_c} \qquad \text{(F2.1)}$$

Neglecting changes in fluid properties due to temperature changes, h_h will remain constant. However h_c will change because of the increasing velocity on the tube-side as the scale thickness increases (the mass flow rate being constant). This effect is allowed for by writing:

$$h_c = \frac{0.0115\, k_c}{(R - x)} \left[\frac{2\dot{m}_c}{\pi \mu (R - x)}\right]^{0.8} \left[\frac{C_c \mu_c}{k_c}\right]^{0.4} \qquad \text{(F2.2)}$$

The heat flow through the element is calculated from:

$$\Delta q = \frac{2\pi R \, \Delta l \, (T_h - T_c)}{R_{th}} \qquad \text{(F2.3)}$$

Based on this heat flow, the temperature changes for the tube-side and shell-side liquids along the length of the element can be found from

$$\Delta T_h = \frac{\Delta q}{\dot{m}_h \, c_h} \qquad \text{(F2.4)}$$

$$\text{and} \quad \Delta T_c = \frac{\Delta q}{\dot{m}_c \, c_c} \qquad \text{(F2.5)}$$

The calculation is started at zero time for which x = 0.

Equations F2.1 to F2.5 inclusive allow the variation in T_h and T_c with tube length to be found, starting with the specified inlet values T_{hi} and T_{ci} respectively.

The total heat flow is obtained as the summation of elemental heat flow rates Δq along the tube length.

Once the temperature distribution is known, the LMTD can be found from the inlet and outlet temperatures of the tube-side and shell-side liquids according to:

$$\text{LMTD} = \frac{\left[(T_{hi} - T_{ci}) - (T_{ho} - T_{co})\right]}{\ln\left[\frac{T_{hi} - T_{ci}}{T_{ho} - T_{co}}\right]} \qquad \text{(F2.6)}$$

Finally, the overall thermal resistance is given as:

$$R_T = \frac{2\pi RL}{q} \times \text{LMTD} \qquad \text{(F2.7)}$$

Deposition of scale occurs on the inside wall of the tube because of the temperature difference $(T_s - T_c)$ between the scale surface and the tube-side liquid. The scale surface temperature is found from:

$$T_s = \frac{(T_h - T_c)\,R}{h_c\,R_{th}(R - x)} + T_c \qquad (F2.8)$$

This temperature will vary along the length of the tube because of the varying liquid temperatures T_h and T_c. Consequently the amount of scale deposited will vary along the length of the tube since the rate of deposition depends on the temperature difference $(T_s - T_c)$. (See equations C3.1 and C3.7).

For a specified interval of time Δt the corresponding increase in scale thickness for the element of length Δl is given by:

$$\Delta x = \frac{K_1}{\rho_{sc}} (T_s - T_c)^p \Delta t \qquad (F2.9)$$

Therefore, as the temperature distribution along the tube, at zero time, is calculated, the increase in scale thickness for each element of length is found from equation F2.9 for the first increment in time.

Once the scale thickness distribution is known, revised thermal resistances for each element after the first interval of time are calculated from equation F2.1 and the cycle of calculations repeated for successive time intervals.

Computer programs have been written in Elliot-Algol for the system of equations described, and these are reproduced as Fig. F2.1 and Fig. F2.2. Fig. F2.1 shows the program for the parallel flow arrangement, the counterflow arrangement program is Fig. F2.2, and program symbols, together with the corresponding theory symbols and units, are listed in Fig. F2.3.

The numerical data has been listed in Section D, in paragraph D2.2 and in Fig. D2.1, and this data allowed for the effect of three variables on the overall thermal resistance to be investigated. These variables were:

(a) the inlet temperature difference between the tube-side and

shell-side liquids,

(b) the mass flow rate of the tube-side liquid,

(c) the value of the exponent p in equation F2.9.

For both programs the element of length was chosen as $L_1/100$ but, because of the dependence of the scaling rate on the exponent p, the results from trial data showed that it was necessary to adjust the specified time interval according to the value of p. A suitable empirical rule giving Δt seconds was found to be:

$$\Delta t = 3600(9 - 4p)$$

Again, the program was stopped by specifying a limiting value of the overall thermal resistance, and p was introduced empirically so that sufficient results were calculated in a minimum of computing time.

This limit can be written in the form:

$$\frac{R_T \text{ at time } t}{R_T \text{ at time } 0} = p + 0.5$$

In programing for the counterflow heat exchanger an iteration procedure was introduced because the specified inlet temperatures T_{hi} and T_{ci} are at opposite ends of the tube. The program allows for a guessed outlet temperature T_{ho} to be used corresponding to T_{ci} in the first element of length, so that the temperature distributions along the tube can be found according to equations F2.1 to F2.5. This calculated distribution leads to a value of T_{hi} which is compared with the specified T_{hi}. If these values differ by more than 1% the outlet temperature T_{ho} is modified and the calculation repeated. Once agreement is reached the calculation will proceed to the next interval of time.

The results of the heat exchanger analysis are presented and discussed in Section D.

PARALLEL - FLOW HEAT EXCHANGER

```
PROGRAM     P12B'
BEGIN  REAL R,L,L1,DELL,T,DELT,Q,HH,RTA,THIN,TCIN,K1,RHOS,DELTH,
            DELTC,MH,MC,C,LMTD,KS,DELX,K,MU,P,Y,Z'
       INTEGER I,J,B,N'
      ARRAY DELQ,RT,TH,TC,TS,HC,X(1:101)'
       SWITCH S:=START,AGAIN'
      READ R,L1,THIN,TCIN,HH,MH,MC,C,K1,RHOS,KS,K,MU,P'
                DELL:=L1/100'
                                        DELT:=(9-4*P)*3600'
       T:=0'     J:=-1'     B:=0'       N:=1'
      PRINT £P=?,P'
  START:        I:=1'     Q:=0'      L:=0'
                IF B LESS 1 THEN BEGIN  TH(I):=THIN'
                                        TC(I):=TCIN'
                                   END'
       AGAIN:       J:=J+1'
                IF J LESS 100 THEN X(I):=0'
     HC(I):=0.0115*K*(2*MC/(3.1416*MU*(R-X(I))))**0.8
                     *(C*MU/K)**0.4/(R-X(I))'
   RT(I):=1/HH+(R/KS)*LN(1/(1-X(I)/R))+(1/(1-X(I)/R))/HC(I)'
       DELQ(I):=6.2832*R*DELL*(TH(I)-TC(I))/RT(I)'
       TS(I):=(TH(I)-TC(I))/HC(I)/(1-X(I)/R)/RT(I)+TC(I)'
    DELX:=(TS(I)-TC(I))**P*DELT*K1/RHOS'
         X(I):=X(I)+DELX'
            DELTH:=DELQ(I)/(MH*C)'
            DELTC:=DELQ(I)/(MC*C)'
```

FIG.F2.1

PROGRAM P12B (Continued)

```
            I:=I+1'

          TH(I):=TH(I-1)-DELTH'
          TC(I):=TC(I-1)+DELTC'

            L:=L+DELL'
          Q:=Q+DELQ(I-1)'

        IF I LESS 101 THEN GOTO AGAIN'

         LMTD:=(TH(1)-TC(1)-TH(101)+TC(101))/
                        LN((TH(1)-TC(1))/(TH(101)-TC(101)))'

          RTA:=6.2832*R*L1*LMTD/Q'

         IF B=0 THEN Z:=RTA'

         Y:=RTA**(P+1)*1@6'

      IF N=1 THEN BEGIN
           PRINT ££L?T=?,SAMELINE,T,££S4?1/U=?,RTA,
                    ££S4?1/U TO (P+1)=?,Y'
  END'

      B:=1'        N:=-N'          T:=T+DELT/3600'

      IF RTA/(P+0.5) LESS Z THEN GOTO START'
END'
```

FIG.F 2.1

COUNTER - FLOW HEAT EXCHANGER

PROGRAM P13'

```
BEGIN REAL R,L,DELL,T,DELT,Q,HH,RTA,THIN,TCIN,K1,RHOS,DELTH,DELTC,
        MH,MC,C,LMTD,KS,DELX,MU,P,Z,K,A,G'

   INTEGER I,J,Y,N'

  READ R,L,THIN,TCIN,HH,MH,MC,C,K1,RHOS,KS,K,MU,P,Y'

       DELL:=L/(Y-1)'

   DELT:=(9-4*P)*3600'

   T:=0'          J:=0'          N:=1'

  BEGIN ARRAY DELQ,RT,TH,TC,TS,HC,X(1:Y)'

        SWITCH S := START'

 START:       Z:=1@-2'
            TC(1):=TCIN'
          TH(Y):=THIN'
        IF J LESS 1 THEN TH(1):=THIN/2'

  FOR TH(1):=THIN/TH(Y)*TH(1) WHILE Z GR 1@-4 DO

  BEGIN     SWITCH SS:=AGAIN'
              Q:=0'          I:=1'

       AGAIN:   IF J LESS 1 THEN X(I):=0'
 HC(I):=0.0115*K*(2*MC/(3.1416*MU*(R-X(I))))**0.8
                *(C*MU/K)**0.4/(R-X(I))'

 RT(I):=1/HH+(R/KS)*LN(1/(1-X(I)/R))+(1/(1-X(I)/R))/HC(I)'

   DELQ(I):=6.2832*R*DELL*(TH(I)-TC(I))/RT(I)'

   TS(I):=(TH(I)-TC(I))/HC(I)/(1-X(I)/R)/RT(I)+TC(I)'

      DELTH:=DELQ(I)/(MH*C)'
      DELTC:=DELQ(I)/(MC*C)'
```

FIG.F 2.2

PROGRAM P13 (Continued)

```
            I:=I+1'

          TH(I):=TH(I-1)+DELTH'
          TC(I):=TC(I-1)+DELTC'

            Q:=Q+DELQ(I-1)'

    IF I LESS Y THEN GOTO AGAIN'
          Z:=((THIN-TH(Y))/THIN)**2'
       END'

          TH(1):=THIN+MC/MH*(TC(Y)-TCIN)'

        PRINT TH(Y)'

      FOR I:=1 STEP 1 UNTIL (Y-1) DO

                  BEGIN IF J LESS 1 THEN X(I):=0'

                        DELX:=(TS(I)-TC(I))**P*DELT*K1/RHOS'
                          X(I):=X(I)+DELX'
                     END'

          LMTD:=(TH(1)-TC(1)-TH(Y)+TC(Y))/LN((TH(1)-TC(1))/
                                (TH(Y)-TC(Y)))'

          RTA:=6.2832*R*L*LMTD/Q'

          IF T=0 THEN G:=RTA'

         A:=RTA**(P+1)*1@6'

    IF N=1 THEN BEGIN

        PRINT ££L?T=?,SAMELINE,T,££S4?1/U=?,RTA,
                      ££S4?1/U TO (P+1)=?,A'
        END'

      J:=J+2'          N:=-N'        T:=T+DELT/3600'

   IF RTA/(P+0.5) LESS G THEN GOTO START'

  END'

END'
```

FIG.F 2.2

HEAT EXCHANGER PROGRAM SYMBOLS AND UNITS

(program switching parameters are not listed)

PROGRAM SYMBOL	THEORY SYMBOL	UNITS
C	C_h, C_c	J/kg deg C
DELL	Δl	m
DELT	Δt	s
DELTC	ΔT_c	deg C
DELTH	ΔT_h	deg C
DELQ	Δq	W
DELX	Δx	m
HC	h_c	W/m^2 deg C
HH	h_h	W/m^2 deg C
K	k_c	W/m deg C
Kl	K_l	-
KS	k_{sc}	W/m deg C
L	l	m
Ll	L	m
LMTD	LMTD	deg C
MC	$\dot{m}_c$	kg/s
MH	$\dot{m}_h$	kg/s
MU	μ	kg/ms
P	p	-
Q	q	W
R	R	m
RHOS	ρ_{sc}	kg/m^3
RT	R_{th}	m^2 deg C/W
RTA, 1/U	R_T	m^2 deg C/W
T	t	h
TC	T_c	^oC
TCIN	T_{ci}	^oC
TH	T_h	^oC
THIN	T_{hi}	^oC
TS	T_s	^oC
X	x	m

FIG.F2.3

SECTION G

REFERENCES

REFERENCES

1. HUDSON, D. "Fouling of shell and tube exchangers" Joint symposium on heat exchangers, I.Mech.E., Manchester, April 1969.

2. KERN, D.Q. and R. E. SEATON. "A theoretical analysis of thermal surface fouling" Brit.Chem.Eng., 1959, 4 (5), 258-262.

3. KERN, D.Q. "Heat exchanger design for fouling services" Proc. of 3rd International Heat Transfer Conf., A.I.Ch.E. 1966, 1, 170-178.

4. KELLY, B.J., and P. R. PUCKORIUS. "Waterside fouling and scaling of heat exchangers" Materials Protection, 1964, 3 (5), 30.

5. KRUPICZKA, R. "Analysis of thermal conductivity in granular materials" Internat. Chem. Eng., Jan. 1967, 7, 122-144.

6. HASSON, D. "Rate of decrease of heat transfer due to scale deposition" Dechema Monograph, 1962, 47, 233.

7. EMERSON, W. E. "Heat exchangers" The Chartered Mech. Engr., 1969, 16 (7), 317.

8. Standards of the Tubular Exchangers Manufacturers Association, Inc., New York. 1st Ed.(1941), 2nd Ed. (1949), 3rd Ed.(1952), 4th Ed.(1959), 5th Ed.(1968)

9. McCABE, W. L. and C. S. ROBINSON. "Evaporator scale formation" Ind. Eng. Chem., 1924, 16, 478.

10. WEILAND, J. H. et al. "Rates of fouling and cleaning of unfired heat exchanger equipment" Trans. A.S.M.E., 1949, 71, 849-853.

11. BANCHERO, J. T. and K. F. GORDON. "Scale deposition on heated surfaces" Advan. Chem. Series, 1960, No. 27, 105.

12. KERST, H. "Laboratory investigation of water-side scale and corrosion in presence of high process - side temperatures" Corrosion, 1960, 16 (10), 523t-528t.

13. McALLISTER, R. A. et al. "Study of scaling and corrosion in condenser tubes exposed to river water" Corrosion, 1961, 17 (12), 579t - 588t.

14. KERST, H. "Influence of inhibitors on corrosion and scale deposition on heat transfer surfaces in fresh water cooling systems" Materials Protection, Oct. 1962, 1, 10-19.

15. HASSON, D. et al. "Mechanism of calcium carbonate scale deposition on heat transfer surfaces" Ind. and Eng. Chem. Fundamentals, 1968, 7 (1), 59.

16. FISHER, A. O. "Improved laboratory technique for investigating corrosion by recirculating cooling water" Corrosion, 1963, 19 (3), 91t-101t.

17. CHANDLER, J. L. "Effect of supersaturation and flow conditions on the initiation of scale formation" Trans. Instn. Chem. Engrs., 1964, 42 (1), T24-T34.

18. REITZER, B. J. "Rate of scale formation in tubular heat exchangers" Ind. and Eng. Chem. Process Design and Development Quarterly, Oct. 1964, 3, 345-348.

19. GUTZIET, J. "Corrosion and fouling of admiralty, aluminium and steel tubes in open recirculating cooling-water systems" Materials Protection, 1965, 4 (7), 28-34.

20. GILMOUR, C. H. "No fooling - no fouling" Chem. Engng. Prog., 1965, 61 (7), 49-54.

21. BRENNAN, P. "Chemical descaling of industrial heat exchangers" Heat. Air Condit., 1962, 29 (5), 452-454.

22. "Design of evaporators: Report of a meeting at NEL, 10th January, 1967" NEL Report No. 329. East Kilbride, National Engineering Laboratory, 1967.

23. SHERWOOD TAYLOR, F. "Inorganic and theoretical chemistry" London: Heinemann, 1959.

24. GROVE, C. S. et al. "Crystallisation from solution" Adv. in Chem. Eng., 1962, 3, 1-60.

25. GOLIGHTLY, D. R. and E. R. McCARTNEY. "A study of the effect of air bubbles on the nucleation and growth of calcium sulphate scale on a heat transfer surface" Chem. Eng., 1963, 169 (6), CE170-175 and CE183.

26. FREEBORN, J. and D. LEWIS. "Initiation of boiler scale formation" J. Mech. Eng. Sci., 1962, 4 (1) 46-52.

27. BADGER, W. L. and J. T. BANCHERO. "Introduction to chemical engineering" New York: McGraw Hill. 1955.

28. BRANSOM, S. H. "Factors in the design of continuous crystallisers" Brit. Chem. Eng., 1960, 5, 838.

29. FREEDMAN, A. J. et al. "Design of equipment and laboratory tests for heat transfer surface inhibition in cooling water" Materials Protection, 1962, 1 (10), 22-31.

30. DAVIS, E. J. "Heat transfer and pressure drop in annuli" 1943, Trans. ASME, 65, 755-760.

31. GUNN, D. J. and C. W. W. DARLING. "Fluid flow and energy losses in non-circular conduits" 1963, Trans. Instn. Chem. Engrs., 41 , 163-173.

32. SCARBOROUGH, J. B. "Numerical mathematical analysis" London: Oxford University Press, 1962.

33. KERN, D. Q. "Process heat transfer" New York: McGraw Hill, 1950.

ACKNOWLEDGEMENTS

The author wishes to thank:

Professor A. J. Ede in his capacity as supervisor, for his assistance and guidance throughout the project. Also in his capacity as Head of Department for making available the facilities of the department.

Those members of the technical staff who gave willing and able assistance in the practical work.

The City of Birmingham Education Committee for granting the author leave of absence to complete the project.